



# A Theory of Crowdfunding Dynamics

**BSE Working Paper 1349**  
**May 2022 (Revised December 2022)**

Matthew Ellman, Michele Fabi

[bse.eu/research](https://bse.eu/research)

# A Theory of Crowdfunding Dynamics\*

Matthew Ellman<sup>†</sup> and Michele Fabi<sup>‡</sup>

December 2022

## Abstract

This paper develops a dynamic model of crowdfunding to characterize success rates and welfare and to identify optimal transparency and design policies. We also characterize average bidding profiles. Bidding costs generate two dynamic forces: (1) *decreasing pivotality*, driven by reduced scope for strategic complementarity as the deadline nears, pushes the slope downwards; (2) a *news effect* from observed bidding further pushes the slope downwards for concave cost distributions, but upwards for convex costs. These effects can explain prominent bidding patterns. Non-disclosure of funding progress yields higher welfare than full transparency given homogeneous costs. However, cost heterogeneity favours disclosure by enabling early bidders to activate otherwise passive, higher cost bidders. We also investigate the tradeoff between raising prices and thresholds and we demonstrate success and welfare gains from the indirect dynamic pricing permitted by current platforms.

*JEL Classifications: D26, C73, L12, M13.*

*Keywords: Strategic complementarity; Subscription games; Disclosure rules; Pivotality; Information acquisition; Crowdfunding dynamics.*

---

\*We thank Ramon Caminal, Vincenzo Denicolò, Ramon Faulí-Oller, Sjaak Hurkens, Ángel López, Carolina Manzano, Chara Papioti and Amedeo Piolatto for valuable discussions, and audiences at IAE, UAB, Ca' Foscari, TSE, SAEe (Alicante, 2019), ASSET (Athens, 2019), WIPE (Reus, 2019), EARIE (Barcelona, 2019) and JEI (Madrid, 2019). We gratefully acknowledge financial support from the Severo Ochoa Programme for Centres of Excellence in R&D (CEX2019-000915-S), Spanish Ministry PID2020-118653GB-I00 (AEI/FEDER, UE), FPI fellowship 914886-79792965, Generalitat of Catalunya (2017 SGR 1136), FBVVA (2016 “Innovación e Información en la Economía Digital”) and the Blockchain & Platform Chair.

<sup>†</sup>Institute of Economic Analysis, IAE-CSIC, and Barcelona School of Economics, BSE ([matthew.ellman@iae.csic.es](mailto:matthew.ellman@iae.csic.es))

<sup>‡</sup>Ecole Polytechnique, CREST, IP Paris ([michele.fabi@ensae.fr](mailto:michele.fabi@ensae.fr))

# 1 Introduction

Strategic complementarities and positive externalities arise in a wide range of games. Simultaneous-move variants are well understood but in reality interactions are often dynamic. This paper characterizes dynamic outcomes, identifying two novel forces and the welfare impact of sequentiality, in a canonical finite-duration game with these features.

Our specific game also has independent interest since it corresponds to reward-based crowdfunding. This, now well-established, way of raising funds for producing new goods, enables entrepreneurs to solicit finance directly from funders. The new good serves as the reward for funders who essentially pledge or bid on the campaign as advance buyers. Projects range from small-scale musical albums to substantial innovations that generate new markets and significant welfare gains.<sup>1</sup> Typically, the entrepreneur describes her planned product and sets its price plus a funding threshold and deadline: she only produces and bidders only buy in the “success” event that aggregate funds reach the threshold in time. If instead the campaign fails, nothing is produced and nothing is paid, giving the name, *all-or-nothing* (AON).

The beauty of crowdfunding is that bidding provides a credible signal of demand before the entrepreneur sinks her costs of production. This market test reduces her exposure to demand uncertainty. On the flip side, bidders face production uncertainty. When campaign failure stops production, bids are reimbursed but any sunk costs of bidding go to waste. So bidders are more willing to bid when a campaign has a higher probability of success. Conversely, each bid raises this success rate. As platforms disclose funding progress in real-time, bidding and success rates co-evolve. Each bid encourages later bidders to bid and benefits them. So the combination of sunk costs and threshold directly create the strategic complementarity and positive externalities that underlie all our results. We characterize the resulting bid dynamics and campaign outcomes. From this, we derive entrepreneurs’ optimal campaign design choices and we establish the welfare implications of crowdfunding platforms’ current disclosure rules.

We also characterize average bidding profiles and compare them with empirically salient patterns. Campaigns that start poorly usually die out, while successful campaigns mostly start up strongly, slow down gradually and then pick up again as the deadline

---

<sup>1</sup>E.g., Kickstarter raised 6.3B USD since 2012, bringing 550K projects to life (Statista, 2021). 40% succeed (Kickstarter, 2021), of which 90% become ongoing ventures (Mollick and Kuppawamy, 2014).

approaches, creating a U-shape (see Fig. 12). Understanding these dynamics is critical for addressing our welfare and design questions. Yet first generation crowdfunding theories only model simultaneous funding choices.

We instead model bidders who arrive over time by a Poisson process. Each bidder observes the “gap” between the campaign’s threshold and funds collected so far and its deadline. He also learns his independent cost of bidding. Any sunk cost has the same implications. We model the case of inspection costs because assessing one’s value for a good *before* it is produced often requires time and effort: bidders must read about the intended good and the entrepreneur and may watch a video pitch. Assuming product prices dissuade uninformed bidding, we show that inspection costs are equivalent to direct sunk costs of bidding. Direct costs include the hassle and opportunity costs of committing to pay by letting the platform hold bids in escrow. As campaign durations rarely exceed two months, such costs may be small but inspection costs are significant for many bidders. Of course, inspection costs are sometimes trivial or even net negative, as when a bidder is already informed or enjoys thinking about the good, but this merely invigorates the analysis because cost heterogeneity is critical to most of our results.

We focus on inspections that reveal private values.<sup>2</sup> A campaign’s date (time since initiation) and gap then form a Markovian state space that determines the probability of success. We show that this (interim) success rate is falling in both date and gap, since later dates leave less time for bidders to arrive and fill the funding gap.

Two forces determine bidding patterns and underlie our welfare results. The first is the *pivotality effect*, denoted PE. We define each bidder’s *pivotality* as the increase in the success rate when he decides to bid, taking as given the state (date and gap) when he arrives.<sup>3</sup> We prove that pivotality has a decreasing trend. This is intuitive: each bidder encourages all followers to also bid and a later bidder expects to have fewer followers; the strategic complementarity operates over a shorter duration as passing time brings the deadline closer. Since a bidder is encouraged by his own pivotality, this *decreasing pivotality* trend, denoted DP, has a negative effect on expected bidding. This is the pivotality effect PE. It is always (weakly) negative. Formally, we show that a bidder only cares about success when he bids, so his incentives rise with the *bidder success rate*, which

---

<sup>2</sup>We discuss common values in Section 7.

<sup>3</sup>Pivotality is often substantial in practice, especially in the early stages of a campaign, because most campaigns are far smaller than those that hit the headlines; on Kickstarter, the median number of bids is 60 and variance is substantial (Fan-Osuala et al., 2018).

is the unconditional success rate plus his pivotality (a martingale plus a supermartingale).

While the PE accounts for the impact of the bidder success rate trend, the second force captures the impact of its variance around that trend. We call this the *news effect*, denoted NE, because later bidders observe more news about bidding outcomes. Comparing an earlier and later bidder, only the later one observes and can respond to the news of how much interim bidders reduce the gap. The later bidder cannot influence interim bidders (whence DP), but can react to deviations in the bidder success rate from its trend. The average impact of these deviations is positive if there are increasing returns to good news about success prospects and negative if the returns are decreasing. Formally, a locally increasing density of bidder costs implies that the mass of higher cost bidders who respond to good news by starting to bid exceeds that of lower cost bidders who respond to bad news by ceasing to bid. An increasing density is equivalent to local convexity of the cumulative distribution function (CDF) of the bidding cost. So the sign of the NE follows directly from Jensen's inequality.

Stochastic calculus allows us to quantify PE and NE and characterize average bidding slopes, both unconditionally and conditional on success and failure, for a range of cost distributions. For the uniform distribution, the NE is neutral so the PE directly guarantees a negative slope. Next, we prove that sufficient convexity plus sufficient success rate variance creates a positive NE that dominates the PE and generates a positive slope. We also highlight the bimodal distributions that arise when bidders split into two classes: close contacts with mostly negative net costs versus distant bidders with mostly prohibitive costs. Single-peaked densities within each class imply concavity followed by convexity on the relevant cost range. As it takes time for enough good news to arrive and activate the distant bidders, the positive NE from the convex region only dominates the negative PE towards a campaign's end. So this setting predicts a U-shape for successful projects and a downward-sloping profile for failed campaigns, consistent with the data.

Our results generalize to discrete distributions. In the homogenous case, for any given state, a project is either active with maximal bidding or frozen with no bidders inspecting. We identify a downward-sloping *wall of ice* that separates the active from frozen states. The frozen state is absorbing, so the probability of staying active falls over time, causing average bidding to also decrease over time. Both bid profile and ice wall consist of downward steps at the critical dates where freezing can occur and a discrete

PE dominates the NE. We provide an efficient joint recursion to compute activity rates and critical dates and thereby infer success rates.

Importantly, our framework permits welfare analysis. Our full disclosure baseline captures the current practice of disclosing funding in real-time but is this better than having no disclosure until after the deadline? We call the full disclosure baseline “SEQ” and the no-disclosure benchmark “SIM” since bidders moves are, respectively, essentially sequential and simultaneous. The answer (SEQ or SIM) again depends on the two forces. If the NE is positive and dominates the PE, disclosure SEQ is beneficial since it allows early arrivals with low costs to activate higher cost bidders who arrive later. This applies when costs are heterogenous and conditions are adverse. When bidders are scarce relative to the campaign threshold, moderate cost bidders do not inspect in SIM. By enabling the activation of late, high cost bidders, associated with the positive NE, SEQ even encourages moderate cost bidders from the start since they anticipate that later activation.

Conversely, when bidders are relatively homogenous, PE dominates in SEQ and disclosure is detrimental because the decreasing pivotality trend reduces success rates and inhibits the positive externalities from inspections. In the extreme case of pure homogeneity, all-inspect must be an equilibrium under no-disclosure else no bidding ever occurs for any information structure. Disclosure can then only reduce inspection and hence success. In principle, disclosure might still raise welfare by reducing wasted inspections.<sup>4</sup> We do identify a delayed disclosure rule that improves on full disclosure, but we prove that SEQ never raises welfare over SIM in the homogenous case. We prove this via a general result: welfare contributions from bidder arrivals are time-decreasing in SEQ since decreasing pivotality has a greater negative impact on surplus than the gains associated with later bidders adapting to news.

Lastly, we use the framework for optimal campaign design. We extend the baseline to endogenize bidder threshold and price. An entrepreneur maximises campaign success subject to a funding need. We show it binds and creates a price-threshold tradeoff. The entrepreneur’s optimal bidder threshold increases with her funding need, limiting required price rises. Her bidder threshold also increases with the expected number of bidders since bidder abundance makes a high threshold safer. Homogeneity is an exception.<sup>5</sup>

---

<sup>4</sup>Bidders under-inspect given a fixed information structure but coordinating inspections also matters.

<sup>5</sup>With its sharp CDF discontinuity, homogeneity inverts the second comparative static. Under bidder scarcity, the main risk of hitting the ice wall is at the start where low pricing is key; bidder abundance postpones this risk so it favours higher prices and lower thresholds.

We close on design by allowing for multiple prices, via gap-dependent pricing. Dynamic pricing can raise both success rates and bidder welfare. Since early bidders face high gaps, low prices on units sold at high gaps represent early discounts (ED) and platforms can readily implement ED by letting bidders choose from a fixed menu of rewards with limited quantities. Late discounts (LD), like time-dependent prices, are not currently feasible but are theoretically instructive. We find that ED is optimal when bidders are abundant since, as in the PE, early bidders have more successors to encourage. Under bidder scarcity, this ED benefit is dominated by LD’s *anticipation effect*: early bidders anticipate that LD will encourage later bidders. Homogeneity is again exceptional.<sup>6</sup> We end the paper with a brief discussion of empirical implications and tests.

**Related theory.** In the literature on private contributions to public goods, AON reward-based crowdfunding is a threshold “subscription game” with exclusion (Admati and Perry, 1991, coin this term in their dynamic extension of Bagnoli and Lipman, 1989). Ellman and Hurkens (2019b) show how crowdfunding credibly reveals market demand before production and potentially complements traditional finance. Other early papers study designs to mitigate entrepreneurial fraud (Strausz, 2017; Chemla and Tinn, 2020; Ellman and Hurkens, 2019a), the flexible funding alternative to AON (Chang, 2020) and investment-based crowdfunding variants (Brown and Davies, 2020), all with a single period of crowdfunding. In this paper, we sidestep the price discrimination in Ellman and Hurkens’s (2019b) binary private value model by setting the low valuation to zero, as do the entrepreneurial fraud papers. Our key departure is to introduce dynamics via bidding costs (with an inspection-based microfoundation).

The two closest papers (Alaei et al., 2021; Deb et al., 2021) are contemporaneous studies of similar dynamic subscription games that also feature bidding costs. They both assume a direct sunk cost of bidding so, as explained above, our inspection cost microfoundation complements their work. We now highlight the more important differences. Alaei et al. (2021) solve a discrete version of our model with homogenous costs. They show that bidding has momentum effects that lead to polarized crowdfunding outcomes, consistent with the increasing variance behind NE in our analysis. They do not compute average profiles. Deb et al. (2021) model bidders with homogenous costs in the same way,

---

<sup>6</sup>Bidder scarcity then promotes ED to avoid early freezing, while bidder abundance promotes LD.

but with the time interval converging to zero and they add a single donor with uncertain wealth. From a range of signalling equilibria, they emphasize how discrete donation spikes at the start and finish of a campaign can explain a rectangular U-shape (i.e., a  $\sqcup$ -shaped bid profile). They assess bid profiles empirically using data they scraped from Kickstarter, but their theory does not solve for average bidding. A unique contribution of our paper is to use stochastic calculus (which circumvents the need for shrinking time intervals) and to compute Markov state probabilities to precisely predict profiles. This enables us to derive explicit theoretical results, including our two novel forces and analysis of welfare and entrepreneurial design. In so doing, we prove that bidding profiles are in fact downward-sloping in Alaei et al. (2021) and Deb et al.’s (2021) no donor benchmark, since both assume homogenous costs. Importantly, we go beyond the extreme discontinuity of the homogenous case. Cost heterogeneity proves vital for explaining positive bidding slopes, the U-shape and our key result on welfare gains from bidding disclosure.<sup>7</sup>

**Related empirics.** Many papers highlight the U-shape or bathtub bidding patterns in AON crowdfunding. Kuppuswamy and Bayus (2018) establish this for bid values and bid counts in Kickstarter data. They normalize durations and average over campaigns for each block in a time partition. Deb et al. (2021) provide richer evidence for Kickstarter and Crosetto and Regner (2018) corroborate the U-shape for Germany’s Startnext platform but only when conditioning on success. Conditioning on failure, they find a simple downward slope. Rao et al. (2014); Etter et al. (2013); Crosetto and Regner (2018); Colombo et al. (2015) predict success based on the bid process, campaign attributes and social activity. Pledging during the early days of a campaign is a powerful predictor of success, in line with our decreasing pivotality insight. Section 7 presents further evidence.

## 2 Model

We construct the simplest reward-based crowdfunding campaign to analyse bid dynamics in continuous time. The entrepreneur specifies a product as the *reward* for crowdfunders, a price  $p$  of that single reward, a funding threshold or goal and her campaign deadline. Funders can pledge  $p$  if they hear about the campaign before its deadline. The campaign

---

<sup>7</sup>Alaei et al. (2021); Deb et al. (2021) both neglect welfare, but the latter study how disclosure rules affect success rates. They claim that a donor is needed for Kickstarter’s disclosure policy to raise success rates. We prove that with heterogenous costs, it can in fact raise success rates without any donor.

is said to *succeed*, denoted  $\mathcal{S}$ , if and only if the sum of these pledged funds (each restricted to  $p$  or 0) reach or exceed the funding threshold. Equivalently, the number of bids must exceed a bidding threshold, denoted  $g_0$ . The campaign is *All-or-Nothing*: after a success ( $\mathcal{S}$ ), each funder pays his pledge  $p$  to the entrepreneur who must invest in production and deliver a unit reward to each funder. After a *failure*, denoted  $\mathcal{F}$ , there are no payments (pledges held in escrow are reimbursed) and there is no production. These crowdfunding rules are perfectly enforced. A pledge is a binding commitment to pay  $p$  in return for the product, *contingent* on funding success  $\mathcal{S}$ . Pledges are subscriptions in the terminology of Admati and Perry (1991); we use the briefer term, *bids*.

Setting time  $t$  to zero on campaign initiation, the campaign's deadline is its duration, denoted  $\tau$ . We say that a bidder arrives at the project at the date  $t \leq \tau$  when he hears about it. Bidders arrive at a constant Poisson intensity  $\lambda > 0$  over the campaign, giving  $\lambda\tau$  expected bidders. Neglecting zero probability events where multiple bidders arrive at an identical instant  $t \in [0, \tau]$ , we uniquely associate each bidder with his arrival date  $t$ .

On arrival, bidder  $t$  perceives project characteristics  $\tau, g_0, p, \lambda$ , his arrival time  $t$ , his inspection cost  $c_t$  and the current gap  $g_t$  between the threshold  $g_0$  and the number of bids  $B_t$  collected by  $t$ . We focus on  $g_t \equiv g_0 - B_t$  instead of working with the equivalent bid count  $B_t$ , so the project's publicly observable state at  $t$  is  $(t, g_t)$ . The gap  $g_t$  evolves over time as a function of bidder arrivals and choices.

On arrival,  $t$  does not know his private valuation  $v_t$  of the product but can learn it immediately if he pays  $c_t$ .  $c_t$  represents  $t$ 's cost of inspecting the proposed product and introspecting as motivated above. Bidders always know the common and fully independent distributions of these valuations and costs. For each  $t$ ,  $v_t \in \{0, v\}$  with probability  $q \in (0, 1)$  on  $v$  and  $c_t$  has cumulative distribution function CDF,  $F(\cdot)$ .<sup>8</sup> To simplify the exposition, we assume that  $F(\cdot)$  is continuously differentiable, generalizing later.

Until design Section 6, we analyse dynamics within the bidding phase given exogenous project variables,  $\tau, g_0, p, \lambda$ . We set  $p = v - 1$ , normalizing the price discount  $d \triangleq v - p$  to unity. So, gross of  $c_t$ ,  $t$ 's expected net benefit from buying after learning  $v_t = v$  is  $qd = q$ . This justifies restricting the support of  $c_t$  to  $[0, q]$ : (a) negative costs, as from curiosity, enjoyment or caring for the entrepreneur, are equivalent to a zero cost, since we assume bidders inspect when indifferent; (b) a bidder with cost strictly above  $q$  is equivalent to

---

<sup>8</sup>A non-zero low valuation strictly below  $p$  leads to identical outcomes.

a non-arrival, so any support above  $q$  is equivalent to reducing arrival rate  $\lambda$ .

Bidders are risk neutral. Each  $t$  gets 0 by not bidding,  $v_t - p$  by bidding  $p$  if the project succeeds (event  $\mathcal{S}$ ) and 0 by bidding on a project that fails. So bidding without inspecting gives him an expected payoff conditional on  $\mathcal{S}$  of  $qv - p$  and 0 if  $\mathcal{F}$ ; there is no resale. We assume  $p > qv$  to focus on the plausible case where bidders never blindly bid without inspecting to check that they value the good. As  $p = v - 1$ , this is equivalent to

**Assumption 1** (*No blind bidding, NBB*).  $q < 1 - 1/v$ .

Move orders are exogenously determined by arrival dates  $t$ . Each bidder takes all his decisions in a single episode of negligible duration so that moves are sequential (see [Section 7](#)). On arrival, a bidder either: **(A)** Avoids the project and **A**voids bidding, **(B)** **B**lind bids in that he bids without inspecting to see  $v_t$ , **(C)** or **C**hecks out the project by paying  $c_t$  and bids if he learns that  $v_t = v$ . Inspecting and always bidding or inspecting and only bidding when  $v_t = 0$  are strictly dominated.<sup>9</sup> So is **B** under [Assumption 1](#), so we need only consider **A** and **C**.

**In sum**, bidders arrive sequentially at Poisson arrival times  $t$ ; each bidder  $t$  observes  $\tau, \lambda, q, F(\cdot)$  and  $c_t$  and state  $(t, g_t)$  on arrival and chooses between substrategies **A** and **C**. The currently superfluous notation  $B_t$  and  $v, p, d$  reappear in the design analysis.

**Equilibrium concept.** We solve for undominated Perfect Bayesian Equilibria, abbreviated to PBE. Undominated refers to the fact that we restrict to weakly undominated strategies. For concreteness, we tie-break in favour of **C** among equilibria that generate identical payoff distributions. Thanks to the sequentiality of moves, this leads to a unique PBE. So there is no strategic uncertainty, but uncertainty in arrivals, inspection costs and valuations generate the shocks to aggregate demand and success prospects  $S$  that are central to our study. Valuation uncertainty provides the motive for costly inspection. Inspection cost uncertainty enriches the dynamics and is crucial for a positive slope. Arrival uncertainty is needed for finite aggregates with continuous time.

### 3 Analysis

To solve for bidding equilibria given a campaign  $g_0, \tau, p = v - 1$  with parameters  $\lambda, q, F(\cdot)$ , we study the incentives of a bidder  $t$  after he observes his inspection cost  $c_t$  and campaign

---

<sup>9</sup>Even if  $c_t \leq 0$ , inspecting and not bidding is strictly dominated if success can ever occur.

state  $(t, g)$ , indicating that  $g_t = g$ . State  $(t, g)$  matters to bidders purely via its impact on the project's success prospects and bidders only affect each other via this success rate.<sup>10</sup> Using  $t_+$  to indicate infinitesimally after  $t$ , that subgame starts at  $(t_+, g)$  if he does not bid and at  $(t_+, g - 1)$  if he does bid. We denote the evolving, state-contingent success probability by

$$S_{(t,g)} \triangleq \mathbb{P}(\mathcal{S}|(t, g)) \equiv \mathbb{E}_{(t,g)} \left( \mathbb{1}_{g_{\tau_+} \leq 0} \right), \quad (1)$$

where  $\mathbb{E}_{(t,g)}(\cdot) \triangleq \mathbb{E}(\cdot|(t, g))$ . This conditions on knowing  $g_t = g$  but not on whether a bidder arrives at  $t$ . If there *is* a bidder at  $t$ , the success probability rises to  $S_{(t,g-1)}$  if he bids and stays at  $S_{(t,g)}$  if not.<sup>11</sup> In choosing what to do, he only cares about success prospects if he bids. We denote this bid-contingent success probability by

$$S_{(t,g)}^{\text{bid}} \triangleq S_{(t,g-1)}. \quad (2)$$

The *pivotality* of a bidder arriving at  $t$  is  $\Delta S_{(t,g_t)}$  where difference operator  $\Delta$  denotes the impact of a unit reduction in  $g$ ;  $\Delta Y_{(t,g)} \triangleq Y_{(t,g-1)} - Y_{(t,g)}$  for a generic function  $Y$ . So

$$S_{(t,g)}^{\text{bid}} \equiv S_{(t,g)} + \Delta S_{(t,g)}. \quad (3)$$

This decomposition is helpful because  $S_{(t,g_t)}$  is a martingale: by the Law of Iterated Expectations,  $\mathbb{E}_{(t,g)} \left( \mathbb{E}_{(x,g_x)} \left( \mathbb{1}_{g_{\tau_+} \leq 0} \right) \right) = \mathbb{E}_{(t,g)} \left( \mathbb{1}_{g_{\tau_+} \leq 0} \right)$  for any  $x \in [t, \tau]$ , so, by Eq. (1),

$$\mathbb{E}_{(t,g)}(S_{(x,g_x)}) = S_{(t,g)}. \quad (4)$$

Section 3.3 will prove that pivotality  $\Delta S_{(t,g_t)}$  is a supermartingale which drives towards decreasing bidding profiles. First, we show how  $S_{(t,g_t)}^{\text{bid}}$  determines bidder  $t$ 's choice.

Bidder  $t$ 's simplest option is to choose to **A**void the project entirely by doing nothing, **A**. Not inspecting and not bidding always gives the same payoff,  $u_t^{\mathbf{A}} = 0$ . So for any  $(t, g)$ ,  $t$ 's expected utility from **A** is  $U_{(t,g)}^{\mathbf{A}} = 0$ .

Bidding is the only weakly undominated action of a bidder  $t$  who learns that  $v_t = v$ . Conversely, not bidding is his only undominated action if he knows  $v_t = 0$ . So the only relevant substrategy involving inspection is **C**: **C**heck by paying  $c_t$  and bid if and only if

<sup>10</sup>By type independence, bidders infer nothing about their own or future bidder valuations and costs. Bidder  $t$  takes the strategies of later bidders as given by the PBE; they cannot detect deviations.

<sup>11</sup>We can write  $t$  instead of  $t_+$  because  $S_{(t,g)}$  is continuous in  $t$  for any gap  $g$ .

the inspection reveals that  $v_t = v$ . This yields ex post payoff and expected utility

$$\begin{aligned} u_t^{\mathbf{C}} &= \mathbb{1}_{g_{\tau_+} \leq 0} (v_t - (v - 1))^+ - c_t, \\ U_{(t,g)}^{\mathbf{C}} &= qS_{(t,g)}^{\text{bid}} - c_t. \end{aligned} \quad (5)$$

In sum, a generic bidder's strategy is a mapping from each possible observed history or time, gap and cost trio to this duo of relevant choices,  $a : (t, g, c) \mapsto \{\mathbf{A}, \mathbf{C}\}$ . PBE require Bayes rational beliefs and choice  $a$  to be a best response at every possible information set  $(t, g, c)$ .<sup>12</sup> Bayes rationality requires every bidder to hold the correct state-contingent probability assessment  $S^{\text{bid}}$  of success given he bids, as derived below.

Eq. (5) shows that  $\mathbf{C}$  is chosen whenever  $c_t \leq qS_{(t,g)}^{\text{bid}}$ . This has probability  $F(qS_{(t,g)}^{\text{bid}})$ . Since bidders arrive with Poisson intensity  $\lambda$  and  $\mathbf{C}$  results in a bid with probability  $q$ , this generates non-homogenous Poisson bidding intensity

$$\beta_{(t,g)} \triangleq \lambda q F(qS_{(t,g)}^{\text{bid}}). \quad (6)$$

Arrival rate  $\lambda$  and taste parameter  $q$  are fixed, so the systematic variations in  $S_{(t,g)}^{\text{bid}}$  and resulting inspection rate  $F(qS_{(t,g)}^{\text{bid}})$  fully determine the temporal pattern of bidding. We now analyse these co-moving variables.

### 3.1 The co-evolution of success probabilities and bids

We characterize success rates by studying how bid-conditional success rates  $S_{(t,g)}^{\text{bid}} \equiv S_{(t,g-1)}$  and bidding intensity  $\beta_{(t,g)}$  interact. By the definition of a success,  $S_{(\tau,g)} = 1$  for  $g \leq 0$ . As  $g$  can only decrease over time,  $S_{(t,g)} = 1$  for  $g \leq 0$  and any  $t \leq \tau$ . From this initial condition, we solve for higher gaps via a recursive step grounded in two facts. First, by Eqs. (2) and (6), the bidding rate  $\beta_{(t,g)}$  at gap  $g$  depends on  $S_{(t,g)}^{\text{bid}}$ , the success rate at gap  $g - 1$ . Second, any successful path from  $(t, g)$  with  $g \geq 1$  must have its next bid's stopping time  $T \in (t, \tau]$ .<sup>13</sup>  $T$ 's density equals bidding intensity  $\beta_{(T,g)}$  at  $(T, g)$  times the probability  $n_T^{(t,g)}$  of no bid on interval  $(t, T)$ ,

$$n_T^{(t,g)} \triangleq \exp\left(-\int_t^T \beta_{(x,g)} dx\right). \quad (7)$$

<sup>12</sup>All sets are reached with positive probability except in trivial cases where success is impossible.

<sup>13</sup> $g_T = g$ ,  $g_{T_+} = g - 1$  and distinguishing by bid number,  $T = T_{1+g_0-g}$ .

The success rate from  $(T, g - 1)$  is  $S_{(T, g-1)}$ . So, taking expectations over  $T$  given  $(t, g)$ ,

$$S_{(t, g)} = \int_t^\tau n_T^{(t, g)} \beta_{(T, g)} S_{(T, g-1)} dT. \quad (8)$$

This recursion yields a unique solution for  $S_{(t, g)}$  given a unique solution for  $S_{(t, g-1)}$ . As the solution is unique at unity for  $g \leq 0$ , with Eq. (6), this proves:

**Proposition 1.** *The crowdfunding game has a unique PBE characterized by  $a_{(t, g, c)} = \mathbf{C}$  if and only if  $c \leq \hat{c}_{(t, g)} \triangleq qS_{(t, g)}^{\text{bid}} \equiv qS_{(t, g-1)}$ , generating bid intensity  $\beta_{(t, g)}$ , where*

$$\beta_{(t, g)} = \lambda q F \left( qS_{(t, g)}^{\text{bid}} \right) \equiv \lambda q F \left( qS_{(t, g-1)} \right), \quad (9)$$

$$S_{(t, g)} = 1 \text{ for } g \leq 0, \quad (10)$$

$$S_{(t, g)} = \int_t^\tau \exp \left( - \int_t^T \beta_{(x, g)} dx \right) \beta_{(T, g)} S_{(T, g-1)} dT \text{ for } g \geq 1. \quad (\text{REC-S})$$

Success rates affect bidding which in turn affects success. Notice that choices and outcomes only depend on current states and beliefs about future bidding, so  $S_{(t, g)}(\tau)$  is invariant to  $g_0$  and to changes in  $t$  and  $\tau$  that fix  $\tau - t$ :  $S_{(t, g)}(\tau) \equiv S_{(0, g)}(\tau - t)$  where  $\tau - t$  is time remaining. We now probe further using martingales, pivotality and shocks.

### 3.2 Basic dynamic properties of the success rate

The success rate  $S_{(t, g_t)}$  is a martingale by Eq. (4). This fact implies a differential equation linking success dynamics to bid rates and pivotality. We use it to prove that pivotality is positive while time's direct effect on success is negative.

At any instant, there are essentially two possibilities: either a new bid is collected so that the gap drops one unit from  $g_t = g$  to  $g_{t+} = g - 1$ , or the gap stays fixed. Formally, over the infinitesimal interval  $[t, t + dt)$ , one bid arrives with probability  $\beta_{(t, g_t)} dt$  and otherwise no bid is collected. Since  $S_{(t, g_t)}$  is a martingale,  $S_{(t, g)} = (1 - \beta_{(t, g)} dt) S_{(t+dt, g)} + \beta_{(t, g)} dt S_{(t+dt, g-1)}$ . This yields an ordinary differential equation (ODE) for  $S$ ,

$$\dot{S}_{(t, g)} \triangleq \frac{\partial S_{(t, g)}}{\partial t} = -\beta_{(t, g)} \left( S_{(t, g-1)} - S_{(t, g)} \right). \quad (\text{ODE-S})$$

That is, the partial time derivative  $\dot{S}_{(t, g)} \equiv -\beta_{(t, g)} \Delta S_{(t, g)}$ .<sup>14</sup> Jump term  $\Delta S_{(t, g)}$  is the

<sup>14</sup>This also follows by differentiating Eq. (REC-S). Conversely, Online Appendix B derives Eq. (REC-S) from Eq. (ODE-S) using  $n_T$  of Eq. (7) as integrating factor.

*pivotality* of a bid at  $t$ . Eq. (ODE- $S$ ) shows how pivotality weighted by bid intensity exactly counterbalances the effect of time passing. We can readily sign both terms:

**Lemma 1** (Success rate properties). (i)  $\Delta S_{(t,g)}, \Delta S_{(t,g)}^{\text{bid}} \geq 0$ , (ii)  $\dot{S}_{(t,g)}, \dot{S}_{(t,g)}^{\text{bid}} \leq 0$ .

The proof in Appendix A uses induction on  $g$  but both results are highly intuitive. Pivotality is never negative: each new bid is good news for success, weakly raising  $S$  by reducing the remaining funding gap. Conversely, no news is bad news: time passing with no new bids lowers  $S$  by leaving less time to cover the current gap by deadline  $\tau$ . Together with Eq. (6), Lemma 1 proves that higher gaps lower success and bidding rates:

**Corollary 1.** For any  $t$ ,  $S_{(t,g)}$ ,  $S_{(t,g)}^{\text{bid}}$  and  $\beta_{(t,g)}$  are all weakly decreasing in the gap  $g$ .

Lemma 1(i) shows that  $S_{(t,g)}^{\text{bid}}$  falls with  $t$  for a fixed gap  $g$  but the gap  $g_t$  falls over time and each drop pushes  $S_{(t,g_t)}^{\text{bid}}$  upwards by Lemma 1(ii). Next, Section 3.3 shows that the first effect dominates, creating a negative average effect of time on  $S_{(t,g_t)}^{\text{bid}}$  and pivotality. Section 3.4 derives PE, the effect of this pivotality trend on bidding. Section 3.5 derives NE, the news effect from variance in  $S_{(t,g_t)}^{\text{bid}}$ . Pivotality plus news effects determine bid dynamics from a given state. Section 3.6 computes  $g_t$  distributions and the slope of the bidding profile averaged across campaigns.

### 3.3 Decreasing pivotality (DP)

Given that  $S_{(t,g_t)}$  is a martingale, any systematic effect of time on  $S_{(t,g_t)}^{\text{bid}}$  must come from the pivotality term  $\Delta S_{(t,g_t)}$ . A two step logic proves that expected pivotality decreases over time. First, a bid at  $t$  strategically complements inspection and bidding by all *subsequent* bidders. Second, a later bidder has fewer such followers to influence. Each follower is influenced positively, so higher  $t$  implies a weaker average impact on success. That is, lower pivotality.

Formally, the change in pivotality at future date  $x$  expected from initial state  $(t, g)$ ,

$$\mathcal{D}_x^{(t,g)} \triangleq \mathbb{E}_{(t,g)}(\Delta S_{(x,g_x)}) - \Delta S_{(t,g)}, \quad (11)$$

is always negative or zero. We prove this by showing that  $\Delta S_{(t,g_t)}$  is a supermartingale. The infinitesimal generator for studying expected rates of change of a generic stochastic

process  $Y_{(t,g_t)}$  is  $\mathcal{L}_{(t,g)}^Y \triangleq \lim_{dt \downarrow 0} \left( \frac{1}{dt} \left( \mathbb{E}_{(t,g)} \left( Y_{(t+dt,g_t+dt)} \right) - Y_{(t,g)} \right) \right)$ . In the case of pivotality,

$$\mathcal{D}_{(t,g)} \triangleq \lim_{dt \downarrow 0} \left( \frac{1}{dt} \left( \mathcal{D}_{t+dt}^{(t,g)} \right) \right) \equiv \mathcal{L}_{(t,g)}^{\Delta S}. \quad (12)$$

The key result on generators from Itô's formula (mathematical details in [Online Appendix B](#)),

$$\mathcal{L}_{(t,g)}^Y = \dot{Y}_{(t,g)} + \beta_{(t,g)} \Delta Y_{(t,g)}, \quad (\text{GEN})$$

is very intuitive:  $\dot{Y}_{(t,g)}$  captures time's direct effect while  $\Delta Y_{(t,g)}$  weighted by the bidding intensity  $\beta_{(t,g)}$  captures time's expected impact via negative unit jumps in the gap  $g_t$ .

[Online Appendix B](#) also shows (via Dynkin's theorem) that  $Y_{(t,g_t)}$  is a martingale if and only if its generator is identically zero, i.e.,  $\mathcal{L}_{(t,g)}^Y \equiv 0, \forall t, g$ . Similarly, supermartingales and submartingales respectively correspond to everywhere weak negativity and positivity of  $\mathcal{L}_{(t,g)}^Y$ . Note that  $\mathcal{L}_{(t,g_t)}^S = 0$  as  $S_{(t,g_t)}$  is a martingale, so [\(GEN\)](#) immediately reconfirms [Eq. \(ODE-S\)](#). We now apply [\(GEN\)](#) to pivotality  $\Delta S_{(t,g_t)}$  to prove that  $\mathcal{D}_{(t,g)} \leq 0$ .

**Proposition 2** (Decreasing pivotality).  $\Delta S_{(t,g_t)}$  and  $S_{(t,g_t)}^{\text{bid}}$  are supermartingales.

**Proof.** As  $S_{(t,g_t)}$  is a martingale, [Eq. \(3\)](#) implies  $\mathcal{L}_{(t,g)}^{\Delta S} = \mathcal{L}_{(t,g)}^{S^{\text{bid}}}$ . By [\(ODE-S\)|<sub>g-1</sub>](#),  $\dot{S}_{(t,g-1)} = -\beta_{(t,g-1)} \Delta S_{(t,g)}^{\text{bid}}$ . So applying [\(GEN\)](#) to  $S_{(t,g_t)}^{\text{bid}}$ ,

$$\mathcal{D}_{(t,g)} = \mathcal{L}_{(t,g)}^{\Delta S} = \mathcal{L}_{(t,g)}^{S^{\text{bid}}} = \dot{S}_{(t,g-1)} + \beta_{(t,g)} \Delta S_{(t,g)}^{\text{bid}} = -\Delta \beta_{(t,g)} \Delta S_{(t,g)}^{\text{bid}} \leq 0. \quad \blacksquare \quad (13)$$

The formula  $\mathcal{D}_{(t,g)} = -\Delta \beta_{(t,g)} \Delta S_{(t,g)}^{\text{bid}}$  neatly captures the insight that a later bidder has fewer successor bidders to encourage with his bid.  $\Delta \beta_{(t,g)}$  is the encouragement effect on imminent followers and  $\Delta S_{(t,g)}^{\text{bid}}$  is the success impact of an induced bid.

[Appendix C.1](#) illustrates the stochastic variation behind this pivotality trend. Maximal pivotality sometimes obtains in the last moments of a campaign but DP remains true since low and minimal pivotality are more common near the deadline: pivotality hits zero whenever the threshold is reached before the deadline and it also tends to zero whenever the gap is above two with the approaching deadline making failure near certain. DP, quantified by [Eq. \(13\)](#), creates the first dynamic force, the PE explained next. Then we show how these stochastics generate the second dynamic force, the NE.

### 3.4 The pivotality effect (PE)

From Eq. (6) and the fact that  $F$  is an increasing function, decreasing pivotality implies a tendency for bidding to fall.  $S_{(t,g_t)}$  is a martingale so  $S_{(t,g_t)}^{\text{bid}}$  falls at the same rate as pivotality  $\Delta S_{(t,g_t)}$  in expectation. The expected fall in  $S_{(t,g_t)}^{\text{bid}}$  over  $(t, x)$  changes an arrival at  $x$ 's inspection rate by the *pivotality effect*

$$\mathcal{E}_x^{(t,g)} \triangleq F\left(\mathbb{E}_{(t,g)}\left(qS_{(x,g_x)}^{\text{bid}}\right)\right) - F\left(qS_{(t,g)}^{\text{bid}}\right). \quad (14)$$

The effect on the bidding rate is  $\lambda q$  times  $\mathcal{E}_x^{(t,g)}$ . For any gap  $g$ ,  $\mathcal{E}_x^{(t,g)} \leq 0$  if  $t \leq x$  because  $\mathbb{E}_{(t,g)}\left(qS_{(x,g_x)}^{\text{bid}}\right) \equiv q\left(S_{(t,g)}^{\text{bid}} + \mathcal{D}_x^{(t,g)}\right)$ ,  $\mathcal{D}_x^{(t,g)} \leq 0$  from Eq. (13) and  $F$  is increasing. If  $F$  is differentiable,  $\mathcal{D}_{t+dt}^{(t,g)} = \mathcal{D}_{(t,g)} dt + O(dt^2)$  and the rate of change PE is

$$\mathcal{E}_{(t,g)} \triangleq \lim_{dt \downarrow 0} \left(\frac{1}{dt} \left(\mathcal{E}_{t+dt}^{(t,g)}\right)\right) = qF_c(qS_{(t,g)}^{\text{bid}})\mathcal{D}_{(t,g)}. \quad (15)$$

### 3.5 Expected bid dynamics and the news effect (NE)

We apply (GEN) to the stochastic process  $\beta_{(t,g_t)}$  to reveal expected changes in the bid rate from a generic state  $(t, g)$ . Bidding  $\beta_{(t,g)}$  is proportional to  $F\left(qS_{(t,g)}^{\text{bid}}\right)$ . Like  $S_{(t,g_t)}^{\text{bid}}$ ,  $\beta_{(t,g_t)}$  falls gradually as time passes without bids and jumps up whenever a bid occurs; time's direct negative effect is  $\dot{\beta}_{(t,g)} < 0$  and its indirect positive effect *per bid* is  $\Delta\beta_{(t,g)} \equiv \beta_{(t,g-1)} - \beta_{(t,g)}$ . In contrast with  $S_{(t,g_t)}^{\text{bid}}$  and  $\Delta S_{(t,g_t)}$ , for bidding  $\beta_{(t,g_t)}$ , time's direct negative effect does not always dominate its positive effect via expected gap reductions. The average effect depends on uncertainty and the cost distribution as we explain now.

Over an infinitesimal time interval, either one bid arrives or none do (Fig. 1 adds details below). A bid arrival is good news, raising  $S^{\text{bid}}$ , while no bid is bad news, lowering  $S^{\text{bid}}$ . The good news outweighs the bad news if an arrival is more likely inspect at  $(t + \epsilon, g_{t+\epsilon})$  than when facing the  $(t, g)$  expectation of  $qS^{\text{bid}}$  at  $t + \epsilon$ . This occurs if the density of inspection costs just above  $qS_{(t,g)}^{\text{bid}}$  is greater than the density just below it. Increasing density is equivalent to CDF convexity. In economic terms, there are increasing returns to good news: the bidders with higher inspection costs who become willing to inspect after good news outweigh those with lower inspection costs who cease to inspect after bad news. In the opposite case where  $F$  is concave, the returns are decreasing. Formally, we define the *news effect* as the impact of uncertainty in state  $(t, g)$  about

bidding over interval  $(t, x)$  on the probability that a bidder arriving at  $x$  would inspect,

$$\mathcal{N}_x^{(t,g)} \triangleq \mathbb{E}_{(t,g)} \left( F \left( qS_{(x,g_x)}^{\text{bid}} \right) \right) - F \left( \mathbb{E}_{(t,g)} \left( qS_{(x,g_x)}^{\text{bid}} \right) \right). \quad (16)$$

By Jensen's inequality, this is positive if  $F$  is convex, negative if concave and zero if affine.

[Appendix A's proof of Proposition 4](#) proves that the rate of change of the NE is

$$\mathcal{N}_{(t,g)} \triangleq \lim_{dt \downarrow 0} \left( \frac{1}{dt} \left( \mathcal{N}_{t+dt}^{(t,g)} \right) \right) = \beta_{(t,g)} \left( \Delta F(qS_{(t,g)}^{\text{bid}}) - q\Delta S_{(t,g)}^{\text{bid}} F_c(qS_{(t,g)}^{\text{bid}}) \right). \quad (17)$$

It is immediate that this NE rate is positive for convex  $F$  since the graph of a convex function lies above its tangent. Similarly, it is negative if  $F$  is concave.

Time's overall average impact sums the pivotality and news effects: by [Eq. \(6\)](#),

$$\mathbb{E}_{(t,g)} \left( \beta_{(x,g_x)} \right) - \beta_{(t,g)} \equiv \lambda q \left( \mathcal{N}_x^{(t,g)} + \mathcal{E}_x^{(t,g)} \right), \quad (18)$$

$$\text{and if } F \text{ is continuous, } \quad \mathcal{L}_{(t,g)}^\beta \equiv \lambda q \left( \mathcal{N}_{(t,g)} + \mathcal{E}_{(t,g)} \right). \quad (19)$$

Since PE  $\mathcal{E}_x^{(t,g)}$  is always weakly negative, bidding is expected to fall if the NE  $\mathcal{N}_x^{(t,g)}$  is small, neutral (as for affine  $F$ ), or negative (as for concave  $F$ ). In the last case, the NE and PE push downwards together and [Eq. \(18\)](#) implies:

**Proposition 3.** *A flat or decreasing inspection cost density on  $[0, q]$  (weakly concave  $F$ ) generates expected bid rates that fall from any state  $(t, g)$ :  $\forall x > t, \mathbb{E}_{(t,g)} \left( \beta_{(x,g_x)} \right) \leq \beta_{(t,g)}$ .*

In the uniform case with  $F_c \equiv 1/q$  on cost range  $[0, q]$ , generalized in [Section 4.1](#), as  $F$  is linear,  $\beta$  and  $S^{\text{bid}}$  are exactly proportional and  $\mathbb{E}_{(t,g)} \left( \beta_{(x,g_x)} \right) - \beta_{(t,g)} = \lambda q \mathcal{E}_x^{(t,g)} \leq 0$ . The NE is then null and  $\mathcal{L}_{(t,g)}^\beta = \lambda q \mathcal{E}_{(t,g)} = \lambda q \mathcal{D}_{(t,g)} \leq 0$ .

When instead  $F$  is convex, the positive NE from increasing returns to good news counteracts the PE and potentially causes the expected bid rate to rise. [Fig. 1](#) illustrates. Over the infinitesimal delay  $\epsilon$ , a bid arrives with probability  $\epsilon\beta_{(t,g)}$  leading to  $\tilde{g}_{t+\epsilon} = g - 1$  so  $S_{(t,g)}^{\text{bid}}$  jumps up to  $S_{(t+\epsilon, g-1)}^{\text{bid}}$ . Otherwise, no bid arrives (probability  $1 - \epsilon\beta_{(t,g)}$ ) and the bid-contingent success rate  $S_{(t,g)}^{\text{bid}}$  moves down to  $S_{(t+\epsilon, g)}^{\text{bid}}$ .

The average change in  $S_{(t,g)}^{\text{bid}}$  is negative since  $\mathcal{D}_{t+\epsilon}^{(t,g)} = \mathbb{E}_{(t,g)} S_{(t+\epsilon, \tilde{g}_{t+\epsilon})}^{\text{bid}} \leq S_{(t,g)}^{\text{bid}} \leq 0$ . The DP arrow indicates this negative trend. This DP reduces the expected incentive to inspect at  $t + \epsilon$  by  $-q\mathcal{D}_{t+\epsilon}^{(t,g)}$ . Green arrow PE shows its negative effect on expected inspections.

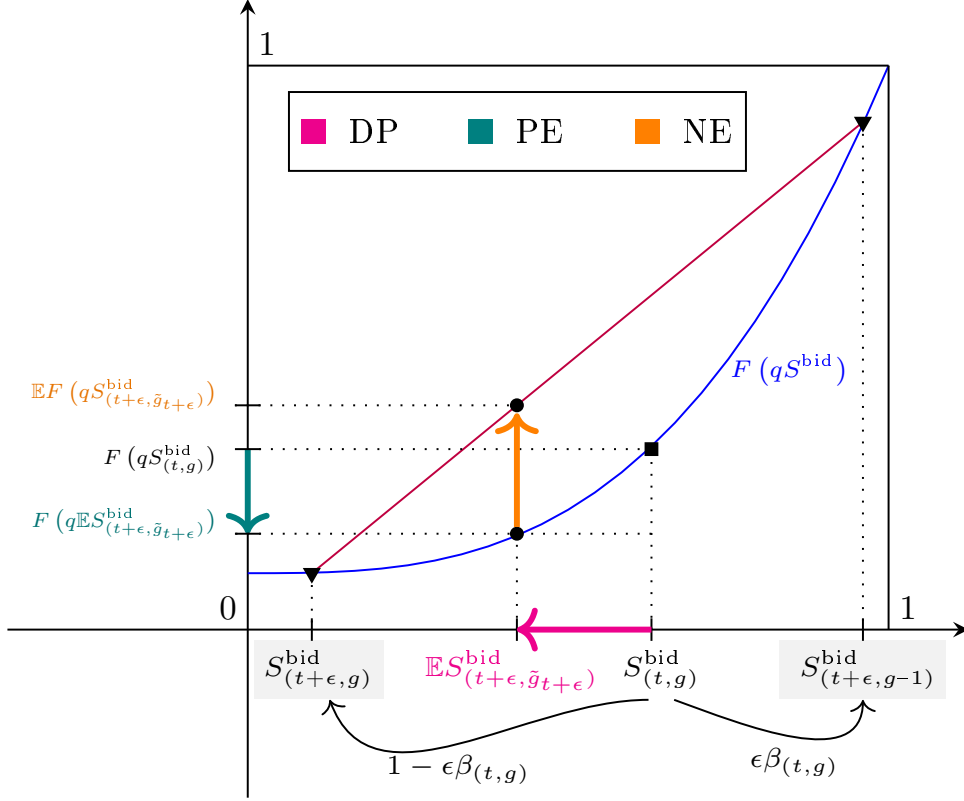


Figure 1: Decreasing pivotality DP, its effect PE and the news effect NE for convex  $F$ .\*

\*  $\mathbb{E}$  is shorthand for  $\mathbb{E}_{(t, g)}$ , expectations given  $(t, g)$ . Curved arrows indicate state-transition probabilities.

As the density of marginal bidders is  $F_c$ , the size of the PE effect is approximately

$$-\mathcal{E}_{t+\epsilon}^{(t, g)} \approx -qF_c(S_{(t, g)}^{\text{bid}}) \mathcal{D}_{t+\epsilon}^{(t, g)}.$$

Finally, the orange NE arrow indicates the impact of the variance in  $S_{(x, g_x)}^{\text{bid}}$  at  $x = t + \epsilon$ ,

$$\mathcal{N}_{t+\epsilon}^{(t, g)} = \mathbb{E}_{(t, g)} \left( F(qS_{(t+\epsilon, \tilde{g}_{t+\epsilon})}^{\text{bid}}) \right) - F \left( \mathbb{E}_{(t, g)} \left( qS_{(t+\epsilon, g_{t+\epsilon})}^{\text{bid}} \right) \right).$$

In Fig. 1,  $F$  is sufficiently convex for the NE to dominate the PE (the NE arrow exceeds the PE arrow). The generator  $\mathcal{L}_{(t, g)}^\beta$  of  $\beta_{(t, g_t)}$  provides a precise *sufficient* condition. For affine and quadratic  $F$ , the [proof of Proposition 4](#) shows that

$$\mathcal{L}_{(t, g)}^\beta = \lambda q \left[ qF_c(qS_{(t, g)}^{\text{bid}}) \mathcal{L}_{(t, g)}^{S^{\text{bid}}} + \frac{q^2}{2} F_{cc}(qS_{(t, g)}^{\text{bid}}) \nu_{(t, g)}^{S^{\text{bid}}} \right], \quad (20)$$

where  $\nu_{(t, g)}^{S^{\text{bid}}} \triangleq \lim_{dt \downarrow 0} \left( \frac{1}{dt} \left( \mathbb{V}_{(t, g)} \left( dS_{(t, g_t)}^{\text{bid}} \right) \right) \right) = \beta_{(t, g)} \left( \Delta S_{(t, g)}^{\text{bid}} \right)^2$  is  $S_{(t, g_t)}^{\text{bid}}$ 's jump variance given  $g_t = g$ . As  $\mathcal{L}_{(t, g)}^{S^{\text{bid}}} = \mathcal{L}_{(t, g)}^{\Delta S}$ , the first term in Eq. (20) represents PE, the expected

impact of decreasing pivotality. The second term is NE, the news effect, driven by variance and convexity:  $\mathcal{N}_{(t,g)} = \frac{1}{2} \beta_{(t,g)} \left( q \Delta S_{(t,g)}^{\text{bid}} \right)^2 F_{cc}$ .

Beyond the quadratic case, we prove that  $\tilde{\mathcal{L}}_{(t,g)}^\beta \triangleq \text{RHS}(20)$  is a lower bound on the bid rate generator for a polynomial  $F$  with all nonlinear coefficients weakly positive, i.e. any  $F = \sum_{k \in \{0,1,\dots,\rho\}} \gamma_k c^k$  with  $\gamma_k \geq 0$  for  $k \neq 1$ . So,

**Proposition 4.** *Sufficient uncertainty and convexity guarantee a rising expected bid rate: for a polynomial  $F$  with non-negative coefficients on powers two and above,  $\mathcal{L}_{(t,g)}^\beta > 0$  if*

$$\frac{q}{2} F_{cc} \left( q S_{(t,g)}^{\text{bid}} \right) \nu_{(t,g)}^{S^{\text{bid}}} > F_c \left( q S_{(t,g)}^{\text{bid}} \right) \left| \mathcal{L}_{(t,g)}^{S^{\text{bid}}} \right|. \quad (21)$$

**Proof** in [Appendix A](#). When  $F$  is a power  $\rho$  function,  $\frac{cF_{cc}}{F_c} = \rho - 1$ . Then inequality (21) is also necessary so a positive slope at  $(t, g)$  is equivalent to

$$\frac{1}{2} \frac{\Delta S_{(t,g)}^{\text{bid}}}{S_{(t,g)}^{\text{bid}}} (\rho - 1) > \frac{\Delta \beta_{(t,g)}}{\beta_{(t,g)}}. \quad (22)$$

### 3.6 Average bidding and the state transition process

Determining average bidding at time  $t$  after the initial state  $(0, g_0)$  requires finding probability weights on the bid rate over possible gaps  $g_t$  at  $t$ . Denoting the transition probability from  $(t', g')$  to  $(t, g)$  by  $Q_{(t,g)}^{(t',g')}$  and letting  $Q_{(t,g)} \triangleq Q_{(t,g)}^{(0,g_0)}$ , the *average bid rate* is given by

$$A_t = \sum_{g=-\infty}^{g_0} Q_{(t,g)} \beta_{(t,g)}. \quad (23)$$

Its time derivative is  $\dot{A}_t \triangleq \frac{\partial}{\partial t}(A_t) \equiv \frac{d}{dt}(A_t)$  as  $A$  only depends on  $t$ . The bidding profile plots  $A_t$  against time. To characterize its slope, we solve recursively for transition matrices  $Q_{(t,g)}^{(t',g')}$  to find  $Q_{(t,g)}$ .

**Lemma 2.** *For any  $t \geq t'$ , the transition process is characterized by*

$$Q_{(t,g)}^{(t',g')} = 0 \text{ for all } g > g'; \quad Q_{(t,g)}^{(t',g')} = \exp \left( - \int_{t'}^t \beta_{(x,g)} dx \right), \quad (24)$$

$$Q_{(t,g)}^{(t',g')} = \int_{t'}^t \exp \left( - \int_{t'}^T \beta_{(x,g')} dx \right) \beta_{(T,g')} Q_{(t,g)}^{(T,g'-1)} dT, \text{ for } g \leq g' - 1. \quad (\text{REC-Q})$$

**Proof.** Clearly,  $Q_{(t,g)}^{(t',g')} = 0$  for all  $g > g'$  and any  $t \geq t'$ , since the gap cannot rise. For  $g = g'$ ,  $Q_{(t,g)}^{(t',g')}$  is the probability of no bid on  $(t', t)$ , giving the second equation in [Eq. \(24\)](#). Notice that  $Q_{(t,g)}^{(t',g')} \equiv n_t^{(t',g')}$  defined in [Eq. \(7\)](#). The recursive step parallels [Eq. \(REC-S\)](#):

for any  $g \leq g' - 1$ , conditioning on  $(t', g')$  and on the first stopping time  $T$  after  $(t', g')$  with density  $n_T^{(t', g')} \beta_{(T, g')}$ , the Law of Iterated Expectations yields Eq. (REC-Q). ■

Online Appendix B.3 adds an alternative derivation of (REC-Q) via the ODE for  $Q_{(t, g)}^{(t', g')}$  varying  $t'$ . It also derives the adjoint ODE (used in the final subsection) by varying  $t$ :

$$\dot{Q}_{(t, g)} = Q_{(t, g+1)} \beta_{(t, g+1)} - Q_{(t, g)} \beta_{(t, g)}. \quad (\text{ODE-Q})$$

Intuitively, the rate of change in the probability that gap  $g_t = g$  is the probability of reaching this gap via a bid from state  $(t_-, g+1)$  minus the probability that the gap falls below  $g$  via a bid in state  $(t_-, g)$ .

## Conditioning

Profiles conditioned on campaign success or failure restrict to paths ending with  $g_{\tau_+} \leq 0$  or  $g_{\tau_+} > 0$ , respectively. A path with a bid in state  $(t, g)$  ends in success with probability  $S_{(t, g-1)}$ . So conditioning on success rescales the probability weights by  $S_{(t, g-1)}/S_0$ . Similarly, conditioning on failure rescales by  $(1 - S_{(t, g-1)})/(1 - S_0)$ . This gives,

$$A_t^{\mathcal{S}} = \frac{1}{S_0} \sum_{g=-\infty}^{g_0} Q_{(t, g)} \beta_{(t, g)} S_{(t, g-1)}, \quad (25\text{-}\mathcal{S})$$

$$A_t^{\mathcal{F}} = \frac{1}{1 - S_0} \sum_{g=-\infty}^{g_0} Q_{(t, g)} \beta_{(t, g)} (1 - S_{(t, g-1)}). \quad (25\text{-}\mathcal{F})$$

Conditioning on success *selects* for paths with more bidding. This has a gap-selection effect: it places more weight on lower gaps where  $\beta_{(t, g)}$  is higher. At  $t = 0$ , the gap is always  $g_0$  so there is no scope for gap-selection. Success-conditioning then multiplies the bid rate by one plus relative pivotality:

$$A_0^{\mathcal{S}}/A_0 = \frac{\beta_{(0, g_0)} S_{(0, g_0)}^{\text{bid}}}{S_0} / \beta_{(0, g_0)} = 1 + \frac{\Delta S_{(0, g_0)}}{S_{(0, g_0)}}.$$

Gap-selection kicks in as the range of possible gaps expands over time. This pushes the conditional bid profiles towards fanning out over time relative to the unconditional profile as illustrated by Fig. 3(b). It also explains Fig. 2(b) relative to 2(c) and the conditionality of the U-shape on success.

### 3.7 The slope of the average bid profile

The slope of the bid profile can be expressed as a weighted average of  $\mathcal{L}_{(t,g)}^\beta$ .

**Lemma 3.** *The time gradients of (i) unconditional, (ii)  $\mathcal{S}$ -,  $\mathcal{F}$ -conditional average bid rates are*

$$\begin{aligned} \dot{A}_t &= \sum_{g=-\infty}^{g_0} Q_{(t,g)} \mathcal{L}_{(t,g)}^\beta, \\ \dot{A}_t^{\mathcal{S}} &= \frac{1}{S_0} \sum_{g=-\infty}^{g_0} Q_{(t,g)} \mathcal{L}_{(t,g)}^\beta S_{(t,g-1)}, \quad \dot{A}_t^{\mathcal{F}} = \frac{1}{1-S_0} \sum_{g=-\infty}^{g_0} Q_{(t,g)} \mathcal{L}_{(t,g)}^\beta (1-S_{(t,g-1)}). \end{aligned} \quad (26)$$

The proof in [Appendix A](#) uses [\(ODE-Q\)](#) to show that for any  $Y_{(t,g)}$ ,  $A_t^Y \triangleq \mathbb{E}_{(0,g_0)} Y_{(t,g_t)}$ ,

$$\dot{A}_t^Y \equiv D_t \left( \mathbb{E}_{(0,g_0)} Y_{(t,g_t)} \right) = D_t \left( \sum_{g=-\infty}^{g_0} Q_{(t,g)} Y_{(t,g)} \right) = \sum_{g=-\infty}^{g_0} Q_{(t,g)} \mathcal{L}_{(t,g)}^Y \equiv A_t^{\mathcal{L}^Y}. \quad (27)$$

Setting  $Y_{(t,g)} = \beta_{(t,g)}$  proves part (i). (ii) follows from the product rule and [Eq. \(ODE-S\)](#). This lemma implies that an everywhere positive  $\mathcal{L}_{(t,g)}^\beta$  is sufficient for a monotone increasing bid profile, and everywhere negative  $\mathcal{L}_{(t,g)}^\beta$  guarantees a decreasing profile.

**Corollary 2.** *If  $\mathcal{L}_{(t,g)}^\beta \geq 0$  for all  $(t,g)$ , the aggregate and conditional bid profiles are increasing over time. If instead  $\mathcal{L}_{(t,g)}^\beta \leq 0 \forall (t,g)$ , they are decreasing.*

Applying [Corollary 2](#) to [Propositions 3](#) and [4](#), delivers two results:

**Proposition 5.** *A weakly concave CDF  $F(c)$  generates a weakly decreasing average bid profile:  $\dot{A}_t \leq 0, \forall t$ . Strict concavity implies a strictly negative slope if  $g_0 \geq 2$ .*

The strict claim uses two facts:  $Q_{(t,g_0)} > 0$  for any  $t$  and if the cost distribution has full support, [Lemma 1](#) holds with strict inequalities for any  $g_0 \geq 2$ .

**Proposition 6.** *Imposing [Proposition 4](#)'s convexity and uncertainty conditions [\(21\)](#) at all  $g \geq 2$  guarantees a strictly increasing average bid profile,  $\dot{A}_t > 0, \forall t$ , if  $g_0 \geq 2$ .*

Both [Propositions 5](#) and [6](#) also hold for the conditional bid profiles. By contrast, conditioning does affect the sign of bid profile slopes when the sign of the infinitesimal generator varies across states. [Section 4.3](#) shows how this sheds light on the U-shape.

## 4 Canonical Distribution Classes

In this section, we apply our results to specific functional forms of the CDF  $F(c)$  of inspection costs, beginning with linear, quadratic and higher power distributions. Linear and general affine CDF's correspond to uniform distributions, precluding any news effect. The pivotality effect then perfectly explains the shape and negative slope of the bidding profile. Quadratic and power CDF's illustrate the impact of positive and negative NE's. Turning to single-peaked distributions, the NE is always negative if the modal cost is negative and always positive if the mode is above  $q$ . Combining these cases gives a bimodal distribution that generates a U-shaped bid profile.

When  $F$  contains atoms, it is neither concave nor convex. Atoms cause bid rate discontinuities on a zero measure set of critical dates where PE's are discrete. Our generator-based results hold at all other dates. NE's remain continuous and are positive in states corresponding to cost atoms. We characterize the case of homogeneous bidder inspection costs via campaign survival probabilities.

As justified in [Section 2](#), we restrict  $F(c)$ 's support to  $[0, q]$  by truncating a generic  $F$  to  $F/F(q)$  on  $0 < c \leq q$  while reducing the arrival rate to  $\lambda' = \lambda F(q)$  and then replacing negative values by a mass  $z = F(0)/F(q)$  atom at 0. This atom represents bidders who already know their taste for the entrepreneur's product *or* have negative (net) inspection costs, perhaps because they are fans, friends or contacts. Later comparative statics use the fact that first-order stochastic domination (FOSD) raises  $S$ .

**Lemma 4.** *If  $F(\cdot) \underset{FOSD}{\succeq} F'(\cdot)$  then  $S_{(t,g)}(F') \geq S_{(t,g)}(F)$  for all  $t, g$ .*

Intuitively, high costs dissuade inspection so they lower success rates. By corollary, proportionate probability shifts from positive costs to zero raise success rates. Also,

**Lemma 5.**  *$\lambda$  and  $q$  both increase  $S_{(t,g)}$  for all  $t, g$ .*

This intuitive result uses [Eq. \(9\)](#) within the inductive [Appendix A](#) proof of [Lemma 4](#).

### 4.1 Affine CDF

If inspection costs follow a uniform distribution with atom  $z$  at  $c = 0$ , the CDF is affine (linear if  $z = 0$ ):

$$F(c) = z + (1 - z) \left( \frac{c}{q} \right). \quad (28)$$

$F_{cc} \equiv 0$ , so the news effect is null. With decreasing pivotality as the only force, the bid profile has a negative slope. The bid rate generator for the quadratic CDF applies to the affine CDF. Setting  $F_c = \frac{1-z}{q}$  in (20) and recalling  $\mathcal{L}_{(t,g)}^{S^{\text{bid}}} = \mathcal{L}_{(t,g)}^{\Delta S}$ ,

$$\mathcal{L}_{(t,g)}^\beta = \lambda q(1-z)\mathcal{L}_{(t,g)}^{\Delta S} \leq 0, \quad (29)$$

so average bid slopes are decreasing. [Online Appendices C.2 and C.3.1](#) use this to compute average pivotality and bidding for distinct thresholds  $g_0$  (explicitly for  $g_0 = 2$ ). Empirical tests could combine the comparative static effects of changing  $g_0$  with [Section 6.1](#) predictions of how  $p$  and  $g_0$  vary as a function of the funding need  $G$ .

## 4.2 Quadratic CDF

A linear density with atom  $z \in [0, 1)$  at  $c = 0$  produces the quadratic CDF,

$$F(c) = z + (1-z) \left( \frac{c}{q} \right)^2. \quad (30)$$

[Proposition 4](#) applies to this convex polynomial so we expect a positive bidding slope given enough news. That is, sufficient variance in  $S^{\text{bid}}$  for the NE to dominate the PE. A sufficient mass  $z$  of the zero-cost types guarantees this by raising bidding enough to activate late-arriving higher cost bidders often enough.

**Proposition 7.** *Quadratic CDF (30) creates a strictly increasing profile for any  $z > 3/4$ .*

**Proof** in [Appendix A](#). The zero atom  $z$  has a non-monotonic effect on the slope. As  $z$  approaches 1, the bidding slope flattens since neither the PE nor NE affect zero-cost types. The slope is always positive at  $z < 1$  because the PE goes to zero faster than the NE (arrival and taste uncertainty maintain success rate variance,  $\nu_{(t,g)}^{S^{\text{bid}}}$ , while  $\mathcal{L}_{(t,g)}^{S^{\text{bid}}}$  is proportional to  $\Delta\beta_{(t,g)}$  which converges to zero as  $z$  tends to 1). [Online Appendix C.3.2](#) illustrates while [C.4](#) shows how higher power distributions generate steeper slopes.

## 4.3 A compelling bimodal distribution

Empirical studies of crowdfunding highlight two relevant classes of bidders. One consists of the entrepreneur’s fans, friends and family. These “close” bidders are often reasonably informed about the entrepreneur’s project in advance or more curious or feel obliged to

show an interest in it. As a result, their net inspection costs are mostly negative. They are well-represented by a single-peaked density with mode below 0. Normalizing onto the  $[0, q]$  cost range censors costs above  $q$  as non-arrivals and truncates negative costs into an atom of zero types who are irresponsive to the PE and NE. The normalized density of close bidders is monotonic decreasing on  $(0, q]$ . If all bidders were close, this fact would guarantee a negative NE and therefore a negative sloped bid profile.

The second class of standard or “distant” bidders have costs high enough to make most of them unwilling to inspect a given crowdfunding project. So their cost distribution is best captured by a single-peaked density with mode above  $q$ . That normalizes to give an increasing density or convex CDF on  $(0, q]$  and possible positive NE and bidding slope.

Fig. 2(a) illustrates the bimodal density from combining these two classes: the left peak represents the “close” bidders (the blue area creates an atom  $z$  at 0) and the right peak represents “distant” bidders, shown with a tight, low variance.<sup>15</sup> As the lower tail of distant bidders barely extends below  $q$ , the positive NE from distant bidders is only significant late in a campaign. In successful campaigns, this creates a late upward slope after an early downward slope from the negative NE and PE arising when close bidders dominate activity. This combination creates the U-shape shown in Fig. 2(b). On failing campaigns, the NE remains essentially dormant and always dominated by the PE, explaining Fig. 2(c). This conditionality of the U-shape on success concords with the evidence in Fig. 3(ii) of Crosetto and Regner (2018) and our Kickstarter data computations in Online Appendix F. Raising the success rate  $S_0$  places more weight on the U-shaped curve so that the unconditional average can also be U-shaped. See also Section 7 on final bidding spikes caused by bidders delaying.

#### 4.4 The homogenous case

Cost homogeneity implies a discontinuous CDF:  $F(c_t) = 1$  if  $c_t \geq c$  and 0 otherwise. Average pivotality still decreases continuously but this smooth DP now has discrete PE’s at a finite set of critical date and gap states where all bidders switch from inspecting to avoiding. The NE is either zero or dominated by the PE in this special case. As a result, the bid profile is a downward flight of steps. We provide a succinct characterization that is useful for optimizing design in the next section. See Online Appendix D for details.

<sup>15</sup>A full analysis would add valuation differences; e.g., zealous fans and close family always bid.

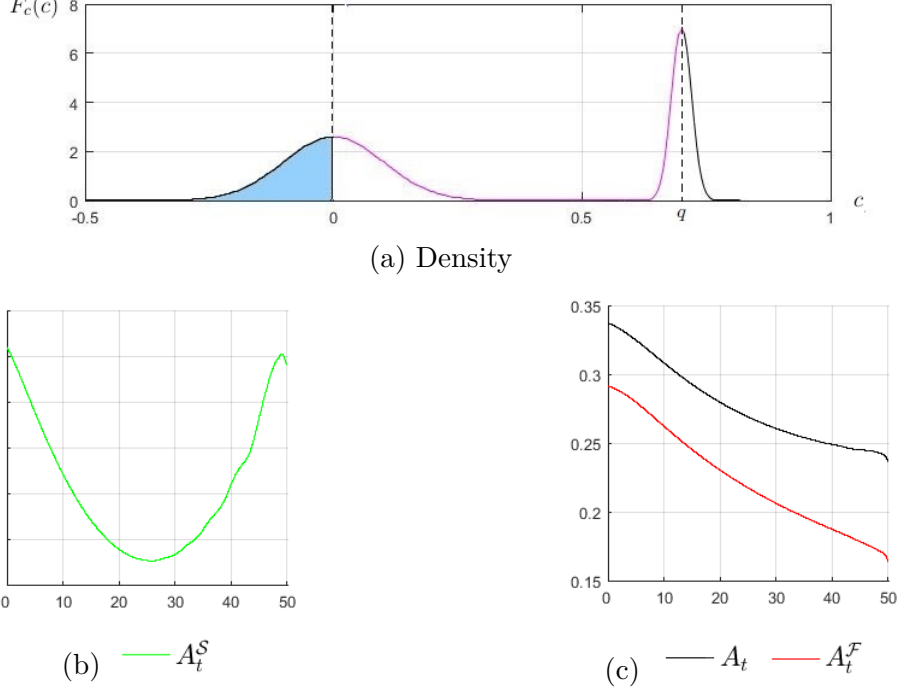


Figure 2: Bimodal density from two normal distributions, 0.65 on  $N(0, 0.1)$ , 0.35 on  $N(q, 0.02)$ ;  $g_0 = 20$ ,  $(\tau, \lambda, q) = (50, 0.7, 0.75)$ . Blue area in (a) truncates to atom  $z$  at 0.

We focus on a cost  $c \in (0, q)$  because the average bid profile is flat at zero for  $c \geq q$  and flat at  $\lambda q$  for  $c \leq 0$ . As bidders are identical, strategic complementarity implies that states  $(t, g)$  can be categorized as *active*, all bidders choose  $\mathbf{C}$  at  $(t, g)$ , or *frozen*, all choose  $\mathbf{A}$ . The frontier between frozen and active states is defined by the critical or maximal gaps for activity,  $\hat{\mathbf{g}} = (\hat{g}_t)_{t \in [0, \tau]}$  and associated critical dates  $\hat{t}_g$  or least durations  $\hat{\tau}_g \equiv \tau - \hat{t}_g$  sufficient for activity;  $\hat{g}_t \triangleq \sup \{g \in \mathbb{Z} : S_{(t, g)}^{\text{bid}} \geq \frac{c}{q}\}$ ; for  $g \geq 2$ ,  $S_{(\hat{t}_g, g)}^{\text{bid}} \equiv S_{(\tau - \hat{\tau}_g, g)}^{\text{bid}}(\tau) \equiv S_{(0, g)}^{\text{bid}}(\hat{\tau}_g) \equiv \frac{c}{q}$ . We call it the *wall of ice* since a campaign instantly freezes when its path crosses into the region with  $g_t > \hat{g}_t$ . Fig. 3(a) illustrates this wall in violet. The region above it is frozen and a campaign is active at  $t$  if its trajectory  $\mathbf{g} = (g_t)_{t \in [0, \tau]}$  has not crossed  $\hat{\mathbf{g}}$  before  $t$ . Setting  $\hat{g}_{\tau_+} \triangleq 0$ , success is equivalent to staying weakly below the wall until  $\tau_+$ . If  $g_0 > \hat{g}_0$ , equivalent to  $\tau < \hat{\tau}_{g_0}$  and  $\hat{t}_{g_0} < 0$ , the campaign is born frozen. So we focus on  $g_0 \leq \hat{g}_0$ . 3(a) also exhibits four possible paths: (1) and (2), in red, end up failing: they freeze on crossing the wall at  $t = 23.5$  and  $49.5$  where  $\hat{g}_{23.5} = 14$  and  $\hat{g}_{49.5} = 2$ ; (3) and (4), in green, successfully stay below the wall,  $g_t \leq \hat{g}_t$  for all  $t \leq \tau$  and  $g_{\tau_+} \leq \hat{g}_{\tau_+} \equiv 0$ .

3(b) shows discrete drops in average bidding precisely coinciding with the vertical steps of the wall in 3(a). 3(c) shows the smoothly decreasing pivotality. This DP generates

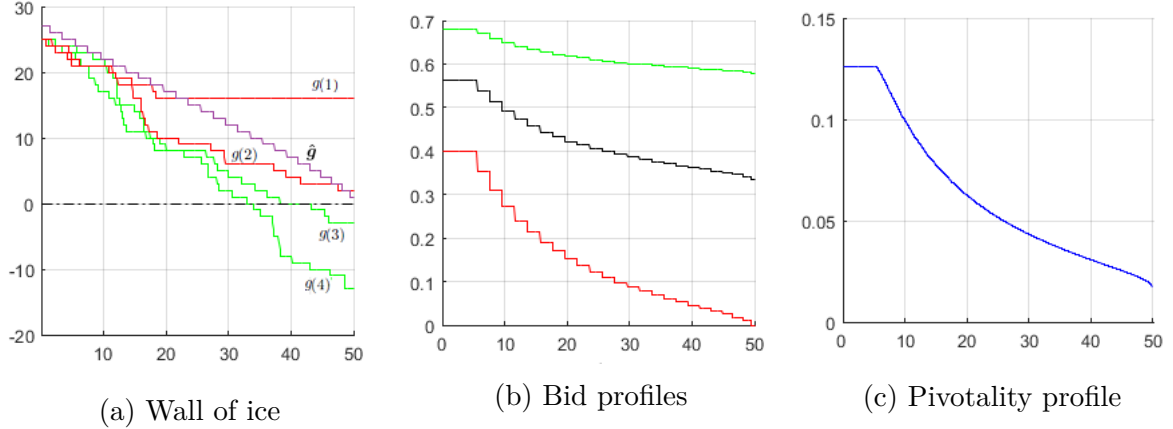


Figure 3: Wall of ice and simulated gap paths beside pivotality and average bid profiles for homogenous inspection cost  $c=0.2$ ,  $g_0=25$ ,  $(\tau, \lambda, q)=(50, 0.75, 0.75)$ , giving  $S_0 = 0.57$ .

Legend: (a) —  $\hat{g}_t$  —  $g(\bullet)$  successful —  $g(\bullet)$  failed (b) —  $A_t^S$  —  $A_t$  —  $A_t^F$  (c) —  $A_t^{\Delta S}$

discrete PE's at each critical date. The bid rate on an active campaign is  $\lambda q$  since each arrival inspects and therefore bids with probability  $q$ . On freezing at any  $t = \hat{t}_g \equiv \tau - \hat{\tau}_g$ , all inspections stop, giving discrete PE,  $\mathcal{E}_{t_+}^{(t,g)} \triangleq \lim_{dt \downarrow 0} (\mathcal{E}_{t+dt}^{(t,g)}) = -z = -1$ . The PE rate  $\mathcal{E}$  is zero in all other states. At critical states, the NE rate  $\mathcal{N}$  is positive but dominated by the discrete PE. Elsewhere the NE is zero unless the gap is exactly one above the wall or critical gap but then the variance is zero so the NE is again zero.

The fall at  $\hat{t}_g$  is  $\lambda q$  times the atom  $z = 1$  times the probability of hitting the vertical segment of the ice wall at  $\hat{t}_g$ , namely  $\mathbb{P}(g_{\hat{t}_g} = g)$ . The vertical drops decrease over time because paths that cross the wall by  $t$  never hit it again, while paths that diverge below the wall rarely come back to cross it. The wall-of-ice is approximately linear so the bid profile is approximately convex from the first critical date onwards. Red profile  $A_t^F$  has bigger drops as the ice wall directly influences failing paths. Despite never freezing, the green profile  $A_t^S$  still has downward steps via selection of enough early bids to stay below the wall. Conditioning on failure selectively weights lower gaps as the campaign progresses, causing the profiles in 3(b) to fan out over time (see Section 3.6).

Appendix D.2 illustrates for  $g_0 = 2$ :  $\hat{\tau}_2 : q(1 - e^{-\lambda q \hat{\tau}_2}) = c$  so  $\hat{t}_2 = \tau - \frac{1}{\lambda q} \ln \left(1 - \frac{c}{q}\right)^{-1}$ . Averaging bidding  $A_t$  is  $\lambda q$  till  $\hat{t}_2$  where it drops by  $\lambda q$  times the probability of hitting the vertical wall of ice at  $\hat{t}_2$  to give  $A_t = \lambda q (1 - e^{-\lambda q \hat{t}_2})$  from then on.

### Explicit recursion for bidding and success rates.

The active-frozen dichotomy under homogeneity permits an explicit characterization

of bid rates via survival probabilities. It replaces [Proposition 1](#)'s generic integral-based recursion for success rates with a finite recursive sum. [Section 3.6](#)'s transition probabilities give the probability that a campaign survives from state  $(t, g)$  till  $t' > t$ ,

$$\alpha_{t'}^{(t,g)} \triangleq \sum_{g' \leq \hat{g}_{t'}} Q_{(t',g')}^{(t,g)}. \quad (31)$$

The probability of surviving till  $t$  given starting gap  $g_0$  is  $\alpha_t^{(0,g_0)}$ . The average bid rate is  $A_t = \lambda q \alpha_t^{(0,g_0)}$  and the success rate is  $S_{(t,g)} = \alpha_{\tau_+}^{(t,g)}$ . Using Poisson probability function,

$$\mathcal{P}(b; \Lambda) \triangleq \frac{\Lambda^b e^{-\Lambda}}{b!}, \quad (32)$$

for  $b \geq 0$  bidding events and Poisson parameter  $\Lambda \geq 0$ , we prove in [Appendix A](#),

**Proposition 8.** *Success and average bid rates under homogeneity are characterized by*

$$S_{(t,g)} = \alpha_{\tau_+}^{(t,g)}, \quad A_t = \lambda q \alpha_t^{(0,g_0)}, \quad (33)$$

where  $\forall g, t \leq t'$ , (i)  $\alpha_{t'}^{(t,g)} = 1$  if  $t' \leq \hat{t}_g$ , (ii)  $\alpha_{t'}^{(t,g)} = 0$  if  $\hat{t}_g < t$ , (iii) on  $t \leq \hat{t}_g < t' \leq \tau_+$ ,

$$1 - \alpha_{t'}^{(t,g)} = \mathcal{P}\left(0; \lambda q(\hat{t}_g - t)\right) + \sum_{b=1}^{g - \hat{g}_{t'} - 1} \mathcal{P}\left(b; \lambda q(\hat{t}_g - t)\right) \left(1 - \alpha_{t'}^{(\hat{t}_g, g-b)}\right); \quad (\text{REC-}\alpha)$$

$$1 - c/q = \mathcal{P}\left(0; \lambda q(\hat{t}_{g-1} - \hat{t}_g)\right) + \sum_{b=1}^{g-2} \mathcal{P}\left(b; \lambda q(\hat{t}_{g-1} - \hat{t}_g)\right) \left(1 - \alpha_{\tau_+}^{(\hat{t}_{g-1}, g-1-b)}\right). \quad (\text{REC-}\hat{t}_g)$$

**Corollary 3.**  $S_{(t,g)} \equiv 1$  for all  $g \leq 0$  initiates a recursive solution for generic  $S_{(t,g)}$  via

$$1 - S_{(t,g)} = \mathcal{P}\left(0; \lambda q(\hat{t}_g - t)\right) + \sum_{b=1}^{g-1} \mathcal{P}\left(b; \lambda q(\hat{t}_g - t)\right) \left(1 - S_{(\hat{t}_g, g-b)}\right). \quad (\text{REC-}S\text{-hom})$$

Corollary recursion [\(REC- \$S\$ -hom\)](#) provides  $S_{(t,g)}$  given  $S_{(\hat{t}_g, g-1)}, \dots, S_{(\hat{t}_g, 1)}$  and  $\hat{t}_g$ . As [\(REC- \$\hat{t}\_g\$ \)](#) reveals  $\hat{t}_g$  given  $\hat{t}_{g-1}$  and  $S_{(\hat{t}_g, g-1)}, \dots, S_{(\hat{t}_g, 1)}$ , combining these recursions solves for both  $S_{(t,g)}$  and  $\hat{t}_g$  given their solutions at gaps  $g-1$  and below; recall that  $\hat{t}_1 = \tau$ .

This explicit linear recursion greatly speeds up computations which is useful for optimizing design where numerical calculations become more intensive.

## 5 Welfare and Transparency

Our baseline model SEQ is transparent as it fully discloses the gap, summarizing past bidding, in real time. To investigate transparency’s welfare and success consequences, we define the no-disclosure benchmark SIM and characterize its outcomes in [Section 5.1](#). In [Section 5.2](#), [Proposition 10](#) shows DP drives decreasing welfare contributions in SEQ, albeit neutral under homogeneity ([Lemma 6](#)). A later decomposition of the binomial case shows how high cost bidders gain more when arriving later. [Section 5.3](#) uses these results to compare SEQ and SIM, first with homogeneity and then heterogeneity with binary costs, uniform costs and a family of atomless distributions, varying bidder scarcity. [Section 5.4](#) concludes by showing the optimality of intermediate transparency rules.

We define expected welfare  $W$  as bidders’ aggregate surplus  $V$  plus a success surplus  $RS_0$  where  $R$  captures societal benefits and the success-maximising entrepreneur’s gains from success. Bidder surplus  $V$  is the expectation over realized arrival sequences  $\{t_n\}_{n=1}^N$ ,

$$V = \mathbb{E} \left( \sum_{n=1}^N u_{t_n}^{a_{t_n}} \right), \quad (34)$$

where  $a_{t_n} \equiv a_{(t_n, g_{t_n}, c_{t_n})} \in \{\mathbf{A}, \mathbf{B}, \mathbf{C}\}$  is the substrategy chosen by bidder  $n$ . In sum,

$$W = V + RS_0. \quad (35)$$

Superscripts distinguish the cases so, e.g.,  $W^{\text{SEQ}}$  denotes welfare in SEQ.

### 5.1 The simultaneous move benchmark

In benchmark SIM, bidders arrive over time as in SEQ but their bids are not disclosed (till after bidding ends at  $\tau$ ) so moves are effectively simultaneous. SIM is equivalent to the simultaneous-move Poisson game with parameter  $\lambda\tau$  determining the bidder population ([Myerson, 1998](#)). Favouring SIM, we assume coordination on the unique Pareto efficient equilibrium. This maximises inspection.

In SIM, a bidder  $t$  knows the initial gap  $g_0$  but nothing else about the bidding path  $(g'_t)^{t' \leq t}$ . [Assumption 1](#) again precludes blind bidding so bidders again decide between  $\mathbf{C}$  and  $\mathbf{A}$ . Replacing  $S_{(t,g)}^{\text{bid}}$  with  $S^{\text{bid}^{\text{SIM}}}$  in [Eq. \(5\)](#) for  $\mathbf{C}$ ’s payoff implies a threshold strategy: play  $\mathbf{C}$  if  $c \leq \hat{c}$ , else play  $\mathbf{A}$ , where  $\hat{c} \in \text{supp}\{F\} \cup \{0\}$ ;  $\hat{c} = 0$  indicates always playing

**A** when  $\text{supp}\{F\} \not\equiv 0$ . Each bidder inspects and bids with probability  $qF(\hat{c})$  so the  $\lambda\tau$  Poisson distribution of bidders implies Poisson parameter  $\lambda q\tau F(\hat{c})$  on bids.<sup>16</sup> So

$$S^{\text{bid}^{\text{SIM}}} = \sigma_{g_0-1}(\tau F(\hat{c})) \quad \text{where } \sigma_g(x) \triangleq 1 - \sum_{b=0}^{g-1} \frac{(\lambda qx)^b}{b!} e^{-\lambda qx}. \quad (36)$$

We later suppress  $g$  when  $g = 1$ :  $\sigma(\cdot) \triangleq \sigma_1(\cdot)$ . Setting  $U^{\mathbf{C}^{\text{SIM}}}(c_t; \hat{c}) \triangleq U_t^{\mathbf{C}^{\text{SIM}}}$  of this  $\hat{c}$ -equilibrium,

$$U^{\mathbf{C}^{\text{SIM}}}(c_t; \hat{c}) = q\sigma_{g_0-1}(\tau F(\hat{c})) - c_t. \quad (37)$$

Equilibrium requires  $U^{\mathbf{C}^{\text{SIM}}}(c_t; \hat{c}) \geq 0, \forall c_t < \hat{c}$ ,  $U^{\mathbf{C}^{\text{SIM}}}(c_t; \hat{c}) \leq 0, \forall c_t > \hat{c}$ . As  $g_0 \geq 2$ , a trivial equilibrium exists when  $F(0) = 0$ . Selecting the best equilibrium in SIM,

$$\hat{c}^{\text{SIM}} = \sup\{c \geq 0 : U^{\mathbf{C}^{\text{SIM}}}(c; c) \geq 0\}. \quad (38)$$

So  $\hat{c}^{\text{SIM}} = q\sigma_{g_0-1}(\tau F(\hat{c}^{\text{SIM}})) \geq 0$ , strictly if  $F(0) > 0$ .  $\hat{c}^{\text{SIM}} < q$  since  $U^{\mathbf{C}^{\text{SIM}}}(q; q) < q - q = 0$  as  $\sigma_{g_0-1}(\tau) < 1$  given  $g_0 > 1$ .  $\hat{c}^{\text{SIM}} = 0$  if  $U^{\mathbf{C}^{\text{SIM}}}(c; c) < 0 \forall c \in \text{supp}\{F\}$ . In sum,

**Proposition 9.** *The simultaneous move benchmark SIM has a unique Pareto optimal equilibrium where all bidders play the trigger strategy, **C** when  $c \leq \hat{c}^{\text{SIM}}$ , **A** when  $c > \hat{c}^{\text{SIM}}$ . If  $\hat{c}^{\text{SIM}} = 0$ , the only equilibrium is trivial and  $V^{\text{SIM}} = S_0^{\text{SIM}} = 0$ ; that requires  $F(0) = 0$ . In general, bidder surplus and campaign success rate are given by*

$$V^{\text{SIM}} = \lambda\tau F(\hat{c}^{\text{SIM}}) \left[ \hat{c}^{\text{SIM}} - \mathbb{E}(c_t \mid c_t \leq \hat{c}^{\text{SIM}}) \right], \quad (39)$$

$$S_0^{\text{SIM}} = \sigma_{g_0}(\tau F(\hat{c}^{\text{SIM}})). \quad (40)$$

## 5.2 Bidder surplus dynamics in the baseline model

By [Proposition 1](#), the dynamic cost threshold for **C** is  $\hat{c}_{(t,g)} \triangleq qS_{(t,g)}^{\text{bid}}$  in SEQ. So bidder surplus increases at rate  $\lambda$  times the expected surplus of a bidder arriving at  $(t, g)$ ,

$$V_{(t,g)}/\lambda \triangleq \mathbb{E}_c \left( U_{(t,g,c)}^{a(t,g,c)} \right) = F(\hat{c}_{(t,g)}) \mathbb{E}_{c_t} \left( qS_{(t,g)}^{\text{bid}} - c_t \mid c_t \leq \hat{c}_{(t,g)} \right) = F(\hat{c}_{(t,g)}) \hat{c}_{(t,g)} - \int_0^{\hat{c}_{(t,g)}} c \, dF(c). \quad (41)$$

<sup>16</sup>Arrivals play **C** on measure  $x = \tau F(\hat{c})$  of the campaign.

Aggregating over  $t$ ,

$$V = \int_0^\tau A_t^V dt, \quad \text{where} \quad A_t^V \triangleq \sum_{-\infty}^{g_0} Q_{(t,g)} V_{(t,g)} \quad (42)$$

again averages over gaps. Using Eq. (27),  $\dot{A}_t^V = A_t^{\mathcal{L}^V}$ . Integrating (41) by parts,  $V_{(t,g)} = \int_0^{\hat{c}_{(t,g)}} \lambda F(c) dc$ . Applying Eq. (GEN) and simplifying,

$$\mathcal{L}_{(t,g)}^V = \lambda F(\hat{c}_{(t,g)}) q \mathcal{D}_{(t,g)} + \beta_{(t,g)} \int_{\hat{c}_{(t,g)}}^{\hat{c}_{(t,g-1)}} \lambda F(c) dc = \beta_{(t,g)} \int_{\hat{c}_{(t,g)}}^{\hat{c}_{(t,g-1)}} \lambda (F(c) - F(\hat{c}_{(t,g-1)})) dc. \quad (43)$$

This proves that  $\mathcal{L}_{(t,g)}^V \leq 0$  and bidder surplus trends downwards,  $\dot{A}_t^V \leq 0$  for all  $t$ :

**Proposition 10.** *In SEQ, the average surplus contribution  $A_t^V$  is time-decreasing.*

Decreasing pivotality underlies this result. Bidders with  $c_t = c < \hat{c}_{(t,g)}$  strictly prefer **C** to **A** at all  $(t + dt, g_{t+dt})$ . By DP, these inframarginals' expected payoffs  $U_{t,g}^{\mathbf{C}} = qS_{(t,g)}^{\text{bid}} - c$  trend downwards at rate  $q\mathcal{D}_{(t,g)}$ . Bidders with  $c \in (\hat{c}_{(t,g)}, \hat{c}_{(t,g-1)})$  gain from more information on arriving later as they switch from **A** to **C**, gaining  $U_{t,g-1}^{\mathbf{C}} = \hat{c}_{(t,g-1)} - c$  when, with probability  $\beta_{(t,g)} dt$ , a bid lowers the gap to  $g_{t+dt} = g_t - 1$ . So they generate  $\beta_{(t,g)} \int_{\hat{c}_{(t,g)}}^{\hat{c}_{(t,g-1)}} \lambda (\hat{c}_{(t,g-1)} - c) dF(c)$  which equals the second term of  $\mathcal{L}_{(t,g)}^V$  in Eq. (43).<sup>17</sup> The information gain is bounded by  $q\Delta S_{(t,g-1)}$  and weighted by inframarginal bidding so the DP effect on inframarginals dominates.

In the homogenous case,  $\mathcal{L}_{(t,g)}^V$  is zero at all non-critical dates since  $\beta_{(t,g)} = 0$  if frozen and if active,  $F(c') = F(\hat{c}_{(t,g-1)}) = 1, \forall c' \in [\hat{c}_{(t,g)}, \hat{c}_{(t,g-1)}]$ . At critical states,  $(\hat{t}_g, g)$ ,  $a_{(t,g,c)} = \mathbf{C}$  switches to **A** fixing a 0 payoff by indifference, except in the zero probability event of a bid at that instant. So  $A_t^V$  is constant and  $V = \tau V_{(0,g_0)} = \lambda \tau (qS_{(0,g_0)}^{\text{bid}} - c)$ .

**Lemma 6.**  *$A_t^V$  is time-independent when costs are homogenous.*

### 5.3 Welfare comparisons

**Homogenous costs.** Dynamic responses in SEQ can only reduce the success rate  $S_0$  below  $S^{\text{SIM}}$  because if SIM has a non-trivial equilibrium, it is all-**C**: all arrivals play **C**,  $F(\hat{c}) = 1$ , maximising bidding and success. By Eqs. (37) and (38), the condition is  $\tau \geq \hat{\tau}_{g_0}^{\text{SIM}} \triangleq \sigma_{g_0-1}^{-1}(c/q)$ . Moreover, since all-**C** maximises strategic complementarity

<sup>17</sup>Marginal bidder  $c = \hat{c}_{(t,g)}$  switches from **C** to **A** if no bid arrives, but this has no surplus effect.

and hence the chance that any bidder play **C** in any information structure,  $\tau < \hat{\tau}_{g_0}^{\text{SIM}}$  also implies trivial outcomes in SEQ. SIM strictly raises success rates for any  $\tau \geq \hat{\tau}_{g_0}^{\text{SIM}}$  because a positive mass of SIM's successful bidding paths have late bids and cross the wall of ice (defined in Section 4.4), implying failure in SEQ:  $S_0^{\text{SEQ}} < S_0^{\text{SIM}} \forall \tau \geq \hat{\tau}_{g_0}^{\text{SIM}}$ .

A bidder arriving at  $t = 0$  in SEQ plays **C** in this case, but with  $g_0 > 2$ , the campaign may freeze even if he bids. That strictly lowers  $S_{(0,g_0)}^{\text{bid}}$  so  $V_{(0,g_0)} < V^{\text{SIM}}/\tau$ . Lemma 6 then implies  $V^{\text{SIM}} > V^{\text{SEQ}} \equiv V$ . When  $g_0 = 2$ ,  $V^{\text{SEQ}} = V^{\text{SIM}}$  though  $S_0^{\text{SEQ}} < S_0^{\text{SIM}}$ . This proves,

**Proposition 11.** *With homogenous costs and  $\tau > \hat{\tau}_{g_0}^{\text{SIM}}$ , (i)  $S_0^{\text{SEQ}} < S_0^{\text{SIM}}$ , (ii)  $V^{\text{SEQ}} \leq V^{\text{SIM}}$  with equality only for  $g_0 = 2$ ; (iii)  $W^{\text{SEQ}} < W^{\text{SIM}}$  unless  $g_0 = 2$  and  $R = 0$ .*

Here SIM maximises strategic complementarity and hence also the success rate. It involves more costly inspection than SEQ but generally raises welfare.

**Heterogeneity.** With enough moderate cost bidders, hiding information ensures their mutual positive externalities as with homogeneity. Then SIM still yields higher welfare than SEQ. When instead such bidders are too scarce, SEQ becomes optimal since good success rates require dynamic coordination where moderate and higher cost bidders exploit any good fortune from low cost arrivals in early stages. Anticipation of the possible encouragement in SEQ of bidders who never inspect in SIM can raise  $\hat{c}_{(0,g_0)}$  above  $\hat{c}^{\text{SIM}}$ . We illustrate with binary and uniform distributions and then provide a more general sufficient condition with  $F(\cdot)$  continuous.

**Binary costs.** In general, if  $F(\hat{c}^{\text{SIM}}) = 1$ ,  $S^{\text{bid}^{\text{SIM}}}$  is maximal so  $V_0 \leq V^{\text{SIM}}/\tau$  and by Proposition 10,  $V \leq V^{\text{SIM}}$ . In the binary cost distribution with weight  $z$  on  $c_L = 0$  and  $1-z$  on  $c_H \in (0, q)$ ,  $F(\hat{c}^{\text{SIM}}) = 1$  and SIM is again welfare optimal for  $c_H \leq q\sigma_{g_0-1}(\tau)$ . When instead  $c_H > q\sigma_{g_0-1}(\tau)$ ,  $\hat{c}^{\text{SIM}} < c_H$  and SEQ has uniformly higher bid rates than SIM because  $L$ -types again always inspect, sometimes lowering  $g_t$  fast enough to activate  $H$ -types.<sup>18</sup> Clearly,  $S_0$  and  $L$ -type bidder surpluses rise and  $H$ -types gain too, so:

**Proposition 12.**  *$W^{\text{SEQ}} > W^{\text{SIM}}$  for any binary CDF with  $c_L = 0$  and  $c_H \in (q\sigma_{g_0-1}(\tau), q)$ .*

We know  $\dot{A}_t^V \leq 0$  but it is instructive to decompose  $A_t^V$  by cost type, into  $A_t^{V^L} \triangleq \lambda z \mathbb{E}_{0,g_0} \left( U_{(t,g,c_L)}^{a(t,g,c_L)} \right)$  and  $A_t^{V^H} \triangleq \lambda(1-z) \mathbb{E}_{0,g_0} \left( U_{(t,g,c_H)}^{a(t,g,c_H)} \right)$ . Average surplus contributions

<sup>18</sup>Appendix D.3 generalizes to discrete distributions. With  $c_L = 0$ , there is no wall of ice but there is a frontier  $(t, \hat{g}_t^H)$  below which  $H$ -types activate. Note that  $\mathbb{P}(\hat{c}_{(t,g_t)} \geq c_H) \geq \mathbb{P}(g_t \leq 1) \geq \sigma_{g_0-1}(tz) > 0$ .

are fixed on  $[0, \hat{t}_{g_0}^H]$  while for  $t > \hat{t}_{g_0}^H$ , we readily confirm the negative effect of DP on  $L$ -types and the positive information benefit of time on  $H$ -types, akin to the news effect.<sup>19</sup>

**Proposition 12** is robust to small  $c_L > 0$ : SEQ's welfare gain over SIM holds for small  $c_L$  as  $qS_{(t,g)}^{\text{bid}} > 0$  on  $t < \tau$  when  $c_L = 0$  and equilibrium actions vary continuously as  $c_L$  rises from 0.  $c_L > 0$  adds a wall of ice but the risk of freezing vanishes as  $c_L \rightarrow 0$ .

**Uniformly distributed costs.** When  $F(c) \equiv c/q$ ,  $g_0 = 2$  and  $\lambda = 1/q$  has  $V_{(t,g)} = \lambda q^2 / 2q = 1/2, \forall g \leq 1$ ,  $V_{(t,2)} = \sigma(\tau - t)^2 / 2$  and  $Q_{(t,2)} = e^{-t}$ , giving  $V = \frac{1}{2} (\tau(1 - 2e^{-\tau}) + e^{-\tau}(1 - e^{-\tau}))$  which is strictly positive for any  $\tau > 0$ . By contrast,  $V^{\text{SIM}} = \lambda \tau \frac{\hat{c}^{\text{SIM}}}{q} \frac{\hat{c}^{\text{SIM}}}{2} = \frac{\tau}{2} \left( \frac{\hat{c}^{\text{SIM}}}{q} \right)^2$ . Using Lambert productlog's principal branch  $\mathcal{W}(\cdot)$ ,  $\hat{c}^{\text{SIM}} = q \left( 1 + \frac{\mathcal{W}(-\tau e^{-\tau})}{\tau} \right)$ .<sup>20</sup>  $\mathcal{W}(-\tau e^{-\tau}) / \tau = -1$  on  $\tau \leq 1$  and is strictly rising on  $\tau \geq 1$ . So SIM is non-trivial for  $\tau > \hat{\tau} = 1/\lambda q = 1$ .  $V^{\text{SEQ}} > V^{\text{SIM}}$  for all  $\tau$  and  $V^{\text{SEQ}}/V^{\text{SIM}}$  falls as  $\tau$  rises.

Generalizing, bidder scarcity (low enough  $\lambda\tau$ ) eventually leads to zero welfare in SIM for any cost distribution lacking an atom at zero. Then SEQ fares strictly better given any positive mass of bidders in the neighbourhood of zero. Those bidders allow the campaign to heat up and succeed. Formally (**Proof in Appendix A**),

**Proposition 13.** *Any atomless cost distribution with support containing  $(0, \epsilon)$  for some  $\epsilon > 0$  has  $W^{\text{SEQ}} > W^{\text{SIM}}$  for sufficiently low  $\lambda\tau$ .*

When instead  $\lambda\tau$  gets large,  $V^{\text{SIM}}$  and  $V^{\text{SEQ}}$  again converge as success becomes virtually guaranteed with or without information transparency. SEQ is dominant for all  $\tau$  in this specific uniform example but if costs have an upper bound below  $q$  then  $V^{\text{SIM}}$  welfare dominates  $V^{\text{SEQ}}$  at large enough  $\lambda\tau$ .

## 5.4 Constrained social optimum

Crowdfunding platforms *could* adopt time-based disclosure rules, as was standard pre-internet, so we now ask if any intermediate information structure improves on the full and no-disclosure extremes of SEQ and SIM? We answer affirmatively by solving the information design problem of a welfare-maximising platform able to set any rule for disclosing bidding news. For expositional simplicity, we treat homogenous costs and

<sup>19</sup>  $\dot{A}_t^{V^L} = \lambda z Q_{(t,\hat{g}_t+1)} q \mathcal{D}_{(t,\hat{g}_t+1)} = -\lambda^2 z (1-z) Q_{(t,\hat{g}_t+1)} q \Delta \hat{c}_{(t,\hat{g}_t+1)} < 0$ .  $\dot{A}_t^{V^H} = \lambda(1-z) Q_{(t,\hat{g}_t+1)} \lambda z q \times (\hat{c}_{(t,\hat{g}_t+1)} - c_H) > 0$ . Summing confirms  $\dot{A}_t^V = \lambda^2 z (1-z) Q_{(t,\hat{g}_t+1)} q (\hat{c}_{(t,\hat{g}_t+1)} - c_H) < 0$ .

<sup>20</sup>  $\hat{c}^{\text{SIM}}$  is the maximal solution of  $q\sigma(\tau \hat{c}^{\text{SIM}}) = \hat{c}^{\text{SIM}}$ . Equation  $w e^w = x$  has two real solutions in  $w$  for  $x \in [-1/e, 0)$ :  $w = \mathcal{W}_0(x)$  and  $w = \mathcal{W}_{-1}(x)$  of which the principal branch  $\mathcal{W}_0(x) \equiv \mathcal{W}(x)$  is maximal.

$g_0 = 2$ ; the platform can then just commit to **Disclose** gaps from some  $t_2^{\mathbf{D}} \in [0, \tau]$  onwards.

Setting  $t_2^{\mathbf{D}} \leq \hat{t}_2$  is strategically equivalent to SEQ because bidders do not respond to gap changes prior to  $\hat{t}_2$  in SEQ so being uninformed has no impact; the equilibrium remains unique. Setting  $t_2^{\mathbf{D}} = \tau$  hides the gap till the end so that is equivalent to SIM. For  $\tau \geq \hat{t}_2$ , retaining Pareto optimal equilibrium selection, intermediate  $t_2^{\mathbf{D}}$  extends the SEQ equilibrium: bidders always play **C** on  $[0, t_2^{\mathbf{D}}]$ , then only playing **C** if  $g_t \leq 1$  over the later, full transparency phase. This information structure generates  $S_0^{t_2^{\mathbf{D}}} \in (S_0, S_0^{\text{SIM}})$  and

$$V^{t_2^{\mathbf{D}}} = \lambda \left[ t_2^{\mathbf{D}} (q\sigma(\tau) - c) + (\tau - t_2^{\mathbf{D}})(q - c)\sigma(t_2^{\mathbf{D}}) \right]. \quad (44)$$

**Lemma 7.** *With homogenous costs and a threshold of two, the bidder optimal rule has full disclosure from  $t_2^{\mathbf{D}^*} \in (\hat{t}_2, \tau)$ . Transparency is strictly between that of SEQ and SIM.*

[Appendix A](#) proves  $t_2^{\mathbf{D}^*} \in (\hat{t}_2, \tau)$ . The intuition is two-fold. First, raising  $t_2^{\mathbf{D}}$  marginally above  $\hat{t}_2$  induces some near-indifferent bidders in SEQ to switch from **A** to **C**; by **C**'s positive externality, that raises welfare. Second, lowering  $t_2^{\mathbf{D}}$  just below  $\tau$  causes bidders who face  $g \geq 2$  on arriving just before  $\tau$  to switch to **A** from playing **C** in SIM; their cost saving raises expected welfare given the negligible success chances in that contingency.

Maximising social welfare  $W = V + RS_0$  with  $R > 0$  simply raises  $t_2^{\mathbf{D}^*}$  towards  $\tau$ .

## 6 Campaign Design

We study an entrepreneur who designs her campaign to maximise project success subject to a funding constraint: she needs  $G \geq 0$  units of money to fund fixed costs of production. We focus on the uniform distribution. A range of smooth distributions are qualitatively similar. We also treat the special case of homogeneity. [Section 6.1](#) identifies and studies the entrepreneur's price-threshold tradeoff while [6.2](#) studies gap-dependent pricing and the resulting price dynamics driven by DP, anticipation effects and risk compensation. [6.3](#) assesses the welfare-implications of gap-dependent pricing.

### 6.1 Endogenous threshold and pricing with a single reward

The entrepreneur has funding need  $G$  and marginal cost  $\kappa$ , so she sets  $g_0$  and  $p$  to,

$$\max_{g_0, p} S_0(p) \quad \text{subject to} \quad G \leq (p - \kappa)g_0. \quad (45)$$

$S_0(p) \equiv S_{(0, g_0)}(p)$  generalizes [Proposition 1](#)'s recursive solution; see [6.2](#). We justify continued neglect of blind bidding **B** by replacing [Assumption 1](#) with

**Assumption 2** (Sufficient condition for NBB).  $\kappa \geq qv$ .

This suffices since the funding constraint requires price above marginal cost  $\kappa$ . The direct effect of generalizing  $p$  beyond  $p = v - 1$  is that [Eq. \(6\)](#) becomes,

$$\beta_{(t, g)}(p) = \lambda q F\left((v - p)q S_{(t, g-1)}(p)\right). \quad (46)$$

Lowering  $p$  raises the discount  $d \triangleq v - p$ . That encourages inspection given any gap  $g$ , so  $S_{(t, g)}(p)$  rises.<sup>21</sup> This creates a tradeoff because lowering  $p$  obliges a higher initial gap  $g_0$  to cover funding need  $G$ . As raising  $g_0$  lowers  $S_0$ , the success objective implies:

**Lemma 8.** *The funding constraint weakly binds so we can set  $p = p(g_0) \triangleq G/g_0 + \kappa$ .*

With the above machinery, we find the optimal threshold  $g_0^*$  by comparing integers  $g_0$  with  $p = p(g_0)$ .<sup>22</sup> We set  $\kappa=q=0.2$  to satisfy [Assumption 2](#). Normalizing  $v$  to 1, we consider gaps  $g_0 \geq \lceil G/(1 - \kappa) \rceil$  since nobody ever bids if  $p > v$ . We focus on (I) the uniform distribution on  $[0, qv] = [0, q]$ ,  $F(c) = c/q$ , as a neutral case, but also solve special case (II) homogenous cost  $c = 0.07$ . [Fig. 4](#) shows how the resulting optimized thresholds  $g_0^*$  (turquoise, integer-valued) and prices  $p^*$  (brown) depend on  $G$  and  $\lambda\tau$ .<sup>23</sup>

In the uniform case (I), [Fig. 4a](#) shows that  $\lambda\tau$  raises  $g_0^*$  and lowers  $p^*$ . Intuitively, low  $\lambda\tau$  makes it hard to reach a high  $g_0$  even if every bidder bids. [Fig. 4b](#) shows that  $g_0^*$  increases in  $G$ : high budgetary needs amplify price reductions from raising  $g_0$ . Price  $p^*$  also mostly increases in  $G$ , but drops back when integer-valued gap  $g_0$  jumps up.

Homogenous case (II) is special because lowering price only helps by reducing the risk of freezing. Lowering  $p$  rotates the wall of ice up around  $(t, g) = (\hat{t}_1, 1) \equiv (\tau, 1)$  so it is most effective early on. Bidder scarcity, low  $\lambda\tau$ , pushes the wall of ice downwards and low  $p$

<sup>21</sup>Formally, the induction logic used to prove [Lemma 5](#) generalizes so a change that increases  $\beta_{(t, g)}$  at fixed  $S_{(t, g-1)}$ , also increases  $S_{(t, g)}$ . Moreover,  $g_0$  lowers  $S_{(g_0, 0)}$  as [Corollary 1](#) generalizes to any  $p$ .

<sup>22</sup> $p(g_0)$  has negative, increasing first forward differences,  $-G/(g_0(g_0 + 1))$ .

<sup>23</sup>We solved for a range of funding needs  $G$  and expected bidder arrivals  $\lambda\tau$ . In each optimization, the plot of  $S_0$  against  $g_0$  is single-peaked ([Fig. 11](#), [Online Appendix E](#)) and identifies a unique optimal  $g_0$ .

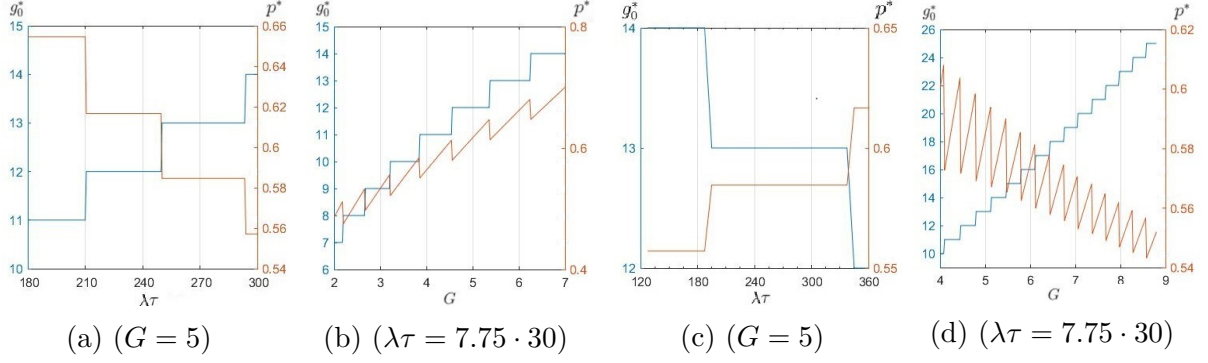


Figure 4:  $g_0^*$  and  $p^*$  for (I) uniform (a,b) and (II) homogenous (c,d) distributions.

mitigates the implied early freezing risk. At high  $\lambda\tau$ , the wall is higher and freezing is only a risk later on where  $p$  is less effective, so the price-threshold tradeoff implies a low  $g_0^*$ . Fig. 4c confirms  $p$  rising and  $g_0$  falling in  $\lambda\tau$ . Similarly, Fig. 4d shows  $g_0^*$  now rising fast enough that  $p^*$  trends downwards in  $G$  to avoid starting too near the wall. In sum,

**Observation 1.** *The optimal threshold  $g_0^*$  is increasing in funding need  $G$  in both (I) and (II);  $g_0^*$  is also increasing in bidder abundance  $\lambda\tau$  in (I) but decreasing in (II).*

*The optimal price  $p^*$  has jumps but neglecting those integer effects: in (I),  $p^*$  is increasing in  $G$  and decreasing in  $\lambda\tau$ ; in (II),  $p^*$  decreases in  $G$  and increases in  $\lambda\tau$ .*

## 6.2 Gap-dependent pricing

With unrestricted gap-dependence, the entrepreneur sets prices  $\mathbf{p}_{g_0} = (p_{g_0}, p_{g_0-1}, \dots, p_1)$  where  $p_g$  applies at gap  $g$  and their sum meets her total budgetary need.<sup>24</sup> She optimizes in two stages, first, for pricing  $\mathbf{p}^*$  given each potentially optimal  $g_0$ , second, for  $g_0^*$ , the optimized threshold under multiple prices. We focus on the first stage which tells us when to expect early bird discounts. Generalizing problem (45), her challenge is to

$$\max_{\mathbf{p}_{g_0}} S_0(\mathbf{p}_{g_0}) \quad \text{subject to} \quad G \leq \sum_{g=1}^{g_0} (p_g - \kappa) = (v - \kappa)g_0 - \sum_{g=1}^{g_0} d_g. \quad (47)$$

As only current and future prices affect bidder incentives, we let  $\mathbf{p}_g \triangleq (p_g, p_{g-1}, \dots, p_1)$ . Again imposing Assumption 2 to justify neglect of blind bidding,<sup>25</sup> we need only derive when bidders choose  $\mathbf{C}$  and the success rate  $S_0(\mathbf{p}_{g_0}) \equiv S_{(0,g_0)}(\mathbf{p}_{g_0})$ , given by:

<sup>24</sup>Prices on post-completion units,  $g \leq 0$ , are not pinned down by success maximization. A lexicographic profit concern would predict price hikes on reaching the threshold.

<sup>25</sup>It suffices since setting any  $p_g < \kappa$  is dominated by removing that price and reducing  $g_0$  by one.

**Proposition 14.** *With gap-dependent pricing, the crowdfunding game has a unique PBE:*

$a_{(t,g,c)} = \mathbf{C}$  if and only if  $c \leq q(v - p_g)S_{(t,g-1)}(\mathbf{p}_{g-1})$ . Bid intensity  $\beta_{(t,g)}(\mathbf{p}_g)$  satisfies

$$\beta_{(t,g)}(\mathbf{p}_g) = \lambda q F \left( q(v - p_g)S_{(t,g-1)}(\mathbf{p}_{g-1}) \right), \quad (48)$$

where  $S_{(t,g)}(\mathbf{p}_g) = 1$  if  $g \leq 0$  and

$$\text{if } g \geq 1, S_{(t,g)}(\mathbf{p}_g) = \int_t^\tau \exp \left( - \int_t^{T_{g_0-g+1}} \beta_{(x,g)}(\mathbf{p}_g) dx \right) \beta_{(T,g)}(\mathbf{p}_g) S_{(T,g-1)}(\mathbf{p}_{g-1}) dT_{g_0-g+1}.$$

$T_n$  is the  $n$ 'th stopping time. Bid intensity  $\beta_{(t,g)}(\mathbf{p}_g)$  depends directly on the price  $p_g$  of unit  $n = g_0 - g + 1$  and indirectly on successive unit prices  $\mathbf{p}_{g-1}$ . Earlier bidders, at gaps  $g' > g$ , anticipate increased bidding at gap  $g$  from a low  $p_g$  raising  $v - p_g$  in Eq. (48), which raises  $S_{(t,g')}^{\text{bid}}$  in Eq. (48)| $_{g=g'}$ . Amplifying gains from later price discounts, this *anticipation effect* suggests lower prices at later/lower gaps; late discounting (LD) has  $p_g$  increase in  $g$ . A high  $S_0$  attenuates this anticipation effect by bunching up  $S_{(t,g')}^{\text{bid}}$  near unity so that late discounts have little effect; high  $S_{(t,g')}^{\text{bid}}$  enhances  $p_{g'}$ 's direct effect.

A low  $p_g$  also creates a *time effect*: more bidding at gap  $g$  shifts down  $T_n$ , the stopping time of the  $g:g-1$  transition so that successors at gaps  $g' \leq g - 1$  have lower  $t$  and by Lemma 1, higher  $S_{(t,g')}^{\text{bid}}$ . This time effect is greater for bidders at higher gaps as they have more successors, so it suggests early discounts (ED) except at low  $S_0$  where LD's strong anticipation effect is a better way to motivate early bidders and create the time effect.

Bidder abundance raises  $S_0$  towards unity while bidder scarcity lowers  $S_0$  to zero. So for the uniform and power distributions, we predict ED at high  $\lambda\tau$  and LD at low  $\lambda\tau$ .

In the special case of homogeneity, extremal elasticities make it optimal to compensate for failure risk  $1 - S^{\text{bid}}$  even though discounts are multiplied by  $S^{\text{bid}}$ .  $S_{(t,g_t)}^{\text{bid}}$  is a supermartingale, as in DP, so failure risks tend to rise, but when  $S_0$  is low, failure risks tend to fall along any path that ends in success. At high  $\lambda\tau$ ,  $S_0$  is high, the campaign starts far from the ice wall, delaying the risk of freezing. LD optimally compensates for this late risk by raising the later section of the ice wall. Conversely, at low  $\lambda\tau$ , it is optimal to use ED to raise the then critical early section of the ice wall.

The above solution method supports these comparative static predictions on all parameter ranges considered. Fig. 5 illustrates graphically: in panel (a), optimal prices in case (I), uniform costs, with  $g_0=10$  feature ED at low  $\lambda\tau$ , moving to LD as  $\lambda\tau$  increases;

panel (b) reveals the converse for case (II), homogenous cost.<sup>26</sup> Formally,

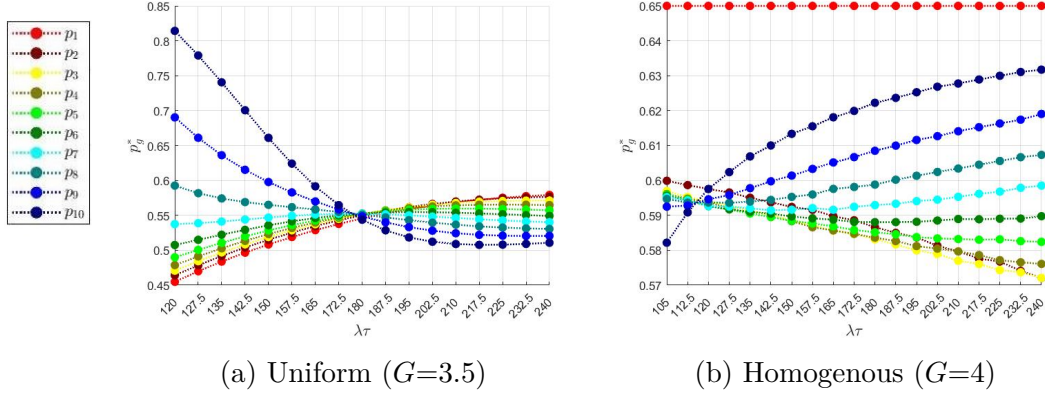


Figure 5: Gap-dependent pricing with  $g_0 = 10$ .

**Observation 2.** *The optimal gap-dependent price scheme given  $g_0$  units has,  $\forall 1 < g' < g$ :  $p_g^* - p_{g'}^*$  is positive at low  $\lambda\tau$  and negative at high  $\lambda\tau$  in case (I);  $p_g^* - p_{g'}^*$  is negative at low  $\lambda\tau$  and positive at high  $\lambda\tau$  in case (II).*

We leave a full analysis to future work but do prove an intuitive explanation in a stylized variant with extreme bidder scarcity: *let exactly  $g_0$  bidders arrive in sequence.* Now success requires every single arrival at each gap  $g \geq 1$  to bid. Having only one possible successful path shuts down time effects. It also implies multiplicative separability, removing risk compensation motives when  $F$  is a homogenous polynomial. So in uniform case (I), only the anticipation effect applies and LD is optimal:<sup>27</sup>

$$p_g^* = v - \frac{1}{2^g} \left( \frac{(v - \kappa)g_0 - G}{1 - 2^{-g_0}} \right), \quad g_0 \geq g \geq 1. \quad (49)$$

Price falls as  $g$  falls over time; the discount doubles on each gap reduction. LD is also optimal for general atomless ( $z = 0$ ) power distributions from Eq. (65); the ratio of optimal discounts is then  $d_{g-1}/d_g = 1 + \rho$ . The extent of late discounting increases with elasticity parameter  $\rho$  as bidders become more sensitive to changes in  $S^{\text{bid}}$ .

Turning to homogenous case (II), ED is optimal, driven by the risk factor:

$$p_g^* = v - \frac{c}{q^g}, \quad g_0 \geq g \geq 1. \quad (50)$$

<sup>26</sup>Observation 2 still holds at  $g_0^*(\lambda\tau)$  instead of fixing  $g_0=10$ ;  $g_0^*=g_0^*=10$  on  $\lambda\tau \geq 210$  in (I), 187.5 in (II). (i)'s LD-ED shift also holds with  $g' = 1$  but in case (II),  $p_1$  is totally inelastic and always maximal.

<sup>27</sup>Online Appendix E.1 provides detailed derivations for all cases.

The anticipation effect is trivial as inspection is necessarily maximal along the one successful path. To motivate those inspections, the discount  $d$  must compensate for risk at every gap  $g$ :  $d_g = c/q^g$  as  $S^{\text{bid}} = q^{g-1}$  on the potentially successful path through  $g$ .<sup>28</sup> Prices (50) are independent of  $G$  and  $\kappa$  but only implementable if  $G \leq (v - \kappa)g_0 - c \left( \frac{q^{-g_0} - 1}{1 - q} \right)$ . Our framework readily permits computation of bidder surplus and total welfare.

### 6.3 Welfare implications of gap-dependent pricing

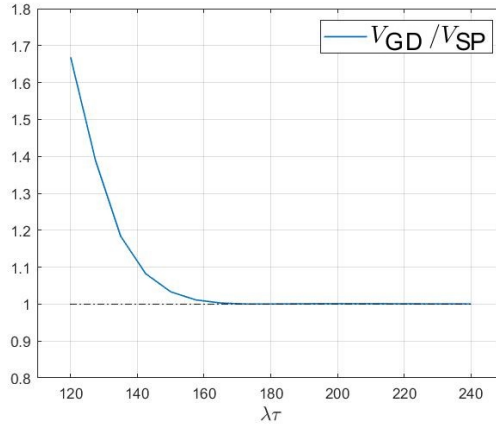


Figure 6: Bidder surplus  $V$  for gap-dependent pricing (GD) relative to a single price (SP).

Gap-dependent pricing unsurprisingly enables the entrepreneur to maximize success more effectively than when restricted to a single price. We find that in our examples, as well as raising the success rate  $S_0$ , gap-dependence raises bidder surplus and therefore welfare. Fig. 6 demonstrates this for the uniform CDF of Fig. 5a by plotting the bidder surplus ratio for the optimized gap-dependent prices,  $\mathbf{p}^{**}$  at  $g_0^{**}$ , relative to the optimized single price  $p^*$  at  $g_0^*$  (equal to  $g_0^{**}$  over the range plotted): the ratio is always above 1.<sup>29</sup> It is highest at low  $\lambda\tau$ , where gap-dependent pricing is most effective at raising the success rate. For example, we have roughly  $V_{SP} = 0.03$ ,  $V_{MP} = 0.05$  at  $\lambda\tau = 120$ ;  $V_{SP} = 0.23$ ,  $V_{MP} = 0.27$  at  $\lambda\tau = 135$ ; and  $V_{SP} \approx V_{MP} = 1.53$ ,  $\lambda\tau = 180$ . The ratio converges to one as  $\lambda\tau$  becomes large. This is intuitive since the entrepreneur can then achieve a very high success rate simply by setting a low single price. This observation is consistent with the

<sup>28</sup>In this special case, the budget constraint need not bind so, for uniqueness, we assume the entrepreneur lexicographically prefers to maximise profits among designs that generate the same  $S_0$ .

<sup>29</sup>To produce Fig. 6, we calculate the surplus contributions under GD by extending Eq. (41) to GD pricing:  $\hat{c}_{(t,g)}$  becomes  $S_{(t,g-1)}(\mathbf{p}_{g-1})(v - p_g)$  and we derive  $V_{(t,g)}/\lambda = [S_{(t,g-1)}(\mathbf{p}_{g-1})(v - p_g)]^2 q/2$  using  $F(c) = c/q$ . Numerical integration, weighted by state-transition probabilities gives  $V$  via Eq. (42). We neglect post-completion surplus contributions, consistent with SP restricting to  $g_0$  units; c.f., Footnote 24.

falling price in Fig. 4a and the concentration of prices in Fig. 5a at high  $\lambda\tau$ .

The homogenous cost case with the parameters of Fig. 5b delivers qualitatively similar results. These welfare results reflect the close alignment between welfare and success motives. However, when entrepreneurs maximize profit, gap-dependent pricing might well raise profits at the expense of  $S_0$  and  $V$ .

## 7 Concluding discussion

This paper’s principal objective was to investigate how strategic complementarities and positive externalities affect dynamic participation and welfare in a canonical finite-duration game. Our key contributions are the explicit welfare results and the novel pair of dynamic forces – the pivotality and news effects. Since the framework that we developed closely fits the most popular crowdfunding paradigm, empirical evidence on funding dynamics can test our theory. We have shown how the new forces, PE and NE, can readily account for prominent dynamics, including the much-commented U-shape. In addition, our results on optimal campaign design can guide entrepreneurs seeking to exploit the potential of crowdfunding, while our welfare results inform debates on platform implementation. Concretely, we established that full dynamic disclosure welfare-dominates static implementation when bidders are scarce, because disclosure allows lower cost types to motivate later high cost types who would otherwise never participate.

As we intentionally chose a parsimonious framework, we close by discussing its limitations in fitting the data, model extensions to improve explanatory power and steps towards testing based on our optimal design results and proxies for the cost distribution. We tentatively illustrate some first steps with a small dataset.

**Delays.** We explained the U-shape profile using only bidding costs, but imposing no delays and no prior arrivals precludes the discrete bidding spikes at campaign start and end dates that some suggest in empirical work (Crosetto and Regner, 2018; Deb et al., 2021). So we now revisit those assumptions. SEQ supposes bidders never delay. This is key for the tractable Markovian state space. No delays is appropriate if bidders generally react to a campaign without delaying, out of curiosity or impulsivity or the efficiency of deciding within a single thinking episode. That is often reasonable since those who contemplate delay must decide on delay, remember to return and then re-focus

on the project to finally decide on bidding. Nonetheless, our welfare analysis in [Section 5](#) indicates how higher cost bidders *might* gain enough from delaying to compensate these added refocusing costs and “Remind-Me” buttons lower memory costs.

So we endogenize delays in a follow-up study, [Ellman and Fabi \(2021\)](#). Delays naturally create bidding spikes at campaign deadlines. Additionally recognizing pre-campaign arrivals, who wait to bid when the campaign starts, creates a sharp U-shape. [Deb et al. \(2021\)](#) instead explain these spikes as early signalling and last-minute top-ups by a single donor (see also [Crosetto and Regner, 2018](#), on self-bidding by entrepreneurs). They use a price proxy to decompose bids between donations and purchases and to estimate separate profiles. The U-shape is more pronounced for purchases, supporting our explanation. The decomposition also indicates multiple actors delaying, as in our sequel.

**Endogenous arrivals.** Advertising drives, word-of-mouth and platforms’ promotion strategies shift bidding dynamics by making the arrival rate  $\lambda$  depend on both time and gap. Click data onto campaign pages could proxy for arrival rates ([Kuppuswamy and Bayus, 2017](#); [Kim et al., 2019](#)) to identify dynamics in  $\lambda$ . Platforms’ revenue shares give them an interest in helping to convert near-successes into successes. Consistent with this, Kickstarter’s “Nearly funded” list raises bidding near completion ([Deb et al., 2021](#)).

**Common values.** At the individual campaign level, common values would readily create momentum effects in the form of positive and negative cascades, but no obvious prediction for the bid profile averaged across campaigns. Extending to common values greatly impedes tractability as gaps no longer summarize bidding paths.<sup>30</sup>

**Making a difference and warm-glow.** [Kuppuswamy and Bayus \(2017\)](#) suggest that when bidders gain a utility from *making a difference*, goal proximity raises the motive to bid. We formally capture *making a difference* as pivotality and show that it is non-monotonic in goal proximity but we support [Kuppuswamy and Bayus’s \(2017\)](#) refined and more conclusive test which interacts goal and deadline proximity. By DP, such motivations would reinforce the downward-sloping tendency.

Pivotality motives also predict decreased bidding after the *completion* date at which funds reach the threshold ([Kuppuswamy and Bayus, 2017](#)). Our SEQ model can predict a post-completion decrease but only for high thresholds or early completions. In any case, such motives only predict that donations should decrease and there is no strong evidence

---

<sup>30</sup>Absent bidding costs, *relative* bid timings perfectly reveal bidder signals in [Liu’s \(2020\)](#) common value equilibria but *absolute* timings are indeterminate, precluding bid profile conclusions.

of post-completion decreases in purchases. To fully investigate this motive, plus altruism and warm-glow, increasing in bid size (Andreoni, 1990), requires multiple bid options by multiple actors as in Ellman and Hurkens’s 2019b’s (static) model.

**Cost distribution proxies.** The bid profile predictions in Section 4.3 from combining “close” and “distant” bidders depend on the relative prevalence of close and distant bidders, so they can be tested using recent proxies for proximity from geographic data (Agrawal et al., 2011) and link traffic data that identifies arrival via social media (Kuppuswamy and Bayus, 2017; Kim et al., 2019). Online Appendix F uses Fan-Osuala et al.’s (2018) Kickstarter dataset to break down profiles by outcome and project category. Emerging patterns fit Section 4.3’s bimodal case: most categories feature appreciable downward slopes, especially early on, with flatter, late upward slopes that are mostly absent when conditioning on failure.

**Design-based predictions.** Section 6 predicts that bidder threshold  $g_0$  rises with funding goal. In the uniform case of Section 4.1, raising  $g_0/\lambda\tau$  makes the initial decreasing slope steeper. A tentative comparison of categories with relatively large campaign funding goals (technology, design, games, and film-and-video) versus relatively small goals (music, comics, dance and craft) is broadly supportive (Appendix F), though highly tentative since, while  $\tau$  varies minimally, parameters including  $\lambda$  may vary systematically.<sup>31</sup>

Future work could find proxies for entrepreneur preferences and move beyond success-maximization. We conjecture higher welfare gains from disclosure if entrepreneurs maximize profit since dynamic coordination polarizes failures and successes and only profit-maximisers value the additional marginal revenues of an extreme success. Much remains to be done on design as well. Beyond multiple prices, rebates when the crowdfunding threshold is strictly exceeded would help encourage inspection. Most platforms do not allow endogenous prices but some allow profit-sharing which works like a rebate and others, like Kickstarter, allow stretch goals which similarly encourage inspection by promising to use additional funding to improve quality. Finally, we hope that recent progress on crowdfunding with inspection and common values in the static case will inspire attempts to study dynamics despite the lack of a Markovian state space.

---

<sup>31</sup>Cordova et al. (2015) and Mollick (2014) associate high funding thresholds with poor success rates. Cordova et al. (2015) find a positive effect of campaign duration in a technology projects sample. Mollick (2014) finds the opposite for generic campaigns. Higher duration may reduce bidders’ attention because of increased inter-project competition, impatience or changing tastes.

## References

- Admati, A. R. and Perry, M. (1991). Joint projects without commitment. *Review of Economic Studies*, 58(2):259–276.
- Agrawal, A. K., Catalini, C., and Goldfarb, A. (2011). The geography of crowdfunding. *NBER Working Paper*.
- Alaei, S., Malekian, A., and Mostagir, M. (2021). A dynamic model of crowdfunding. *Mimeo*.
- Andreoni, J. (1990). Impure altruism and donations to public goods: A theory of warm-glow giving. *The Economic Journal*, 100(401):464–477.
- Bagnoli, M. and Lipman, B. L. (1989). Provision of Public Goods: Fully Implementing the Core through Private Contributions. *The Review of Economic Studies*, 56(4):583–601.
- Brown, D. C. and Davies, S. W. (2020). Financing efficiency of securities-based crowdfunding. *The Review of Financial Studies*, 33(9):3975–4023.
- Chang, J.-W. (2020). The economics of crowdfunding. *American Economic Journal: Microeconomics*, 12(2):257–80.
- Chemla, G. and Tinn, K. (2020). Learning through crowdfunding. *Management Science*, 66(5):1783–1801.
- Colombo, M. G., Franzoni, C., and Rossi-Lamastra, C. (2015). Internal social capital and the attraction of early contributions in crowdfunding. *Entrepreneurship Theory and Practice*, 39(1):75–100.
- Cordova, A., Dolci, J., and Gianfrate, G. (2015). The determinants of crowdfunding success: evidence from technology projects. *Procedia-Social and Behavioral Sciences*, 181:115–124.
- Crosetto, P. and Regner, T. (2018). It’s never too late: Funding dynamics and self pledges in reward-based crowdfunding. *Research Policy*, 47(8):1463–1477.

- Deb, J., Öry, A., and Williams, K. (2021). Aiming for the goal: Contribution dynamics of crowdfunding. *Cowles Foundation Discussion Papers*. 2597.
- Ellman, M. and Fabi, M. (2021). Crowdfunding with endogenously timed moves. *Mimeo*.
- Ellman, M. and Hurkens, S. (2019a). Fraud tolerance in optimal crowdfunding. *Economics Letters*, 181(C):11–16.
- Ellman, M. and Hurkens, S. (2019b). Optimal crowdfunding design. *Journal of Economic Theory*, 184:104939.
- Etter, V., Grossglauser, M., and Thiran, P. (2013). Launch hard or go home! Predicting the success of kickstarter campaigns. In *Proceedings of the First ACM Conference on Online Social Networks*, pages 177–182.
- Fan-Osuala, O., Zantedeschi, D., and Jank, W. (2018). Using past contribution patterns to forecast fundraising outcomes in crowdfunding. *International Journal of Forecasting*, 34(1):30–44.
- Kickstarter (2021). Kickstarter statistics. <https://www.kickstarter.com/help/stats>. Accessed: 2021-12-15.
- Kim, J.-H., Newberry, P., and Qiu, C. (2019). The role of information signals in determining crowdfunding outcomes. *Proceedings of the 12th Digital Economics Conference*.
- Kuppuswamy, V. and Bayus, B. L. (2017). Does my contribution to your crowdfunding project matter? *Journal of Business Venturing*, 32(1):72–89.
- Kuppuswamy, V. and Bayus, B. L. (2018). Crowdfunding creative ideas: The dynamics of project backers. In *The Economics of Crowdfunding*, pages 151–182. Springer.
- Liu, S. (2020). A theory of collective investment with application to venture funding. *Mimeo*.
- Mollick, E. (2014). The dynamics of crowdfunding: An exploratory study. *Journal of Business Venturing*, 29(1):1–16.
- Mollick, E. R. and Kuppuswamy, V. (2014). After the campaign: Outcomes of crowdfunding. *UNC Kenan-Flagler Research Paper*, (2376997).

Myerson, R. B. (1998). Population uncertainty and Poisson games. *International Journal of Game Theory*, 27(3):375–392.

Rao, H., Xu, A., Yang, X., and Fu, W.-T. (2014). Emerging dynamics in crowdfunding campaigns. In *International Conference on Social Computing, Behavioral-Cultural Modeling, and Prediction*, pages 333–340. Springer.

Statista (2021). Total amount of funding pledged on Kickstarter 2012-2021. <https://www.statista.com/statistics/310218/total-kickstarter-funding>. Accessed: 2022-02-09.

Strausz, R. (2017). A theory of crowdfunding: A mechanism design approach with demand uncertainty and moral hazard. *American Economic Review*, 107(6):1430–76.

## Appendix A Proofs

**Proof of Lemma 1.** Bid intensity  $\beta_{(t,g)}$  cannot be negative so (i) and Eqs. (2) and (ODE-S) immediately imply (ii). So we need only prove  $\Delta S_{(t,g)} \geq 0, \forall g$ ; this implies the second inequality in (i) since  $S_{(t,g)}^{\text{bid}} \equiv S_{(t,g-1)}$ . We prove  $\Delta S_{(t,g)} \geq 0$  by induction. First, if  $g \leq 0$ ,  $S_{(t,g)} \equiv 1$  so  $\Delta S_{(t,g)} = 0$ . Second,  $\Delta S_{(t,1)} = 1 - S_{(t,1)} = e^{-\lambda q(\tau-t)} \in (0, 1]$ . For  $g \geq 2$ , we integrate Eq. (8) by parts, using  $dn_T = -n_T \beta_{(T,g)} dT$  from Eq. (7), to give

$$S_{(t,g)} = - \int_t^\tau S_{(T,g-1)} dn_T = \int_t^\tau n_T \dot{S}_{(T,g-1)} dT - [n_\tau S_{(\tau,g-1)} - n_t S_{(t,g-1)}]. \quad (51)$$

$S_{(\tau,g-1)} = 0 \forall g \geq 2$  and  $n_t = e^0 = 1$  imply  $[n_T S_{(T,g-1)}]_t^\tau = S_{(t,g-1)}$ . So using Eq. (ODE-S),

$$\Delta S_{(t,g)} = - \int_t^\tau n_T \dot{S}_{(T,g-1)} dT = \int_t^\tau n_T \beta_{(T,g-1)} \Delta S_{(T,g-1)} dT.$$

Now  $\beta_{(t,g)} \geq 0$  and  $n_x > 0 \forall x \leq \tau$ , so (i) holds at  $g-1 \implies$  (i) holds at  $g$ . ■

**Proof of Lemma 3.** Eq. (27) follows from (ODE-Q),  $\dot{Q}_{(t,g)} = Q_{(t,g+1)} \beta_{(t,g+1)} - Q_{(t,g)} \beta_{(t,g)}$ , as follows:

$$D_t \left( \mathbb{E}_{(0,g_0)} Y_{(t,g)} \right) = D_t \left( \sum_{g=-\infty}^{g_0} Q_{(t,g)} Y_{(t,g)} \right) = \sum_{g=-\infty}^{g_0} \left( \dot{Q}_{(t,g)} Y_{(t,g)} + Q_{(t,g)} \dot{Y}_{(t,g)} \right)$$

$$\begin{aligned}
&= \sum_{g=-\infty}^{g_0} \left( (Q_{(t,g+1)}Y_{(t,g+1)} - Q_{(t,g)}Y_{(t,g)})Y_{(t,g)} + Q_{(t,g)}\dot{\beta}_{(t,g)} \right) \\
&= \sum_{g=-\infty}^{g_0} Q_{(t,g)} \left( Y_{(t,g)} (\beta_{(t,g-1)} - \beta_{(t,g)}) + \dot{\beta}_{(t,g)} \right) = \sum_{g=-\infty}^{g_0} Q_{(t,g)} \mathcal{L}_{(t,g)}^Y \quad (52)
\end{aligned}$$

since  $Q_{(t,g_0+1)} = 0$  implies  $\sum_{g=-\infty}^{g_0} Q_{(t,g+1)}\beta_{(t,g+1)}\beta_{(t,g)} = \sum_{g=-\infty}^{g_0} Q_{(t,g)}\beta_{(t,g)}\beta_{(t,g-1)}$ .

(i)  $\dot{A}_t = D_t(\mathbb{E}_{(0,g_0)}\beta_{(t,g)})$  so the result is immediate [Eq. \(27\)](#).

(ii) As shown in part (i) for the average of  $Y_{(t,g)} = \beta_{(t,g)}$ , the time derivative of any average with weights  $Q_{(t,g)}$  is the same weighted average of the generator of  $Y_{(t,g)}$ . By [Eq. \(GEN\)](#),  $\mathcal{L}_{(t,g)}^{\beta S^{\text{bid}}} = \beta_{(t,g)}\dot{S}_{(t,g-1)} + \dot{\beta}_{(t,g)}S_{(t,g-1)} + \beta_{(t,g)}(\beta_{(t,g-1)}S_{(t,g-2)} - \beta_{(t,g)}S_{(t,g-1)}) = \mathcal{L}_{(t,g)}^{\beta}S_{(t,g-1)} + \beta_{(t,g)}(\beta_{(t,g-1)}\Delta S_{(t,g-1)} + \dot{S}_{(t,g-1)}) = \mathcal{L}_{(t,g)}^{\beta}S_{(t,g-1)}$  as  $\mathcal{L}_{(t,g-1)}^S \equiv 0$  given  $S_{(t,g_t)}$  is a martingale. Hence,  $\dot{A}_t^S = \frac{1}{S_0} \sum_{g=-\infty}^{g_0} (Q_{(t,g)}\mathcal{L}_{(t,g)}^{\beta S^{\text{bid}}}) = \frac{1}{S_0} \sum_{g=-\infty}^{g_0} Q_{(t,g)}\mathcal{L}_{(t,g)}^{\beta}S_{(t,g-1)}$ . Similarly,  $\mathcal{L}_{(t,g)}^{\beta(1-S^{\text{bid}})} = \mathcal{L}_{(t,g)}^{\beta}(1 - S_{(t,g-1)})$ . So  $\dot{A}_t^F = \frac{1}{1-S_0} \sum_{g=-\infty}^{g_0} Q_{(t,g)}\mathcal{L}_{(t,g)}^{\beta}(1 - S_{(t,g-1)})$ . ■

**Proof of Lemma 4.** Let  $F'$  have lower costs than  $F$  in that  $F \succeq_{\text{FOSD}} F'$ :  $F'(c) \geq F(c)$  for all  $c \in [0, q]$ . Let  $H', H$  denote the CDF of  $T_g$  under  $F', F$ , respectively and  $\mathbb{E}(S_{(T,g-1)}|H)$  indicates expectation over  $T_g \equiv T$  distributed according to  $H$ . Similarly, we use  $S', \beta'$  and  $S, \beta$  to distinguish results for  $F'$  and  $F$ . By the inductive hypothesis at  $g-1$ ,  $S'_{(t,g-1)} \geq S_{(t,g-1)}$  so  $\beta'_{(t,g)} \geq \beta_{(t,g)}$  by [Eq. \(9\)](#) and so  $n'_T = \exp\left(-\int_t^T \beta'_{(x,g)}(z) dx\right) \leq n_T$  for all  $T$ . For any  $t, g$  (suppressed),  $H_T \equiv 1 - n_T$  so  $H' \geq H$  for all  $T$ ; i.e.,  $H \succeq_{\text{FOSD}} H'$ .

Now,  $S, S'$  are decreasing in  $T$  by [Lemma 1](#) so by FOSD,  $\mathbb{E}(S_{(T,g-1)}|H') \geq \mathbb{E}(S_{(T,g-1)}|H)$ ; to prove this FOSD result, we integrate by parts as in [Eq. \(51\)](#) ( $\dot{S} \leq 0$  by [Lemma 1](#)):

$$\int_t^\tau S_{(T,g-1)} dH'_T - \int_t^\tau S_{(T,g-1)} dH_T = S_{(\tau,g-1)}(H'_\tau - H_\tau) - \int_t^\tau \dot{S}_{(T,g-1)}(H'_T - H_T) dT$$

since  $H_t^{(t,g)} = 0 \implies H_t = H'_t = 0$  and  $S_{(\tau,g-1)} = S'_{(\tau,g-1)}$  ( $= 0$  if  $g \geq 2$ ,  $= 1$  if  $g = 1$ ).

Finally, applying [Eq. \(REC-S\)](#) and then the inductive hypothesis,

$$S'_{(t,g)} - S_{(t,g)} = \mathbb{E}(S'_{(T,g-1)}|H') - \mathbb{E}(S_{(T,g-1)}|H) \geq \mathbb{E}(S_{(T,g-1)}|H') - \mathbb{E}(S_{(T,g-1)}|H) \geq 0. \quad \blacksquare$$

**Proof of Proposition 4.** The chain rule for generators (see [Appendix B.1](#)) states that

$$\mathcal{L}_{(t,g)}^{h(Y)} = h_Y \mathcal{L}_{(t,g)}^Y + \beta_{(t,g)} \left( \Delta h(Y_{(t,g)}) - h_Y \Delta Y_{(t,g)} \right). \quad (53)$$

Setting  $Y_{(t,g)} \equiv qS_{(t,g)}^{\text{bid}}$  and  $h(\cdot) \equiv \lambda qF(\cdot)$  so that  $\beta_{(t,g_t)} \equiv h(Y_{(t,g_t)})$  and  $h_Y(\cdot) \equiv \lambda qF_c(\cdot)$ , provides an expression for  $\mathcal{L}_{(t,g)}^{\beta}$  which we equate with its PE-NE decomposition [\(19\)](#),

$$\lambda q \left( q F_c \mathcal{L}_{(t,g)}^{S^{\text{bid}}} + \beta_{(t,g)} \left( \Delta F(q S_{(t,g)}^{\text{bid}}) - F_c q \Delta S_{(t,g)}^{\text{bid}} \right) \right) = \lambda q \left( \mathcal{E}_{(t,g)} + \mathcal{N}_{(t,g)} \right), \quad (54)$$

where  $F_c \equiv F_c(q S_{(t,g)}^{\text{bid}})$ . Cancelling  $\mathcal{E}_{(t,g)} = q F_c \mathcal{L}_{(t,g)}^{S^{\text{bid}}}$  by Eqs. (13) and (15) proves  $\mathcal{N}_{(t,g)} = \beta_{(t,g)} \left( \Delta F(q S_{(t,g)}^{\text{bid}}) - F_c q \Delta S_{(t,g)}^{\text{bid}} \right)$ . If  $F$  is polynomial with maximal exponent  $\rho \in \mathbb{N}_+$ ,

$$\Delta F(q S_{(t,g)}^{\text{bid}}) = F_c(q S_{(t,g)}^{\text{bid}}) q \Delta S_{(t,g)}^{\text{bid}} + \frac{F_{cc}(q S_{(t,g)}^{\text{bid}})}{2} \left[ q \Delta S_{(t,g)}^{\text{bid}} \right]^2 + \sum_{k=3}^{\rho} \frac{D_c^k(F)}{k!} \left( q S_{(t,g)}^{\text{bid}} \right) \left[ q \Delta S_{(t,g)}^{\text{bid}} \right]^k.$$

The instantaneous variance of  $S_{(t,g)}^{\text{bid}}$  equals the intensity of the underlying Poisson process  $g_t$  times the jump size squared, so  $\nu_{(t,g)}^{S^{\text{bid}}} = \beta_{(t,g)} (q \Delta S_{(t,g)}^{\text{bid}})^2 = q^2 \nu_{(t,g)}^{S^{\text{bid}}}$  (details in B.4).

If  $\rho = 2$ , this implies  $\mathcal{N}_{(t,g)} = \frac{q^2}{2} \nu_{(t,g)}^{S^{\text{bid}}} F_{cc}(q S_{(t,g)}^{\text{bid}})$ . So Eq. (19) implies that  $\mathcal{L}_{(t,g)}^{\beta}$  satisfies (20) and condition (21) guarantees  $\mathcal{N}_{(t,g)} \geq \mathcal{E}_{(t,g)}$ , hence  $\mathcal{L}_{(t,g)}^{\beta} \geq 0$ . If  $\rho \geq 3$ ,

$$\mathcal{N}_{(t,g)} = \frac{q^2}{2} \nu_{(t,g)}^{S^{\text{bid}}} F_{cc}(q S_{(t,g)}^{\text{bid}}) + \beta_{(t,g)} \sum_{k=3}^{\rho} \frac{D_c^k(F(c))}{k!} \left[ q \Delta S_{(t,g)}^{\text{bid}} \right]^k. \quad (55)$$

$k$ 'th derivatives for  $k > \rho$  are zero. If  $F(c) \equiv \sum_{k' \in \{0,1,\dots,\rho\}} \gamma_{k'} c^{k'}$  for  $3 \leq k \leq k' \leq \rho$ , the  $k$ 'th summation term from positive polynomial coefficient  $\gamma_{k'}$  is a positive multiple of  $c^{k'-k}$ . So condition (21) is sufficient for the NE to prevail over the PE and produce an increasing expected bid rate from state  $(t, g)$ ; if  $\rho = 2$ , (21) is also necessary. ■

**Proof of Proposition 7.** Eq. (30) gives  $F_c(q S_{(t,g)}^{\text{bid}}) = \frac{2(1-z)S_{(t,g)}^{\text{bid}}}{q}$  and  $F_{cc}(q S_{(t,g)}^{\text{bid}}) = \frac{2(1-z)}{q^2}$ . Substituting for  $\nu_{(t,g)}^{S^{\text{bid}}}$ ,  $\mathcal{L}_{(t,g)}^{S^{\text{bid}}} = \mathcal{L}_{(t,g)}^{\Delta S}$  from equation Eq. (13), and using the expressions for  $F_c$ ,  $F_{cc}$ , Eq. (20) reduces to

$$\mathcal{L}_{(t,g)}^{\beta} = \lambda q (1-z) \Delta S_{(t,g)}^{\text{bid}} \left( -2 S_{(t,g)}^{\text{bid}} \Delta \beta_{(t,g)} + \beta_{(t,g)} \Delta S_{(t,g)}^{\text{bid}} \right).$$

Simplifying further using  $(S_{(t,g-1)}^{\text{bid}})^2 - (S_{(t,g)}^{\text{bid}})^2 = \Delta S_{(t,g)}^{\text{bid}} (S_{(t,g-1)}^{\text{bid}} + S_{(t,g)}^{\text{bid}})$ , we obtain

$$\mathcal{L}_{(t,g)}^{\beta} = (\lambda q)^2 (1-z) \left( \Delta S_{(t,g)}^{\text{bid}}(z) \right)^2 \left[ z - (1-z) S_{(t,g)}^{\text{bid}}(z) \left( 2 S_{(t,g-1)}^{\text{bid}}(z) + S_{(t,g)}^{\text{bid}}(z) \right) \right]. \quad (56)$$

$$\text{If } z \geq \zeta_{(t,g)}(z) \triangleq 1 - \frac{1}{1 + S_{(t,g)}^{\text{bid}}(z) \left( 2 S_{(t,g-1)}^{\text{bid}}(z) + S_{(t,g)}^{\text{bid}}(z) \right)}, \quad (57)$$

$\mathcal{L}_{(t,g)}^{\beta}$  from Eq. (56) is positive, strictly so for  $z < 1$  and  $g > 1$  which ensure that  $\nu_{(t,g)}^{S^{\text{bid}}} > 0$  and  $F_{cc}(q S_{(t,g)}^{\text{bid}}) > 0$ . Maximising  $S_{(t,g)}^{\text{bid}}$ ,  $S_{(t,g-1)}^{\text{bid}}$  at 1 gives  $\zeta_{(t,g)}(z) \leq 3/4$ . ■

**Proof of Proposition 8.** (i) If  $t' \leq \hat{t}_g$ ,  $\alpha_{t'}^{(t,g)} = 1$  since the project is safely below the

wall of ice and cannot freeze between  $t$  and  $t'$ . (ii) If  $t > \hat{t}_g$ , the campaign is already frozen at  $t$  so it can neither survive nor succeed:  $\alpha_{t'}^{(t,g)} = \alpha_{\tau_+}^{(t,g)} = 0$ . (iii) If  $t \leq \hat{t}_g < t'$ , both freezing and survival are possible. On  $[t, \hat{t}_g]$ , bids arrive with intensity  $\lambda q$  so  $b$  has Poisson parameter  $\Lambda = \lambda q (\hat{t}_g - t)$  there. Eq. (REC- $\alpha$ ) holds because there are two ways to fail to survive till  $t'$ : either  $b = 0$  on  $[t, \hat{t}_g]$  or  $b \in \{1, \dots, g - \hat{g}_{t'} - 1\}$  on  $[t, \hat{t}_g]$  and then the campaign fails to survive from state  $(\hat{t}_g, g - b)$  till  $t'$ . As  $g \leq 0$  guarantees success and implies  $\hat{t}_g = \tau_+$ ,  $\alpha_{\tau_+}^{(t,g)} = 1$  for any  $t \leq \tau_+$ , providing the initial step in Eq. (REC- $\alpha$ ).

Recursion (REC- $\hat{t}_g$ ) for  $\hat{t}_g$  at  $g \geq 1$  combines  $S_{(\hat{t}_g, g-1)} = S_{(\hat{t}_g, g)}^{\text{bid}} = c/q$  from Eq. (66) with recursion Eq. (REC- $\alpha$ ) at  $t' = \tau_+$  and starting state  $(\hat{t}_g, g - 1)$ ; recall that  $\hat{g}_{\tau_+} = 0$ . The initial step for  $\hat{t}_g$  at  $g = 1$  follows from the general result that  $\hat{t}_1 = \tau$  since at  $g = 1$  bidders play **C** at any date during the campaign; conversely,  $\hat{g}_\tau = 1$ . ■

**Proof of Lemma 7.** The first-order condition for the optimal disclosure date  $t_2^{\mathbf{D}^*} \triangleq \arg \max V$ , where  $V$  is given by Eq. (44) is

$$D_{t_2^{\mathbf{D}}} (V) \equiv (q\sigma(\tau) - c) + (q - c) \left[ \lambda q (\tau - t_2^{\mathbf{D}}) \left( 1 - \sigma(t_2^{\mathbf{D}}) \right) - \sigma(t_2^{\mathbf{D}}) \right] = 0. \quad (\text{FOC})$$

This has a unique solution  $t_2^{\mathbf{D}^*}$  that achieves a maximum since  $D_{t_2^{\mathbf{D}}}^2 (V) = -(\lambda q)^2 (\tau - t_2^{\mathbf{D}}) (1 - \sigma(t_2^{\mathbf{D}})) < 0$ .  $t_2^{\mathbf{D}^*}$  lies strictly between  $\hat{t}_2$  and  $\tau$ , as  $D_{t_2^{\mathbf{D}}} (V) = (q - c) \lambda q (\tau - t_2^{\mathbf{D}}) (1 - \sigma(t_2^{\mathbf{D}})) > 0$  at  $t_2^{\mathbf{D}} = \hat{t}_2$ , and  $D_{t_2^{\mathbf{D}}} (V) = -c(1 - \sigma(\tau)) < 0$  at  $t_2^{\mathbf{D}} = \tau$ . ■

**Proof of Proposition 13.** With  $F(0) = 0$ ,  $U^{\mathbf{C}^{\text{SIM}}}(c_t; 0) < 0, \forall c_t > 0$  so  $\hat{c} = 0$  is a PBE of SIM. A sufficient condition for no other equilibria, so  $\hat{c}^{\text{SIM}} = 0$ , is  $D_c (U^{\mathbf{C}^{\text{SIM}}}(c; c)) < 0$ ; that is,

$$D_c (q\sigma_{g_0-1}(\tau F(c))) \equiv [\lambda q^2 \tau F_c(c)] \mathcal{P}(g_0 - 2, \lambda q \tau F(c)) < 1, \quad (58)$$

$$\begin{aligned} \text{as } D_x(\sigma_{g_0}(x)) &= \sum_{b=g_0}^{\infty} D_x \left( \frac{(\lambda q x)^b}{b!} e^{-\lambda q x} \right) = \sum_{b=g_0}^{\infty} \lambda q \left( \frac{(\lambda q x)^{b-1}}{(b-1)!} e^{-\lambda q x} - \frac{(\lambda q x)^b}{b!} e^{-\lambda q x} \right) \\ &= \lambda q \frac{(\lambda q x)^{g_0-1}}{(g_0-1)!} e^{-\lambda q x} \equiv \lambda q \mathcal{P}(g_0 - 1, \lambda q x). \end{aligned}$$

Clearly, condition (58) holds for sufficiently small  $\lambda, q$  and  $\tau$  or sufficiently large  $g_0$  ( $\mathcal{P}$  is the Poisson probability mass defined by Eq. (32)).

By contrast,  $\lambda q \tau > 0$  implies  $S_{(t,g)} > 0$  for all  $t < \tau$  as we now prove by induction. At  $g \leq 0$ ,  $S_{(t,g)} = 1$ . If  $S_{(t,g)} > 0, \forall t < \tau$ , then  $S_{(t,g+1)}^{\text{bid}} > 0$  and  $\beta_{(t,g+1)} > 0$  so the integrand in (REC- $S$ ) is positive, implying  $S_{(t,g+1)} > 0$ . Hence the SEQ equilibrium is non-trivial and  $V^{\text{SEQ}} > V^{\text{SIM}} = 0$  and  $W^{\text{SEQ}} > W^{\text{SIM}} = 0$ . ■

# Online Appendices (NOT FOR PUBLICATION)

## A Theory of Crowdfunding Dynamics

[Appendix B](#) provides background theory behind the main analysis. [Appendix C](#) delves into the stochastic paths of pivotality and offers explicit comparative statics. [Appendix D](#) provides full details on the homogenous case and expands on discrete distributions. [Appendix E](#) covers the optimization procedure employed in [Section 6](#) on design. [Appendix F](#) computes Kickstarter bid profiles using the dataset of [Fan-Osuala et al. \(2018\)](#).

## Appendix B Supplementary theory

This appendix adds details behind the infinitesimal generator and related results used in the paper to characterize dynamics. [B.1](#) provides a full definition. [B.2](#) uses it for a formal proof of [Eq. \(ODE-S\)](#) and offers an alternative derivation of [Eq. \(REC-S\)](#). [B.3](#) presents full details on the differential equations that determine the transition probabilities. [B.4](#) and [B.5](#) derive jump variance and martingale equivalences.

### B.1 Infinitesimal generator

The Poisson count process  $B_t$  equals the number of bids by date  $t$ . Recall our state variable is  $g_t \triangleq g_0 - B_t$ . Denoting the change in  $g_t$  over an infinitesimal interval of length  $dt$  by  $dg_t \triangleq g_{t+dt} - g_t$ , the stochastic differential equation (SDE) for  $g_t$  is  $dg_t = (-1) \times dB_t$  (SDE- $g$ ). Given that the instantaneous probability of a bid is  $\beta_{(t,g)} dt$  and that of two or more bids occurring simultaneously is negligible,  $\mathbb{P}((-dg_t) = 0 | (t, g)) = 1 - \beta_{(t,g)} dt + O(dt)^2$ ,  $\mathbb{P}((-dg_t) = 1 | (t, g)) = \beta_{(t,g)} dt + O(dt)^2$  and other values can be ignored.<sup>32</sup> So for any process  $Y_{(t,g_t)}$  adapted to  $g_t$ , Itô's formula applied to the Poisson jump process (SDE- $g$ ) yields the jump-diffusion

$$dY_{(t,g_t)} = \dot{Y}_{(t,g_t)} dt + \left( Y_{(t,g_t-1)} - Y_{(t,g_t)} \right) (-dg_t). \quad (\text{SDE-}Y)$$

---

<sup>32</sup>We use big-O notation, writing  $y(t) = O(h(t))$  as  $t \rightarrow 0$  if  $\exists M, \epsilon : |y(t)| \leq Mh(t)$  for all  $|t| \leq \epsilon$ .

The *infinitesimal-generator* of  $Y_{(t,g_t)}$  is its limit expected rate of change and satisfies

$$\mathcal{L}_{(t,g)}^Y \triangleq \lim_{dt \downarrow 0} \frac{\mathbb{E}_{(t,g)} \left( Y_{(t+dt, g_{t+dt})} \right) - Y_{(t,g)}}{dt} = \dot{Y}_{(t,g)} + \beta_{(t,g)} \Delta Y_{(t,g)}. \quad (\text{GEN})$$

Recall that  $\Delta Y_{(t,g)} \triangleq Y_{(t,g-1)} - Y_{(t,g)}$ , distinct from  $dY_{(t,g_t)}$ .

Unlike total derivatives in standard calculus, the generator  $\mathcal{L}$  satisfies the following adapted chain rule: for any twice differentiable function  $h(\cdot)$  of  $Y_{(t,g_t)}$  with  $h_Y \triangleq \partial h(Y)/\partial Y$ ,

$$\mathcal{L}_{(t,g)}^{h(Y)} = h_Y \mathcal{L}_{(t,g)}^Y + \beta_{(t,g)} \left( \Delta h(Y_{(t,g)}) - h_Y \Delta Y_{(t,g)} \right). \quad (\text{GEN-}h(Y))$$

To see this, substitute  $h(Y_{(t,g)})$  for  $Y_{(t,g)}$  in Eq. (GEN), noting that  $\frac{\partial}{\partial t} h(Y_{(t,g)}) = h_Y \dot{Y}_{(t,g)}$  and substitute for  $\dot{Y}_{(t,g)}$  from Eq. (GEN).

## B.2 Alternative derivation of the success probability recursion

As  $S_{(t,g_t)}$  is a martingale,  $\mathcal{L}_{(t,g)}^S \equiv 0$  (see B.5), so  $\dot{S}_{(t,g)} = -\beta_{(t,g)} (S_{(t,g-1)} - S_{(t,g)})$ . Since  $\beta_{(t,g)}$  is determined by  $S_{(t,g-1)}$ , we solve this first-order, linear, non-homogeneous differential equation (Eq. (ODE-S)) for  $S_{(t,g)}$  given  $S_{(t,g-1)}$ : the integrating factor is  $n_T^{(t,g)} = \exp\left(-\int_t^T \beta_{(x,g)} dx\right)$  (Eq. (7)'s probability of no bid on  $(t, T)$  given gap  $g_t = g$ ),

$$D_T \left( n_T^{(t,g)} S_{(T,g)} \right) = -n_T^{(t,g)} \beta_{(T,g)} S_{(T,g)} + n_T^{(t,g)} \dot{S}_{(T,g)} = -n_T^{(t,g)} \beta_{(T,g)} S_{(T,g-1)}.$$

Integrating, using  $n_t^{(t,g)} = 1$  and  $S_{(\tau,g)} = 0$  for  $g \geq 1$ , (ODE-S)'s unique solution is

$$S_{(t,g)} = \int_t^\tau n_T^{(t,g)} \beta_{(T,g)} S_{(T,g-1)} dT.$$

$S_{(t,g)} \equiv 1 \forall g \leq 0$  completes this recursive solution as alternative derivation of (REC-S).

## B.3 State transition probabilities

As with the alternative derivation of Eq. (ODE-S) provided in Section 3.2, we begin by proving Eq. (REC-Q) via the adjoint to Eq. (ODE-Q). This adjoint is called the Kolmogorov backward equation because it fixes the target state  $(t, g)$  and solves for  $Q$  by integrating backwards to the earlier state  $(t', g')$ . To derive the adjoint, we sum the

probabilities of reaching  $(t, g)$  from  $(t', g')$  via  $(t' + dt', g')$  with no bid on infinitesimal interval  $(t', t' + dt')$  and the alternative path via  $(t' + dt', g' - 1)$  with one bid on  $(t', t' + dt')$ :

$$Q_{(t,g)}^{(t',g')} = \left(1 - \beta_{(t',g')} dt'\right) Q_{(t,g)}^{(t'+dt',g')} + \left(\beta_{(t',g')} dt'\right) Q_{(t,g)}^{(t'+dt',g'-1)} + O(dt')^2.$$

$$\text{So } \lim_{dt' \rightarrow 0} \frac{Q_{(t,g)}^{(t'+dt',g')} - Q_{(t,g)}^{(t',g')}}{dt'} = -\beta_{(t',g')} \left(Q_{(t,g)}^{(t',g'-1)} - Q_{(t,g)}^{(t',g')}\right).$$

$$\text{So } D_{t'} \left(Q_{(t,g)}^{(t',g')}\right) = -\beta_{(t',g')} \left(Q_{(t,g)}^{(t',g'-1)} - Q_{(t,g)}^{(t',g')}\right). \quad (\text{ODE-}Q\text{-backward})$$

The integrating factor to solve (ODE- $Q$ -backward) is  $n_T^{(t',g')}$ . For  $g \leq g' - 1$ , this generates the recursive solution<sup>33</sup>

$$Q_{(t,g)}^{(t',g')} = \beta_{(T,g')} \int_{t'}^t n_T^{(t',g')} Q_{(t,g)}^{(T,g'-1)} dT \equiv \mathbb{E}_{(t',g')} \left[ Q_{(t,g)}^{(T_{g_0-g'+1}, g'-1)} \right],$$

which is precisely Eq. (REC- $Q$ ). For  $g = g'$ , given that  $Q_{(t,g)}^{(t,g)} = 1$  and  $Q_{(t,g)}^{(t,g'')} = 0$  for all  $g'' < g$ , the solution is Eq. (24), confirming the overall solution derived in the text.

To derive the Kolmogorov forward equation that we use in Lemma 3, we instead fix the initial state  $(t', g') = (0, g_0)$ , restricting away from the general case, and look forward to assess the probability of marginal shifts in the later state  $(t, g)$ . A campaign reaches  $(t + dt, g)$  via either a bid from just prior state  $(t, g + 1)$  or via  $(t, g)$  with no intervening bid on the interval  $[t, t + dt)$ . So

$$Q_{(t+dt,g)} = Q_{(t,g)}(1 - \beta_{(t,g)} dt) + Q_{((t,g+1))} \beta_{(t,g+1)} dt.$$

Using  $Q_{(t+dt,g)} - Q_{(t,g)} = \dot{Q}_{(t,g)} dt$  and dividing by  $dt$  and taking limits as  $dt \rightarrow 0$ , this gives the differential equation Eq. (ODE- $Q$ ). We suppress the “-forward” qualification since the main paper only needs this single variant.

---

<sup>33</sup>Since  $T_n$  is the  $n$ 'th stopping time, the next bid after  $(t', g')$  occurs at  $T_{g_0-g'+1}$ .

## B.4 Jump variance

Using Eq. (SDE- $Y$ ) and neglecting terms of order  $O(dt^2)$ ,

$$\begin{aligned} \nu_{(t,g)}^Y &\triangleq \lim_{dt \downarrow 0} \frac{\mathbb{V}_{(t,g)} \left( Y_{(t+dt, g_{t+dt})} - Y_{(t,g)} \right)}{dt} &&= \lim_{dt \downarrow 0} \frac{\mathbb{V}_{(t,g)} \left( dY_{(t,g)} \right)}{dt} \\ &= \lim_{dt \downarrow 0} \frac{\mathbb{E}_{(t,g)} \left[ \left( Y_{(t+dt, g-1)} - Y_{(t,g)} \right) \left( -dg_t \right) \right]^2}{dt} &&= \beta_{(t,g)} \left( \Delta Y_{(t,g)} \right)^2, \end{aligned}$$

since the instantaneous variance of the underlying Poisson process  $g_t$  equals its intensity  $\beta_{(t,g)}$ ; each bid causes  $Y_{(t,g)}$  to jump by  $\Delta Y_{(t,g)}$ ; squaring that scale factor gives the result.

## B.5 Martingale equivalences

Using the transition probabilities determined in Lemma 2, the expected generator at time  $x$  given an initial state  $(t', g')$  can be expressed as

$$\mathbb{E}_{(t', g')} \left( \mathcal{L}_{(x, g_x)}^Y \right) = \sum_{g \leq g'} Q_{(x, g)}^{(t', g')} \mathcal{L}_{(x, g)}^Y.$$

To see that the generator of a martingale process  $Y_{t, g_t}$  must be identically zero and always positive for a submartingale, always negative for a supermartingale, notice that

$$\left. \frac{d}{dt} \left( \int_{t'}^t \sum_{g \leq g'} Q_{(x, g)}^{(t', g')} \mathcal{L}_{(x, g)}^Y dx \right) \right|_{t'=t} = \sum_{g \leq g'} Q_{(t, g)}^{(t', g')} \mathcal{L}_{(t, g)}^Y = \mathcal{L}_{(t, g')}^Y.$$

So the martingale property is violated if there exists a  $(t, g)$  such that  $\mathcal{L}_{(t, g)}^Y \neq 0$ . The proof for supermartingales and submartingales is also immediate from this identity. To prove the converse implication and complete the proof of the equivalences, it suffices to apply Dynkin's Theorem, that for any  $t' \leq t$ :  $\mathbb{E}_{(t', g')}(Y_{(t, g_t)}) - Y_{(t', g')} = \int_{t'}^t \mathbb{E}_{(t', g')} \left( \mathcal{L}_{(x, g_x)}^Y \right) dx$ .<sup>34</sup>

## Appendix C Further analysis of canonical cases

C.1 demonstrates the stochastic paths behind the decreasing pivotality trend, using the uniform distribution. C.2 highlights the exact parallel between pivotality and bidding

<sup>34</sup>See for example Theorem 1.24 in Øksendal and Sulem (2007)—Applied Stochastic Control of Jump Diffusions, Springer, volume 498.

in that case and discusses the impact of bidder scarcity (the threshold relative to the expected number of bidders). C.3 derives explicit slopes and comparative statics.

## C.1 Pivotality and bidder success rates - stochastic paths

It is perhaps surprising that average pivotality decreases from *any* state  $(t, g)$ . If  $g_t$  does not change,  $S_{(t,g_t)}^{\text{bid}}$  falls with  $t$  by Lemma 1 but  $S_{(t,g_t)}^{\text{bid}}$  rises whenever  $g_t$  falls by Corollary 1. Proposition 2 shows that the average direct effect of time always dominates the positive average indirect effect of downward jumps in the gap and does so for any cost distribution. Fig. 7 probes this averaging effect for a project with initial gap  $g_0 = 10$ , duration  $\tau = 20$ , bidder arrival intensity 0.95, valuation probability  $q = 0.8$  and uniform cost distribution on  $[0, q]$ .  $S_{(t,g)}^{\text{bid}} \equiv S_{(t,g-1)}$  and pivotality  $\Delta S_{(t,g)} \equiv S_{(t,g-1)} - S_{(t,g)}$ , so we only plot  $S_{(t,g)}$  against time.

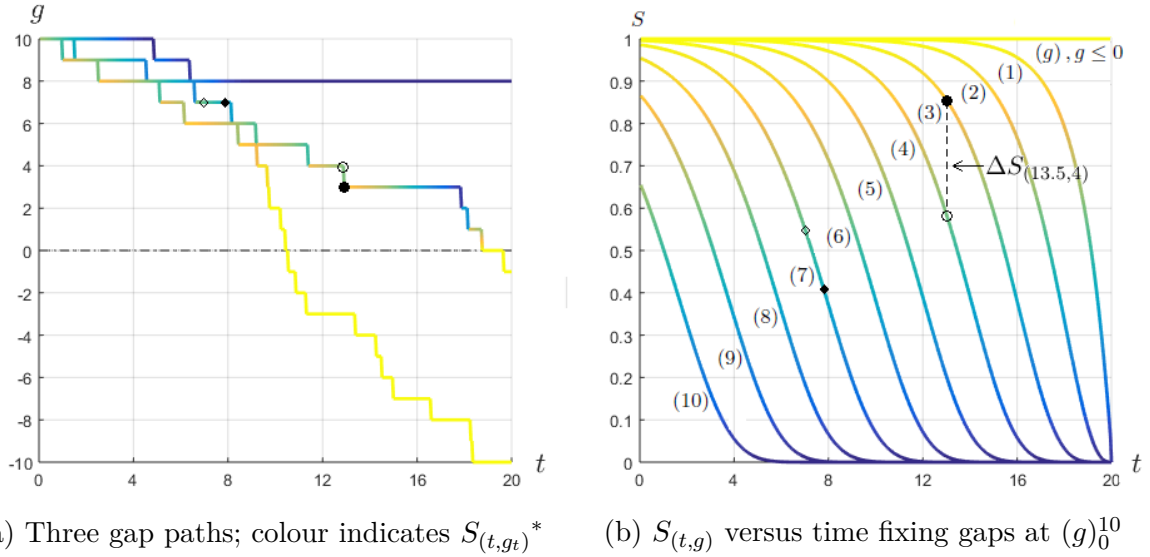
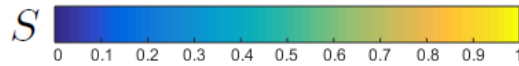


Figure 7: Time profiles of  $g$  and  $S$ ;  $F(c) = \frac{c}{q}$ ,  $c \in [0, q]$ ,  $g_0=10$ ,  $(\tau, \lambda, q) = (20, 0.95, 0.8)$ .\*



\*By Markov property, path likelihoods after crossing points are independent of prior paths.  $S_0=0.65$ .

Panel (a) depicts three simulated paths of  $S_{(t,g_t)}$ . The highest path shows a failing project and the darkening blue colour reflects the increasingly low success prospects with  $S_{(t,g_t)}$  nearing zero by  $t = 10$ : almost all positive cost types choose **A** since gap  $g_{10} = 8$  with  $\tau - 10 = 10$  units of time left is near hopeless. At the other extreme, the path that ends up lowest becomes increasingly yellow, reflecting nearly and then fully, guaranteed success as  $g$  nears 0 with plenty of time left and then falls below 0.

Panel (b) presents curves of  $S_{(t,g)}$  as  $t$  varies for each fixed gap  $g$ . The diamonds in (a) at  $g = 7$  map to those in (b):  $S_{(t,g_t)}$  slides down  $S_{(t,7)}$ , marked (7). By contrast, moving from empty to solid circle at  $t = 13.5$  in (a) depicts a drop in  $g$  from 4 to 3 and causes  $S$  to jump up by pivotality  $\Delta S_{(13.5,4)}$  equal to the dashed vertical distance between curves (4) and (3) in (b). Initial pivotality is about  $0.85 - 0.65 = 0.2$  from curves (10) and (9) at  $t = 0$  in (b) since  $g_0 = 10$ . At any *fixed* gap  $g \geq 2$ ,  $\Delta S_{(t,g)}$  first increases and then decreases over time.  $\Delta S_{(t,g_t)}$  falls to 0 when campaigns are clearly failing or clearly succeeding towards their ends but  $\Delta S_{(t,g_t)}$  *can* stay high if  $g_t$  falls at a specific intermediate rate; indeed if  $g_\tau = 1$ ,  $\Delta S_{(\tau,g_\tau)} = 1$ , the distance between curves (0) and (1) at  $t = \tau = 20$ . *Average* pivotality is still decreasing because this is rare.

## C.2 Pivotality and bidding trends in the uniform case

Fig. 8 exhibits the downward bid slopes for averages across all projects (in black), conditioned on success (in green) and failure (in red). The black, unconditional bid profiles in panels (a) and (d) are exact rescalings of the average pivotality profiles of (b) and (e), because the pivotality effect operates in isolation.

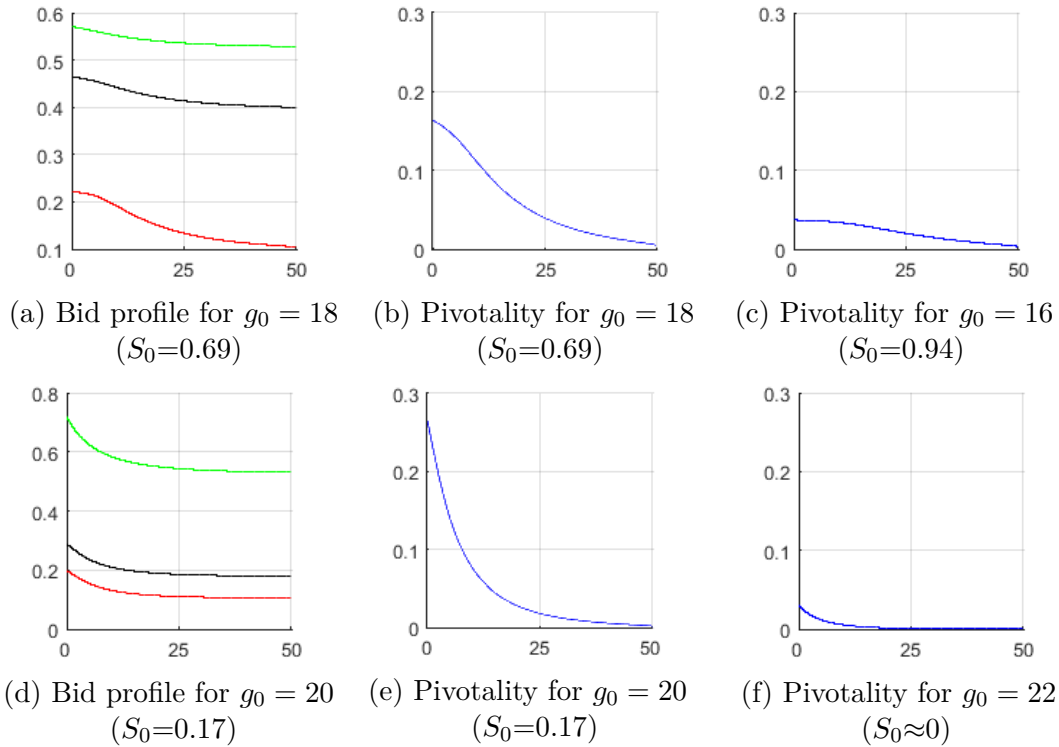


Figure 8: Profiles of bids  $\text{---} A_t^S$   $\text{---} A_t$   $\text{---} A_t^F$  and pivotality  $\text{---} A_t^{\Delta S}$  against time  $t$  for a linear CDF with  $z = 0.2$  given  $g_0 \in \{16, 18, 20, 22\}$  and  $(\tau, \lambda, q) = (50, 0.7, 0.75)$

To see how the threshold  $g_0$  affects the shape, panels (c) and (f) add pivotality profiles for  $g_0 = 16$  and 22 so that  $g_0$  rises from 16 to 18, 20, 22 moving anti-clockwise from panel (c) to (b),(e),(f). Average pivotality and bidding profiles become increasingly convex as  $g_0$  rises. For  $g_0 = 16$  and 18, the pivotality profile is initially concave and becomes convex as the deadline approaches. To see why, recall that pivotality is the vertical difference between the fixed- $g$  success curves in Fig. 7b. When  $g_0$  is low enough to give  $S_0$  near unity, those curves initially bunch up near the unit upper bound; they diverge as time passes, creating the initial concavity. As time starts to run out, the curves are increasingly constrained by the lower bound of 0, causing the later convexity; pivotality ends up at zero in the last moments except, rarely, on ending up with gap exactly 1. More generally,

**Observation 3.** *The pivotality profile is less concave and more convex at higher  $g_0/\lambda\tau$ .*

At very high thresholds, early bids are critical, so pivotality and bid profiles are convex from the start, as in panel (f) where  $g_0 = 22$  and  $S_{(0,22)} \approx 0$ . Higher thresholds do not always raise slopes since they scale down pivotality and bidding (towards  $z\lambda q$ ) but they do raise curvature, which is maximal in (f).

The atom  $z$  of types that always inspect also has a non-monotone effect on the slope. By Lemmas 4 and 5,  $z$  and  $q$  raise  $S$ . If  $g_0$  is high or  $\lambda$ ,  $q$ ,  $\tau$  low, raising  $z$  initially amplifies the downward slope as positive cost bidders react more to gap reductions, but as  $z$  grows, the insensitivity of zero types to  $S^{\text{bid}}$  has the opposite effect. Appendix C.3.1 provides explicit comparative statics when  $g_0 = 2$ .

### C.3 Explicit profile slopes and comparative statics

Lemma 3 permits closed-form profile slopes for the uniform and quadratic distributions of 4.1 and 4.2 with  $g_0 = 2$  and we conduct comparative statics on the atom  $z = F(0)$ .

#### C.3.1 Linear CDF

With the linear CDF of Eq. (28), the constant bid intensity of  $\lambda q$  at any  $g_t \leq 1$  implies a zero generator. When  $g_t = 2$ , Eq. (29) gives,

$$\begin{aligned} \mathcal{L}_{(t,2)}^\beta &= -\lambda q(1-z) \Delta S_{(t,1)} \Delta \beta_{(t,2)} = -(\lambda q)^2(1-z) \left[ 1 - (z + (1-z)S_{(t,1)}) \right] (1 - S_{(t,1)}) \\ &= -(\lambda q(1-z))^2 (1 - S_{(t,1)})^2 = -(\lambda q(1-z))^2 e^{-2\lambda q(\tau-t)}. \end{aligned} \quad (59)$$

To weight this by the probability  $Q_{(t,2)}$  that  $g_t = 2$ , we use [Eq. \(24\)](#) to find

$$\begin{aligned} Q_{(t,2)} &= \exp \left[ - \int_0^t \lambda q \left( z + (1-z)S_{(x,1)} \right) dx \right] \text{ so, as } S_{(x,1)} = 1 - e^{-\lambda q(\tau-x)}, \\ &= \exp \left[ -\lambda q \left( t - (1-z) \int_0^t e^{-\lambda q(\tau-x)} dx \right) \right] = \exp \left[ -\lambda q t + (1-z) \left( e^{-\lambda q(\tau-t)} - e^{-\lambda q \tau} \right) \right]. \end{aligned}$$

Hence, the slope of the average profile equals

$$\dot{A}_t = Q_{(t,2)} \mathcal{L}_{(t,2)}^\beta = - \left( \lambda q (1-z) \right)^2 \exp \left[ -\lambda q (2\tau - t) + (1-z) \left( e^{-\lambda q(\tau-t)} - e^{-\lambda q \tau} \right) \right] < 0. \quad (60)$$

The partial derivative of this slope's magnitude with respect to  $z$  is negative:

$$\begin{aligned} D_z |\dot{A}_t| &= -(\lambda q)^2 (1-z) \exp \left[ -\lambda q (2\tau - t) + (1-z) \left( e^{-\lambda q(\tau-t)} - e^{-\lambda q \tau} \right) \right] \\ &\quad \times \left( 2 + (1-z) \left( e^{-\lambda q(\tau-t)} - e^{-\lambda q \tau} \right) \right) \leq 0. \quad (61) \end{aligned}$$

This monotonicity is specific to  $g_0 = 2$  and to the uniform distribution as we show next.

### C.3.2 Quadratic CDF

For  $g_0 = 2$ , similar to the affine case, the slope is determined by the product of

$$\begin{aligned} \mathcal{L}_{(t,2)}^\beta &= (\lambda q)^2 (1-z) e^{-2\lambda q(\tau-t)} \left[ z - (1-z) \left( 1 - e^{-\lambda q(\tau-t)} \right) \left( 3 + e^{-\lambda q(\tau-t)} \right) \right] \quad (62) \\ \text{and } Q_{(t,2)} &= \exp \left[ -\lambda q \int_0^t z + (1-z) \left( 1 - e^{-\lambda q(\tau-x)} \right)^2 dx \right] \\ &= \exp \left\{ -\lambda q t + (1-z) \left[ 2 \left( e^{-\lambda q(\tau-t)} - e^{-\lambda q \tau} \right) - \frac{1}{2} \left( e^{-2\lambda q(\tau-t)} - e^{-\lambda q \tau} \right) \right] \right\}. \end{aligned}$$

$$\begin{aligned} \text{So } \dot{A}_t &= (\lambda q)^2 (1-z) \left[ z - (1-z) \left( 1 - e^{-\lambda q(\tau-t)} \right) \left( 3 + e^{-\lambda q(\tau-t)} \right) \right] \\ &\quad \times \exp \left\{ \lambda q (t - 2\tau) + (1-z) \left[ 2 \left( e^{-\lambda q(\tau-t)} - e^{-\lambda q \tau} \right) - \frac{1}{2} \left( e^{-2\lambda q(\tau-t)} - e^{-\lambda q \tau} \right) \right] \right\}. \quad (63) \end{aligned}$$

The first term in square brackets determines the sign of the profile slopes. It is positive if condition [Eq. \(57\)](#) holds, i.e., for

$$z \geq \zeta_{(t,2)} = 1 - \left( 1 + S_{(t,2)}^{\text{bid}} \right)^{-2} = 1 - \left( 4 - 4e^{-\lambda q(\tau-t)} + e^{-2\lambda q(\tau-t)} \right)^{-1} \quad \forall t \in [0, \tau]. \quad (64)$$

A strict inequality implies a strictly positive slope for any  $\zeta_{(t,2)} < z < 1$ . For  $t = 0$  and  $\lambda q \tau = 0.126$ , the lower bound on  $z$  is  $\zeta_{(0,2)} = 0.2$ .

## C.4 Higher power distributions

Generalizing to the power- $\rho$  CDF

$$F(c) = z + (1 - z) \left( \frac{c}{q} \right)^\rho, \quad \rho \geq 0. \quad (65)$$

This is concave for  $\rho \in (0, 1]$  and yields a decreasing profile.  $\rho > 2$  gives a steeper positive slope than the quadratic case owing to the higher convexity of  $F$ , when we raise  $z$  to fix  $S_0$ ; higher  $\rho$  raises inspection costs and this lowers  $S_0$  by Lemma 4. Fig. 9 illustrates:  $S_0$  is lower in panel (a) than (b) so we raise  $z$  to compensate and fix  $S_0$  at its value in (a), giving the steeper slope of (c). Raising the power  $\rho$  creates more convex profiles; the NE arises later in the campaign as high-cost types are mostly activated increasingly late.

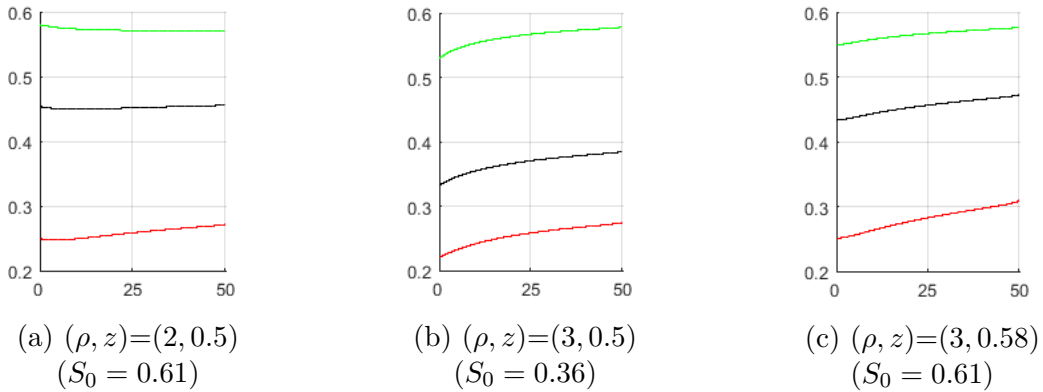


Figure 9: Average bids  $\text{---} A_t^S \text{ ---} A_t \text{ ---} A_t^F$  against time  $t$ , for a power- $\rho$  CDF and a campaign with  $g_0 = 20$ ,  $(\tau, \lambda, q) = (50, 0.7, 0.8)$

## Appendix D Discrete distributions

This appendix provides full details and derivations for the homogenous case of Section 4.4, digging deeper into the intuitions and extending some of the ideas (in D.1 and D.2). We also briefly explain the extension to general discrete distributions (in D.3).

To be self-contained, we repeat the definitions of the critical states. At  $g \leq 1$ , the project is always active. At  $g \geq 2$ , the campaign freezes when time remaining falls

below the minimal duration  $\hat{\tau}_g$  needed for cost  $c$  bidders to inspect.  $\hat{\tau}_g$  is well-defined by  $S_{(0,g)}^{\text{bid}}(\hat{\tau}_g) = c/q$  since  $S_{(t,g)}^{\text{bid}}(\tau) \equiv S_{(0,g)}^{\text{bid}}(\tau - t) \in [0, 1)$  and continuous, decreasing in  $t$ : as  $\lambda q > 0$ ,  $S^{\text{bid}}$  rises towards unity with enough time left and falls to zero at or before  $t = \tau$ . We also define associated critical dates  $\hat{t}_g \triangleq \tau - \hat{\tau}_g$ , so for  $g \geq 2$ ,

$$S_{(\hat{t}_g, g)}^{\text{bid}} \equiv S_{(\tau - \hat{\tau}_g, g)}^{\text{bid}}(\tau) \equiv S_{(0, g)}^{\text{bid}}(\hat{\tau}_g) \equiv \frac{c}{q}. \quad (66)$$

The frontier between active and frozen states can also be described by the maximal or critical gaps at which the campaign is just active for any given date  $t$ :  $\hat{\mathbf{g}} = (\hat{g}_t)_{t \in [0, \tau]}$  where

$$\hat{g}_t \triangleq \sup \left\{ g \in \mathbb{Z} : S_{(t, g)}^{\text{bid}} \geq \frac{c}{q} \right\}. \quad (67)$$

These gaps and the critical dates trace out the frontier that we called the *wall of ice*.

We explain bidding patterns with PE and JE but note that the survival probability approach of the explicit recursion already proves the slope is downward: (1) The frozen state is absorbing because the gap cannot fall while all bidders play  $\mathbf{A}$ , so  $S_{(x, g)}^{\text{bid}}$  does not rise as time passes and bidders continue to choose  $\mathbf{A}$ . (2) The probability of an absorbing state can only increase over time and bid intensity is 0 when frozen,  $\lambda q > 0$  while active.

## D.1 Bid rate decomposition

The first step towards a dynamic analysis is to capture the evolution of average pivotality. Despite the discontinuity in bidding provoked by homogenous costs, average pivotality decreases smoothly over time, as shown in Fig. 3(c). It is continuous because success rates are integrals over time remaining of the finite functions in Eq. (REC-S).

The perfectly flat plateau at the start of the average pivotality profile in Fig. 3(c) owes to the fact that  $g_0$  must start below the critical gap in a campaign that is not born frozen. Given  $g_0 < \hat{g}_0(\tau)$ , the campaign faces no risk of freezing until  $t = \hat{t}_{g_0}$ . DP is trivial on interval  $[0, \hat{t}_{g_0}]$  because any arriving bidder already inspects there, removing the scope for additional strategic complementarity of earlier bidders *on*  $[0, \hat{t}_{g_0}]$ : they have more successors on  $[0, \hat{t}_{g_0}]$  but cannot influence them as they are already maximally active. Their average influence on *later* successors is the same, fixing average pivotality until  $\hat{t}_{g_0}$ . Eq. (13) confirms this:  $\mathcal{D}^{(t, g)} = 0$  for  $t \leq \hat{t}_{g_0}$  given  $\Delta\beta_{(t, g)} = 0$ . Larger durations  $\tau$  extend this plateau and diminish the downward steps and the failure probability.

Moving to the average effect of pivotality on bidding, this continuity is broken by the discontinuity in  $F(\cdot)$ : bidding  $\beta_{(t,g_t)}$  depends on  $F(S_{(t,g_t)} + \Delta S_{(t,g_t)})$  by Eq. (6). Eq. (15) applies at all non-critical dates since  $F(\cdot)$  is only discontinuous at  $c$ . PE is zero except at critical dates: marginal changes in  $S_{(t,g)}^{\text{bid}}$  only affect bidding  $\beta_{(t,g)} = \lambda q F(q S_{(t,g)}^{\text{bid}})$  at dates when  $q S_{(t,g)}^{\text{bid}} = c$ . On the other hand, since  $F_c = 0$  at non-critical dates, the NE is then given by Eq. (17) as  $\mathcal{N}_{(t,g)} = \beta_{(t,g)} \Delta F(q S_{(t,g)}^{\text{bid}})$ . This product is always zero in the homogenous case because the difference term is zero for gaps below the wall of ice and the bid rate is zero for gaps strictly above the wall of ice. For intuition, recall the NE's two necessary components. First, local convexity or concavity here requires a non-zero difference  $\Delta F$  but  $\Delta F$  is zero below the wall of ice because gap reduction cannot raise the inspection probability when already maximized at unity. Strictly prior to a critical date, the unique cost type always inspects even if a small amount of time passes with no bid. That is, the project is maximally active, and hence equally active after both good and bad news. Second, uncertainty requires the possibility of a bid but strictly above the frontier the campaign is frozen and generates no news at all so the NE is zero there too. For a quick mathematical proof: note that  $\Delta F(q S_{(t,g)}^{\text{bid}}) = 0$  except when the gap  $g_t$  is one unit above the critical gap for that high cost; at such gaps,  $\Delta F(q S_{(t,g)}^{\text{bid}}) = 1$  but then  $\beta_{(t,g)} = 0$  at all such gaps and  $\mathcal{N}_{(t,g)} = 0$  even there. In Appendix D.3, additional mass points allow for positive variance and hence Jensen effects that create positive slopes.

Because all the action takes place in proximity of critical dates, we zoom-in on a small neighbourhood of time starting at a critical date  $\hat{t}_g$  and terminating  $\epsilon$  later. Fig. 10, like Fig. 1, provides a graphical decomposition of the bid rate into PE and NE for a campaign at the edge of the wall of ice, with  $(t, g) = (\hat{t}_g, g)$ . It illustrates how the PE's discrete negative effect always dominates the NE at such moments and creates a discrete downward jump. The DP arrow shown in magenta is negative. It is only of order  $\epsilon$ , but has a discrete effect shown by the PE in green because  $F(\cdot)$  is discontinuous at  $t$ :  $\mathcal{E}_{t+\epsilon}^{(t,g)}$  equals  $-1$  for any  $\epsilon > 0$ . Uncertainty in  $S_{(t+\epsilon, \hat{g}_{t+\epsilon})}^{\text{bid}}$  around  $\mathbb{E} S_{(t+\epsilon, \hat{g}_{t+\epsilon})}^{\text{bid}}$  creates the positive but only order  $\epsilon$  NE  $\mathcal{N}_{t+\epsilon}^{(t,g)}$  shown in orange. So the negative PE dominates as  $\epsilon \rightarrow 0_+$ .

In brief, the NE is positive but infinitesimal, since  $\mathbb{E} S_{(t+\epsilon, \hat{g}_{t+\epsilon})}^{\text{bid}}$  lies just below  $c/q$  but the chance of a bid arriving in any instant  $\epsilon$  converges to zero. In Fig. 10,  $t = \hat{t}_g^c$ , so  $\hat{g}_t^c = g$  and  $\hat{g}_{t+\epsilon}^c = g - 1$  so at  $t + \epsilon$ ,  $g$  is exactly one unit above the wall of ice. By contrast, the PE is discrete; the project freezes if no bid arrives at the critical date. As  $\epsilon \rightarrow 0$ ,

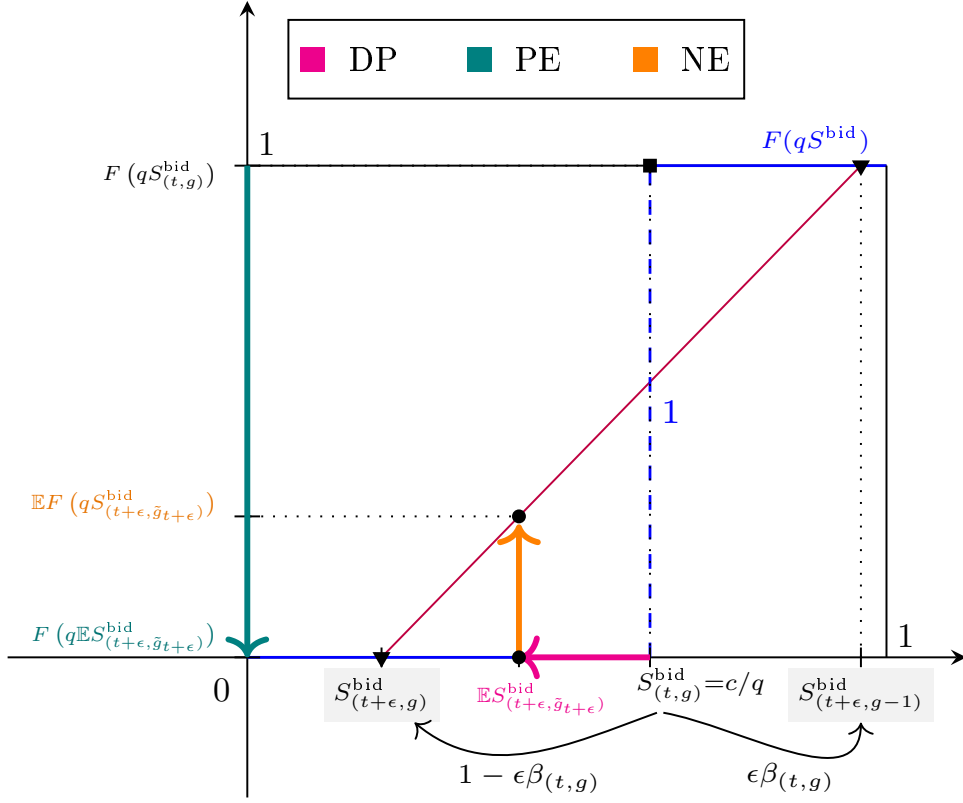


Figure 10: DP, PE and NE for the homogenous case

$S_{(t+\epsilon, g)}^{\text{bid}} \rightarrow S_{(t, g)}^{\text{bid}}$  so DP  $\mathcal{D} \rightarrow 0$  and NE  $\mathcal{N} \rightarrow 0$  but PE  $\mathcal{E}$  stays fixed at  $-1$ .

## D.2 Illustration with initial gap $g_0 = 2$ .

The campaign success rate is  $S_0 = S_{(0,2)}$ . To collect at least two bids, with at least one by  $\hat{t}_2$ ,  $S_{(0,2)} = 1 - \left[ e^{-\lambda q \hat{t}_2} + \left( \lambda q \hat{t}_2 e^{-\lambda q \hat{t}_2} \right) e^{-\lambda q (\tau - \hat{t}_2)} \right]$ . The bracket sums the probability of no bids on  $[0, \hat{t}_2]$  plus the probability of one on  $[0, \hat{t}_2]$  and none on  $[\hat{t}_2, \tau]$ . Simplifying,

$$S_0 = 1 - \left[ e^{-\lambda q \hat{t}_2} + \lambda q \hat{t}_2 e^{-\lambda q \tau} \right]. \quad (68)$$

While  $g = 2$ , bidders only inspect if  $t \leq \hat{t}_2$ , whereas bidders always inspect at  $g \leq 1$ . So the average bid rate is constant at  $A_t = \lambda q$  up till  $\hat{t}_2$  and drops at that date by  $\lambda q$  times the probability  $1 - \alpha_{\hat{t}_2}^{(0,2)} = Q_{(\hat{t}_2, 2)}^{(0,2)} = e^{-\lambda q \hat{t}_2}$  of hitting the vertical wall of ice at  $\hat{t}_2$ . It then remains constant at  $A_t = \lambda q \left( 1 - e^{-\lambda q \hat{t}_2} \right)$ .  $S_{(\hat{t}_2, 1)} = 1 - e^{-\lambda q (\tau - \hat{t}_2)} = c/q$ , so

$$\hat{t}_2 = \tau - \frac{1}{\lambda q} \ln \left( 1 - \frac{c}{q} \right)^{-1}. \quad (69)$$

or equivalently,  $e^{-\lambda q \hat{t}_2} = 1 - c/q$ . Intuitively,  $\hat{t}_2$  is lower in adverse settings as bidders at  $g = 2$  then give up earlier:  $\hat{t}_2$  falls with  $c$  and rises with  $\lambda$  and  $q$ . Substituting in Eq. (68),

$$S_0 = 1 - e^{-\lambda q \tau} \left[ \lambda q \tau + \left(1 - \frac{c}{q}\right)^{-1} - \ln \left(1 - \frac{c}{q}\right)^{-1} \right]. \quad (70)$$

### D.3 Richer discrete distributions

For a generic discrete distribution, let the CDF  $F$  have mass  $z^k$  atoms at  $c = c^k$  for  $k \in \{0, 1, 2, \dots, K\}$  indexed so that  $0 = c^0 < c^1 < \dots < c^K$ ;  $z^0$  can be 0,  $K$  can be infinite. The analysis is similar to the homogenous case except that the multiple atoms now lead to positive news effects away from critical dates because bidding variance is only trivial below the lowest atom's frontier. For example, in the binary case, discrete PE's at critical dates, corresponding to the two cost types punctuate continuous positive NE's associated with the higher type to create a tooth-shaped profile.

Formally, for any  $g$  and  $c^k < q$ , by Lemma 1 and  $\lim_{\tau \rightarrow \infty} S_{(t,g)}^{\text{bid}}(\tau) = 1$ , a unique duration  $\hat{\tau}_g^k$  satisfies  $S_{(0,g)}^{\text{bid}}(\tau) = c^k/q$ . For  $c^K = q$ ,  $g \geq 2$ , we let  $\hat{\tau}_g^K = \infty$ .  $\hat{\tau}_g^k = 0$  if  $g \leq 1$  or  $k = 0$ . Otherwise,  $\hat{\tau}_g^k \in (0, \infty)$ . At  $t = \hat{t}_g^k \triangleq \tau - \hat{\tau}_g^k$ ,  $\mathcal{E}_{t+}^{(t,g)} = -z^k$ . This multiplies the set of NE's but for each type  $k$  and date  $t$ , there is at most one gap  $g = \hat{g}_t^k + 1$  at which type  $k$ 's start to inspect after a bid, creating a positive NE. At non-critical dates, the rate of NE in Eq. (17) is well-defined: as  $F_c = 0$ ,  $\mathcal{N}_{(t,g)} = \beta_{(t,g)} \Delta F(q S_{(t,g)}^{\text{bid}}) = \beta_{(t,g)} \sum_{k: g = \hat{g}_t^k + 1} z^k$ .

## Appendix E Design optimization details

We begin by illustrating optimization of  $g_0$  in case (I) with parameters configured as in Fig. 4b, with  $G=3.5$  and 5, to illustrate the same  $g_0^* = g_0^{**}$  that is convenient for multiple prices in Section 6.2 and a higher value corresponding to a larger financial goal.

Fig. 11 displays  $S_0(g_0, p(g_0))$  for  $g_0 = 1, 2, \dots, 22$ . The bar plot in dark blue corresponds to the higher value  $G = 5$ . Only values  $g_0 \geq 7$ , marked by the solid dark blue line, are feasible. The success rate is essentially zero (below one percent after rounding) outside the range of  $g_0$  values between 8 and 18. The optimal single-price design is  $(g_0^*, p^*(g_0^*)) = (12, 0.6167)$  and achieves a success rate of  $S(12, 0.6167) = 0.53$ . The yellow plot treats  $G = 3.5$ . The now wider range  $g_0 \geq 5$  of feasible  $g_0$  values starts at the solid yellow line. Success rates are also non-trivial for a wider  $g_0$  region, starting at  $g_0 = 5$  and

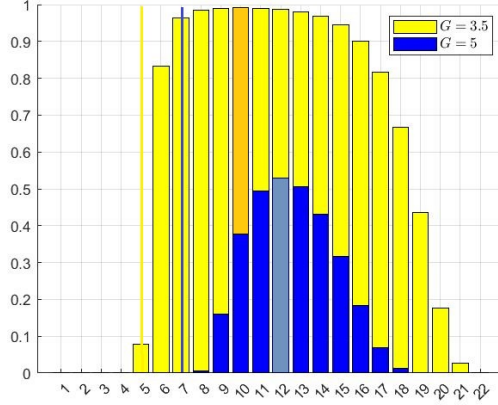


Figure 11:  $S_0(g_0, p(g_0))$  in case (I), highlighting optimal  $g_0$  values

terminating at  $g_0 = 21$ . The optimal single-price design  $(g_0^*, p^*(g_0^*)) = (10, 0.55)$  yields  $S_0 = 0.99$ . Importantly, in both bar plots, reducing the price, or equivalently raising the bidder threshold, initially raises and later decreases  $S_0(g_0, p(g_0))$ . This implies a unique maximizer. For instance, for  $G = 5$ , increasing  $g_0$  from 9 to 10 reduces the implied price by 0.056, more than compensating for its direct effect on  $S_0$ . By contrast, raising  $g_0$  from 14 to 15 reduces the implied price by only 0.024 and the success rate drops.

## E.1 Deterministic sequential arrival of $g_0$ bidders

Since a success requires a bid from every bidder at each of the sequence of gaps from  $g_0$  down to 1, in this simplified model with exactly  $g_0$  bidders known to arrive, every single arrival at every gap  $g \geq 1$  must bid. Letting  $\pi_g$  denote the probability of a bid at  $g$  given bids by all prior bidders, the success probability from gap  $g - 1$  onwards, denoted  $S_{(g-1)}$ , satisfies  $S_{(g)} = \pi_g S_{(g-1)}$  by cost independence and  $S_{(1)} = \pi_1$  since  $S_{(0)} = 1$ . Solving recursively gives  $S_{(g)} = \prod_{g' \leq g-1} \pi_{g'}$  and  $S_0 \equiv S_{(g_0)}$  so

$$S_0 = \prod_{g=1}^{g_0} \pi_g. \quad (71)$$

### Power law distribution

Using the generic power distribution in Eq. (65) with  $z = 0$  and all  $d_g \in [0, q]$ ,  $\pi_g = qd_g^\rho S_{(g-1)}^\rho$ , so that  $S_{(g)} = qd_g^\rho S_{(g-1)}^{1+\rho}$ . Solving recursively Eq. (71) using  $g$  instead of  $g_0$  to

compute intermediate  $S_{(g)}$  combined with  $\pi_1 = qd_1^\rho$  gives

$$S_0 = q \sum_{g=1}^{g_0} (1+\rho)^{g_0-g} \prod_{g=1}^{g_0} d_g^{\rho(1+\rho)^{g_0-g}} = q \frac{(1+\rho)^{g_0-1}}{\rho} \prod_{g=1}^{g_0} d_g^{\rho(1+\rho)^{g_0-g}}. \quad (72)$$

Dropping the discount-independent  $q$  term, (47)'s Lagrangian with budget constraint multiplier  $l$  is

$$L = \prod_{g=1}^{g_0} d_g^{\rho(1+\rho)^{g_0-g}} - l \left[ \sum_{g=1}^{g_0} d_g - ((v - \kappa)g_0 - G) \right]. \quad (73)$$

Differentiating with respect to each  $d_g$  gives first-order conditions

$$\frac{\rho(1+\rho)^{g_0-g}}{d_g} \prod_{g=1}^{g_0} d_g^{\rho(1+\rho)^{g_0-g}} = l \quad \text{so} \quad \frac{d_g}{d_1} = (1+\rho)^{1-g}. \quad (74)$$

Imposing the budget constraint,

$$(v - \kappa)g_0 - G = d_1 \sum_{g=1}^{g_0} (1+\rho)^{1-g} = d_1 \frac{1+\rho - (1+\rho)^{1-g_0}}{\rho}.$$

So  $d_1 = \frac{\rho}{1+\rho - (1+\rho)^{1-g_0}} ((v - \kappa)g_0 - G)$ ,  $d_g = \frac{\rho}{(1+\rho)^g - (1+\rho)^{g-g_0}} ((v - \kappa)g_0 - G)$ .

The optimal prices in Eq. (49) follow on subtracting this  $d_g$  from  $v$ , with  $\rho = 1$  (case I).

## Homogenous inspection costs

The argument given in Section 6.2 proves that prices (50) are optimal. The associated implementability restriction follows on substituting optimal prices (50) into the budget constraint of problem (47):  $G \leq \sum_{g=1}^{g_0} [(v - \kappa) - c/q^g] = (v - \kappa)g_0 - c \left( \frac{q^{-g_0} - 1}{1-q} \right)$ .

## Appendix F Kickstarter profile plots

The dataset from Fan-Osuala et al. contains daily data for 618 Kickstarter campaigns collected between April 1st and May 2nd 2014. The Figs. 12 and 13 profile plots divide campaign duration into 20 blocks and measure bidding as total collected per time block divided by the goal. Data are fitted by a spline with smoothing parameter 0.005.

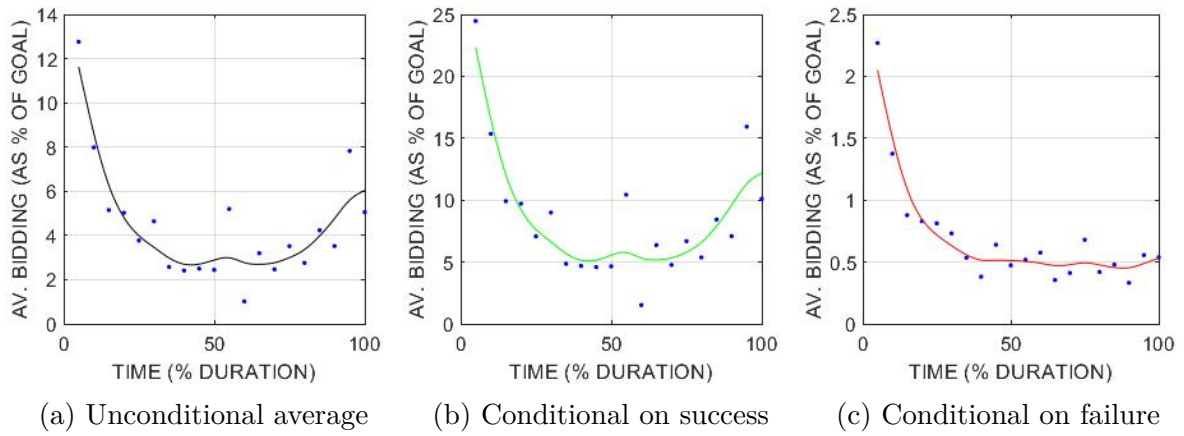


Figure 12: Bid profiles by outcome from Kickstarter data

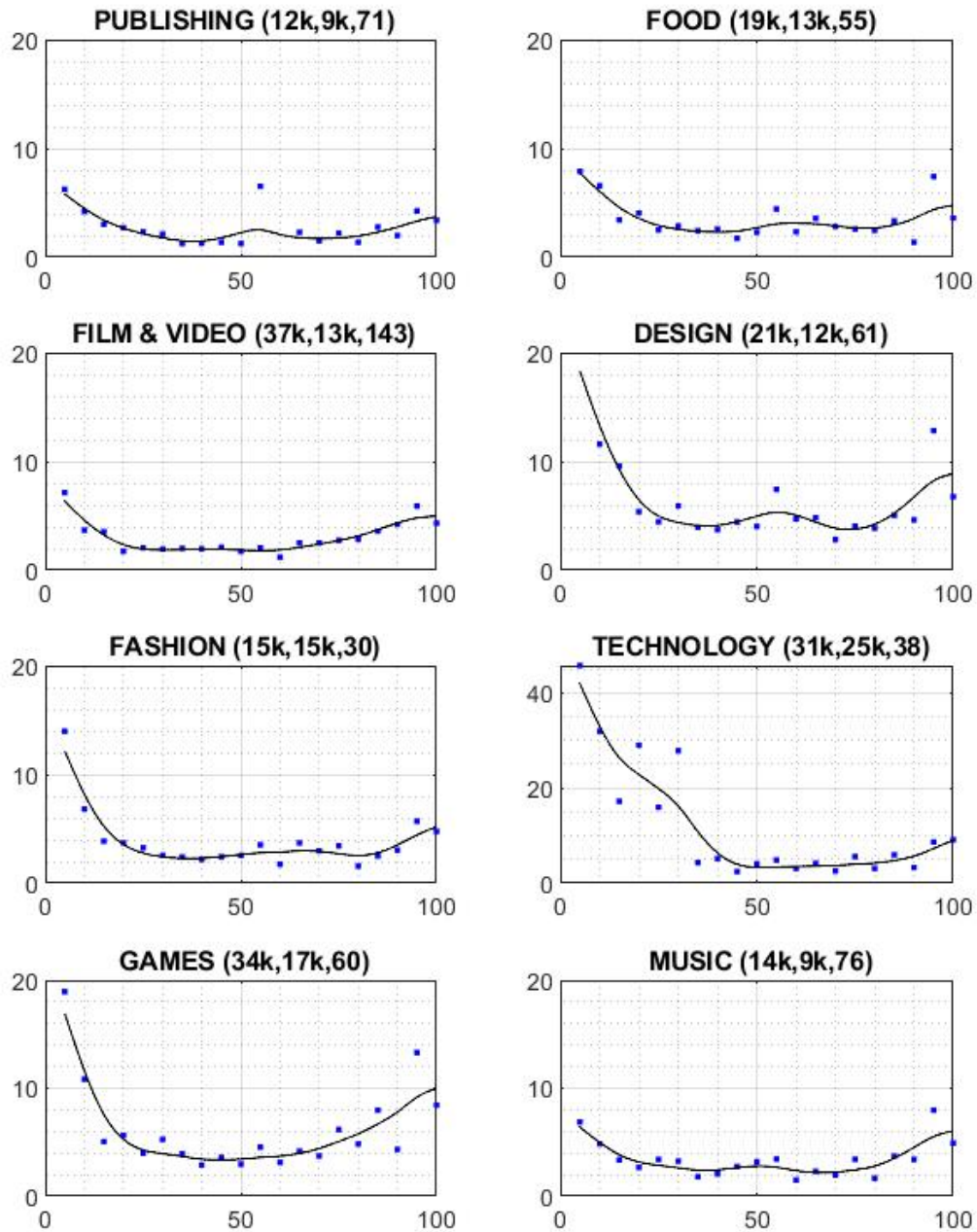


Figure 13: Profiles by category; average and median amounts pledged in USD and number of campaigns observed in parentheses (av,med,#) plotted against time as % of duration. Categories with less than 20 campaigns are omitted.